IntechOpen

Recent Developments in the Field of Carbon Fibers

Edited by Rita Khanna and Romina Cayumil

RECENT DEVELOPMENTS IN THE FIELD OF CARBON FIBERS

Edited by **Rita Khanna** and **Romina Cayumil**

Recent Developments in the Field of Carbon Fibers
http://dx.doi.org/10.5772/intechopen.71346
Edited by Rita Khanna and Romina Cayumil

Contributors

Hassan El-Dessouky, Mohamed Nasr Saleh, Félix A. López, Carlos González, Cláudio S. Lopes, Andrea Fernández, Bo Jin, Aleksandr Evhenovych Kolosov, Elena Kolosova, Yang Liu, Chao Zhang, Xinyu Zhang, Naveen Kumar, Anil Kumar Gangwar, Sangeeta Devi Khangembam, Feng Xu, Xusheng Du, Helezi Zhou, Rita Khanna

Notice

First published in London, United Kingdom, 2018 by IntechOpen
eBook (PDF) Published by IntechOpen, 2019
IntechOpen is the global imprint of INTECHOPEN LIMITED, registered in England and Wales, registration number: 11086078, The Shard, 25th floor, 32 London Bridge Street
London, SE19SG – United Kingdom
Printed in Croatia

British Library Cataloguing-in-Publication Data
A catalogue record for this book is available from the British Library

Additional hard and PDF copies can be obtained from orders@intechopen.com

Recent Developments in the Field of Carbon Fibers
Edited by Rita Khanna and Romina Cayumil

p. cm.

Print ISBN 978-1-78923-518-0

Online ISBN 978-1-78923-519-7

eBook (PDF) ISBN 978-1-83881-562-2

Meet the editors

Associate Professor Rita Khanna holds a PhD degree in condensed matter physics and has extensive research experience (Nuclear Research Centre, Jülich, Germany; Department of Atomic Energy, India; ANU Canberra, Sydney University, University of New South Wales, Sydney, Australia) in the fields of diffuse x-ray scattering, disordered materials, atomistic computer modelling and simulations, high-temperature metallurgical processes, environmentally sustainable waste management, and nanoscale carbon fibres, foams and structures. She has published over 140 peer-reviewed articles including 10 book chapters, 110 journal articles and over 20 papers in conference proceedings. Her group has successfully produced one-, two- and three-dimensional carbons, and hybrid carbon structures from biowaste and is making groundbreaking contributions to the field of novel carbon materials.

Dr. Romina Cayumil is a lecturer and researcher at Universidad Andrés Bello, Chile. She holds a PhD in Materials Science and Engineering from the University of New South Wales, Sydney, Australia, and she is a Metallurgical Engineer at Universidad de Concepción, Chile. Her research is focused on the recycling of electronic waste for the recovery of valuable materials in an environmentally friendly manner, with emphasis on resource recovery and the minimization of the environmental impacts related to the recycling process.
Her background is in extractive metallurgy and high-temperature processes. Her interests are R&D on metallurgical processes for the mining industry, development and optimization of high-temperature processes, and waste management and resource valorization.

Contents

Preface

Carbon fibre-reinforced composites (CFRPs) are materials of choice in several industries with applications in aerospace, marine, construction and automotive sectors. With a combination of high mechanical strength, lightweight, design flexibility, low system cost, functionalities and high fuel efficiencies, the demand for carbon fibre–based components is expected to grow dramatically with expanding opportunities for other composites and lightweight metals. Although this field has achieved a high level of maturity, industrial and commercial success, ongoing developments include, among others, the use of nanocarbons such as graphene, carbon nanotubes, graphite nanoplatelets, nanofillers, bucky papers for creating multiscale hierarchical composites into engineered multifunctional preforms, toughened thermoplastic fibres or nonwoven veils, etc.

With focus on recent developments in the field of carbon fibres, this book presents several new approaches being used to enhance basic and/or specific characteristics of carbon fibres/composites and novel applications such as biological veterinary implants for tissue engineering and scaffoldings. Another key development in the field involves recycling and reuse of end-of-life CFRP waste as well as manufacturing waste, which is becoming a serious issue in the field.

The book has an introductory chapter and seven full chapters with contributing authors from Algeria, Australia, China, India, Spain, the UK and the USA. Global authorship in this book reflects intense research activity in this field worldwide with developments occurring on several fronts.

The Introductory Chapter is focussed on an issue of major concern for the carbon fibre industry: recycling and reuse of burgeoning volumes of end-of-life carbon fibres and manufacturing waste. Challenges during recycling include degradation in carbon fibre quality, limited reuse, landfilling costs and regulatory measures. Key aspects of mechanical processing and thermal and chemical treatments to separate resin and carbon fibres are discussed along with the impact of various treatments on the basic characteristics of recovered carbon fibres.

The table of contents is organized taking into account recent developments in the field of carbon fibres including new products or treatments to enhance product quality and characteristics, novel applications to different fields and approaches being developed for the reuse and recycling of waste CFRPs and other carbon fibre–based products.

The second chapter reports on retrospective aspects of creating classical and nanomodified functional carbon composites for structural applications. Ultrasonic processing for physical

modification was investigated for improving technological operational and physico-mechanical characteristics of composites and structures. Methods for obtaining functional carbon composites with increased strength, electrical conductivity and crack resistance are detailed along with potential applications.

The third chapter reports on the creation of nanostructures on the carbon fibre surface as one of the most effective approaches for additional functions and functional enhancements in mechanical properties, interfacial bonding and electrocatalytic properties of carbon fibres. Different nanostructures including nanoparticles, nanorods, nanotubes, nanosheets, and nanoflowers were grown on the surface of carbon fibres by using a variety of techniques. These multiscale, multifunctional nanostructured carbon fibres are expected to find applications in next-generation fibre-reinforced composites and energy storage devices and for producing green energy.

The fourth chapter presents results on 3D woven carbon fibre composites right from weaving up to manufacturing stages. During weaving, weft, warp and binder fibres run through the fabrics along three directions. Producing a unitised single-piece fabric and subsequently reducing the time required for rapid composite manufacturing are the key advantages of 3D woven preforms. Weaving of 3D fabrics and manufacturing of 3D composites, physical characterisation and mechanical testing of infused composite samples are discussed in this chapter.

The fifth chapter analyses novel surface treatment methods for carbon fibres including grafting of carbon nanotubes, generation of carbon fibre forests by surface brushing and abrading and the growth of ZnO nanowires on fibre surfaces. Improvements in the interfacial shear strength were measured by the single-fibre microbond test. The hierarchical microfibres on CF fabrics were used to fabricate laminates and anti-delamination capacity of composites was determined.

The sixth chapter reports on a biological evaluation of carbon fibre mesh for creating three-dimensional scaffolds for tissue engineering and on using fibrous matrix bioimplants for tissue regeneration by acting as cell-supporting scaffolds. In vivo examination of retrieved sample on day 30 postimplantation showed good adhesion and biocompatibility of carbon fibres with carbon fibre mesh covered with dense thick fibrous connective tissue. Complications like infection or pus formation were not observed in the vicinity of implanted biomaterials.

The seventh chapter presents a report on recycling carbon fibre composites to prepare new low-cost composites with thermoset plastics. Operating parameters of the recycling process including pyrolysis followed by oxidation were optimized, and recycled composites were characterized using tensile tests, Scanning electron microscopy and Raman spectroscopy. With less than 10% loss in tensile strength, these recycled composites could find application in the automotive, wind energy, construction, railway and aeronautics sectors.

The eight chapter focusses on in-depth characterization of reused composite-oriented strand boards (COSB) for stiffness-critical and contoured applications. Development of this product has the potential for significant utilization of prepreg scrap generated during aerospace manufacturing processes. The application of non-destructive techniques such as ultrasound and micro-computed tomography and microscopic imaging for investigating COSBs was evaluated for determining key facets of these products, and their key feature and limitations were identified.

The book covers extensive areas of interest in the field of carbon fibres, carbon fibre–reinforced composites, new developments, applications and recent developments in their recycling and reuse. Current major issues are examined, and future opportunities in this field are revealed. The book has a global perspective and wide coverage of topics for academics, professionals and regional and international organizations.

Associate Professor Rita Khanna (Editor)
School of Materials Science and Engineering
The University of New South Wales
Sydney, Australia

Dr. Romina Cayumil (Coeditor)
Facultad de Ingenieria
Universidad Andres Bello
Santiago, Chile

Chapter 1

Introductory Chapter: Recycling and Reuse of End-of-Life Carbon Fibre Reinforced Polymers

Rita Khanna

Additional information is available at the end of the chapter

http://dx.doi.org/10.5772/intechopen.76709

1. Introduction

Industrial carbon-bearing waste from airliners, trains, cars, boats, turbine blades, sporting, industrial and commercial goods is very hard to recycle or reshape into original components [1, 2]. Carbon fibre-reinforced polymers (CFRPs) (>90% carbon) contain significant fraction of carbon fibres within a polymer matrix, along with varying levels of additives such as silica, alumina and other minerals. Carbon fibres contribute towards high tensile strength, whereas the matrix provides the impact strength [3]. Their key characteristics such as long-term thermal stability, rigidity, dimensional stability, resistance to creep and deformation under load, high electrical and thermal insulating properties and other advantages play an important role in their various applications; however, these create major bottlenecks for their end-of-use disposal [4, 5]. These fire-resistant materials that are designed to resist combustion contain large amounts of pure, disordered carbon with a complex bond network and are difficult to recycle by conventional means.

Aeronautics is one of the biggest consumers of CFRPs due to the recent developments in planes, for example, Boeing 787, Airbus A380 and A350, whereas the growth in the automotive sector is somewhat slow. According to the International Civil Aviation Organisation, the global air transport network has been observed to double in size every 15 years. It is estimated that ~44% of the global fleet of commercial, military and private aircrafts is likely to reach end of life in 20 years or so; between 400 and 600 commercial aircraft are disassembled around the world each year [6]. A cost-effective environmentally sustainable management of large volumes of CFRPs' waste from end-of-life products therefore assumes great significance and urgency.

Protecting the environment for future generations is a fundamental issue and a great challenge; manufacturers are seeking alternatives approaches of waste management.

Key challenge is to find environmentally friendly, alternative recycling approaches and to transform carbon-bearing composite waste into valuable resources. Recycling rates for CFRPs are currently very low, with most of the waste ending up in landfills. While landfilling is a relatively cheap and convenient disposal route, environmental legislation on waste management is also becoming increasingly restrictive.

According to the European Union's Waste Framework Directive [7], landfilling is the least preferred waste management option. Landfilling carbon-bearing waste can be a serious environmental hazard as well. It can lead to the release of greenhouse gases, including huge amounts CO_2 and methane; up to 50% of these emissions are of methane, which is 21 times more potent a greenhouse gas than CO_2. Manufacturers across Europe are required to pay to dispose their production waste if it goes to landfill as well as a climate change levy.

Current approaches for recycling composite materials, reuse and material recovery from waste CFRPs are briefly reviewed in the following section. While several techniques such as pyrolysis, solvolysis, mechanical grinding, chemical, high voltage fragmentation and so on using different approaches have shown feasibility of recycling, commercial/industrial applications of recycled carbon fibres are still very limited. Recycled fibres are generally of lower quality as compared to virgin fibres due to lack of control in fibre length and length distribution, diminished surface quality and multiple sources [8].

Recycling is profitable and sustainable only if the value of the reclaimed materials exceeds the cost of the recycling process. Recycled carbon fibres can be 30–40% cheaper than virgin carbon fibres; however, the degradation of fibre characteristics can be a serious issue during reuse. Process conditions are known to vary significantly depending on the waste CFRP products being recycled. Composite waste, generally sourced across different industries, is also likely to be heterogeneous in nature. A new approach based on using waste CFRPs as a carbon resource in steelmaking will be presented, especially for those CFRPs that cannot be transformed back in to carbon fibres.

2. Recycling approaches for waste CFRPs

Various approaches for recycling and reusing waste CFRPs as carbon fibres as well as a carbon resource are briefly reviewed in this section.

2.1. Mechanical recycling

The key principle of recycling CFRPs involves the separation of carbon fibres from the resin matrix.

Mechanical processing involves crushing and shredding followed by further grinding and milling down to 10–50 mm of fine particles [9]. Recovered materials/flakes are separated into resin-rich powders and carbon fibres of different lengths still embedded in the resin matrix. Resin-rich powders find applications as fillers in bulk as well as sheet-melding composites [10]. While recovered fibre-rich fractions find reuse in composites [11], their cost and quality are key factors affecting efficient reuse.

Cutting mills were found to produce longer as well as more homogeneous fibre lengths as compared to hammer mills [12]. Direct reforming without grinding has also been used in some cases. Due to significant impairment in mechanical properties and poor bonding between the fibrous fraction and resin, recycled materials are still being used in small concentrations only [13]. Electrodynamic fragmentation has been used to shred carbon fibre-reinforced thermoplastics. Milling dust and chips produced during milling operations have found applications as fillers in the production of thermoplastic granulates with increase in tensile strength and overall rigidity [14]. Degradation in carbon fibre quality is a key issue affecting mechanical processing.

2.2. Thermal processing

A variety of thermal processes including pyrolysis (heating in the absence of air), fluidised bed and microwave-assisted pyrolysis as well as combustion (heating in the presence of oxygen) have been used for recycling CFRPs [15–17]. Key purpose of these processes is to devolatilize resin to recover carbon fibres; typical temperatures used range between 450 and 700°C depending on the resin used. As high temperatures (>2200°C) are used in the preparation of carbon fibres, relative lower pyrolysis temperatures do not have much effect on basic characteristics of carbon fibres.

Temperatures up to 1550°C are used for recycling of CFRPs for steelmaking applications [18]. Devolatilised resin produces CO_2, H_2, CH_4 gases, an oily fraction as well as char that may deposit on fibre surfaces. Key advantages of pyrolysis (temperature range: 400–1550°C) include retention of mechanical properties, recovery of carbon fibres and the absence of chemicals. Some of the detrimental factors include the deposition of chars on fibre surfaces and hazardous emissions due to thermal degradation of resin [18].

While higher amounts of energy may be consumed during pyrolysis depending on operating temperatures, this process does not cause local area contamination, typically associated with mechanical and physical processing of waste. Deposition of char from degraded resin can be seen clearly in SEM images of CFRPs treated at a range of temperatures (**Figure 1**). The fibres contaminated by resin char require additional heating in air at 450°C to burn this residual char. However, oxidation can cause strength degradation (up to 50%), shorter fibres and unstructured fibre architecture [20].

In microwave-assisted pyrolysis, direct heating of the material core in inert atmosphere results in fast thermal transfer and energy savings. Lester et al. [17] suspended specimens of carbon fibres and resin in a microwave cavity using quartz sand to suspend the samples and glass wool to limit material loss. Using a bed of silica sand, fluidised bed reactor used hot air for rapid heating and dissociation of resin from the CFRPs matrix [12]. A strength degradation of ~25% was recorded for carbon fibres after heat treatment at 550°C. While this technique can process contaminated as well as end-of-life waste, it is not particularly suitable for recovering carbon fibres.

2.3. Solvolysis

Solvolysis involves chemical degradation of the resin present in CFRPs with the help of chemical solvents. Water is the most commonly used solvent; organic co-solvents, alkaline as well as

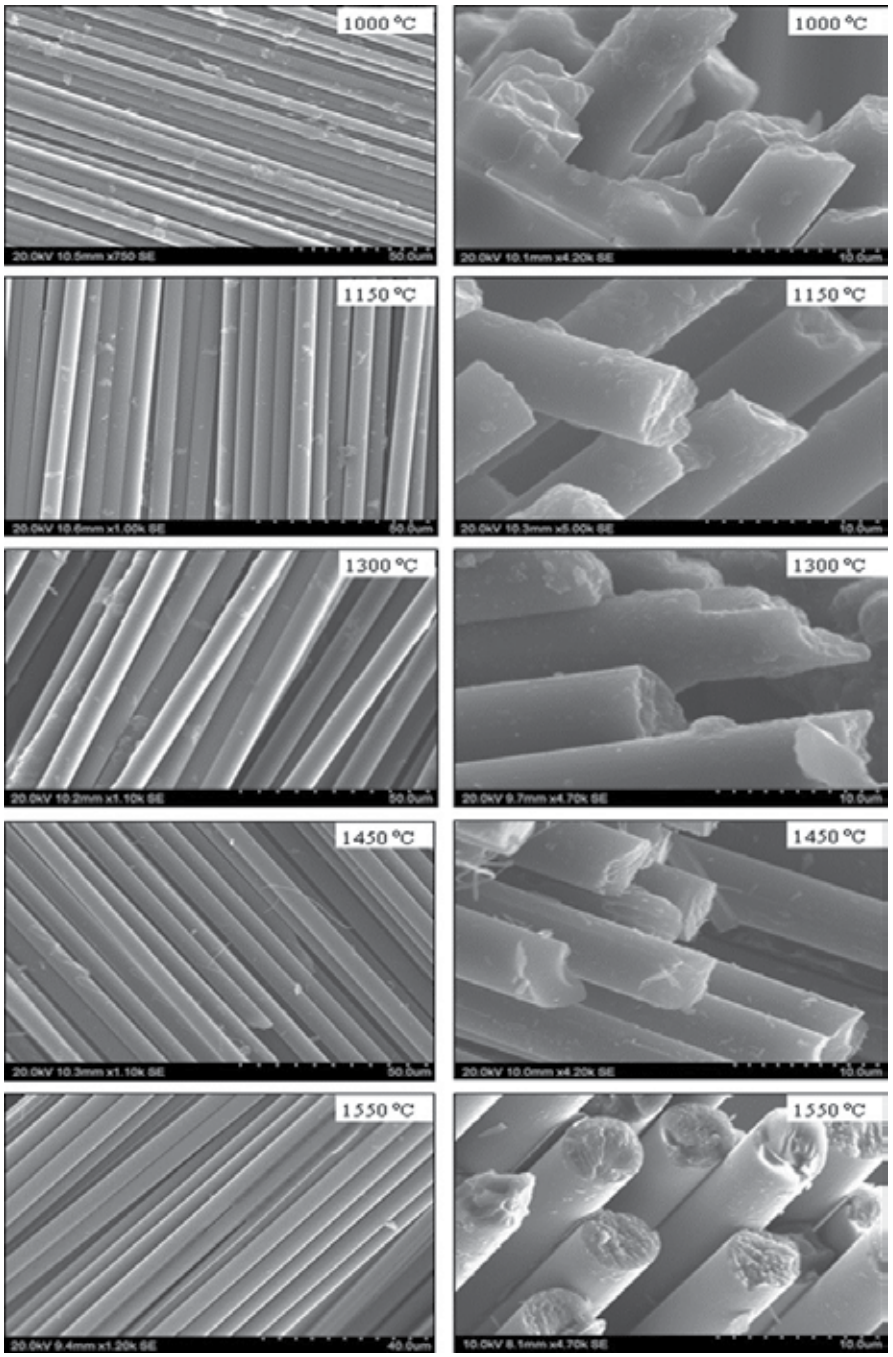

Figure 1. Scanning electron microscopy (SEM) images on pyrolysis residues from CFRPs heat treated at a range of temperatures [19]. Low (left) as well as high (right) resolution images have been presented.

acidic catalysts, are also used along with water depending on the nature of the resin involved [21–23]. Low temperatures as well as pressures are used sometimes in conjunction with various solvents; polyester resins require lower temperatures than epoxy resins for degradation

and solvolysis. The overall process can therefore be a combination of solvolysis and thermal processes, for example, hydrothermal processes for use of water at higher temperatures.

It is also possible to modify the solvent power and basic characteristics, reactivities and so on by operating under subcritical or supercritical conditions as a function of temperature and pressure [24]. These techniques can recover carbon fibres without much detriment of fibre lengths, distributions and mechanical properties. However, these may not be suitable for contaminated waste or could cause environmental damage when hazardous chemicals are either used or produced as spent byproducts.

2.4. Waste CFRPs as a carbon resource

Significant research has been carried out on recycling waste CFRPs in attempts to extract carbon fibres, albeit with reduced mechanical and other capabilities, for further reutilization in a variety of lower-grade applications. As recycling rates continue to be very low and landfilling not a viable option due to high costs and/or legislation, the utilisation of waste CFRPs as a carbon resource in steelmaking is being explored [25]. This technique can process waste CFRPs irrespective of the nature and characteristics of fibres, resin and impurities present due to high temperatures (1550°C).

CFRPs typically contain up to 92 wt.% carbon in form of fibre; fibres containing up to 99 wt.% carbon is generally known as graphite fibres. The atomic structure of carbon fibres is similar to graphite and consists of sheets of carbon atoms (graphene sheets) arranged in a regular hexagonal pattern, the key difference being the manner of interlocking between sheets. Precursors used to prepare carbon fibres have a strong influence on atomic-level fibre structure [26].

Carbon fibres derived from polyacrylonitrile (PAN) have a turbostratic structure (random orientation of graphene sheets), whereas carbon fibres derived from the mesophase pitch have a highly ordered graphitic structure. As a potential carbon resource for steelmaking, waste CFRPs have better characteristics as compared to typical carbons, for example, coals, cokes, chars and so on [27].

Carbon dissolution from CFRP powders into molten iron was investigated at 1550°C using sessile drop arrangement [28]. Carbon dissolution investigations showed a rapid carbon pickup reaching ~5.20 wt.% carbon for CFRPs char (K: 22.2×10^{-3} s^{-1}) within 2 min. This level of carbon pickup was similar to that from synthetic graphite and was much higher than typical results from coke, coal chars and natural graphite.

End-of-life waste CFRPs can be used as an alternative source of carbon for carburising purposes in steelmaking. Such sustainable recycling of CFRP materials for the steelmaking industry will be an important pathway towards solving CFRPs' disposal problems such as waste management and landfilling. This research is presently in initial stages. Significant testing and development will be required for commercial-scale applications.

3. Concluding remarks

A brief review has been presented on recycling CFRPs, recovering carbon fibres as reusable products, degradation of fibre characteristics after mechanical, thermal and chemical

processing of waste. Significant success has been achieved using a wide variety of techniques depending on the nature/type of resin used, fibre precursors, manufacturing source and waste CFRP products being recycled. Commercial industrial scale recycling is not yet economically feasible in most cases. Utilisation of waste CFRPs as an alternate carbon resource in steelmaking is an emerging technology that could reduce the carbon footprint of the steel sector and help redirect this carbonaceous waste from landfills and associated economic and environmental impact.

Author details

Rita Khanna

Address all correspondence to: rita.khanna66@gmail.com

Centre for Sustainable Materials Research and Technology, School of Materials Science and Engineering, UNSW Australia, Sydney, NSW, Australia

References

[1] Goodship V, editor. Management, Recycling and Reuse of Waste Composites. Cambridge, England: Woodhead Publishing Co.; 2008

[2] Marsh G. Reclaiming value from post-use carbon composite. Reinforced Plastics. 2008; **52**:36-39

[3] Chawla KK. Composite Materials: Science and Engineering. New York: Springer-Verlag; 1998

[4] Kubota Y, Furuta T, Aoki T, Ishida Y, Ogasawara T, Yokota R. Long-term thermal stability of carbon fibre-reinforced addition-type polyimide composite in terms of compressive strength. Advanced Composite Materials. 2018. DOI: 10.1080/09243046.2018.1446124

[5] Recycling Carbon Fibres from the Composite Industry. 2005. Available from: http://www.jeccomposites.com/composites-news/1741/carbon-fibres.html

[6] Ribeiro JS, Oliveira Gomes J. Proposed framework for end-of-life aircraft recycling. Procedia CIRP. 2015;**26**:311-316

[7] Jacob A. Composites can be recycled. Reinforced Plastics. 2011;**55**:45-46

[8] McConnell VP. Launching the carbon fibre recycling industry. Reinforced Plastics. 2010; **54**:33-37

[9] Molnar A. Recycling advanced composites. Final Report for the Clean Washington Center (CWC). December 1995

[10] Oliveux G, Dandy LO, Leeke GA. Current status of recycling of fibre rein1forced polymers: Review of technologies, reuse and resulting properties. Progress in Materials Science. 2015;**2072**:61-99

[11] Palmer J, Savage L, Ghita OR, Evans KE. Sheet moulding compound (SMC) from carbon fibre recyclate. Composites Part A Applied Science Manufacturing. 2010;**41**:1232-1237

[12] Pickering SJ. Recycling technologies for thermoset composite materials – Current status. Composites Part A Applied Science and Manufacturing. 2006;**37**:1206-1215

[13] Schinner G, Brandt J, Richter H. Recycling carbon-fiber-reinforced thermoplastic composites. Journal of Thermoplastic Composite Materials. 1996;**9**:239-245

[14] Uhlmann E, Meier P. Carbon fibre recycling from milling dust for the application in short fibre reinforced thermoplastics. Procedia CIRP. 2017;**66**:277-282

[15] Meyer LO, Schulte K. CFRP-recycling following a pyrolysis route: Process optimization and potentials. Journal of Composite Materials. 2009;**43**:1121-1132

[16] López FA, Rodríguez O, Alguacil FJ, García-Díaz I, Centeno TA, García-Fierro J. Recovery of carbon fibres by the thermolysis and gasification of waste prepeg. Journal of Analytical Applied Pyrolysis. 2013;**104**:675-683

[17] Lester E, Kingman S, Wong KH, Chris R, Pickering S, Hilal N. Microwave heating as a means for carbon fibre recovery from polymer composites: A technical feasibility study. Material Research Bulletin. 2004;**39**:1549-1556

[18] Pimenta S, Pinho ST. Recycling carbon fibre reinforced polymers for structural applications: Technology review and market outlook. Waste Management. 2011;**31**:378-392

[19] Mansuri I, Khanna R, Sahajwalla V. Recycling carbonaceous industrial/commercial waste as a carbon resource in steelmaking. Steel Research International. 2017;**88**:1600333

[20] Markovic V, Marinkovic S. A study of pyrolysis of phenolic resin reinforced with carbon fibres and oxidized PAN fibres. Carbon. 1980;**18**:329-335

[21] Fromonteil C, Bardelle P, Cansell F. Hydrolysis and oxidation of an epoxy resin in sub- and supercritical water. Industrial Engineering Chemistry Research. 2000;**39**:922-925

[22] Iwaya T, Tokuno S, Sasaki M, Goto M, Shibata K. Recycling of fibre reinforced plastics using depolymerization by solvothermal reaction with catalyst. Journal of Materials Science. 2008;**43**:2452-2456

[23] Yang P, Zhou Q, Yuan XX, van Kasteren JMN, Wang YZ. Highly efficient solvolysis of epoxy resin using poly(ethylene glycol)/NaOH systems. Polymer Degradation Stability. 2012;**97**:1101-1106

[24] Wu BC, Klein MT, Sandler SI. Solvent effects on reactions in supercritical fluids. Industrial Engineering Chemistry Research. 1991;**30**:822-828

[25] Mansuri I. Recycling waste polymers as a source of carbon in steelmaking: Fundamental high temperature investigations on structure evolution and carbon dissolution into molten iron. [PhD thesis]. Sydney, Australia: University of New South Wales; 2015

[26] Huang X. Fabrication and properties of carbon fibers. Materials. 2009;**2**:2369-2403

[27] Sahajwalla V, Dubikova M, Khanna R. Reductant characterisation and selection: Implications for ferroalloys processing. Proceedings of 10th International Ferroalloys Congress. Capetown, South Africa: South African Institute of Mining and Metallurgy; 2004. p. 2

[28] Rahman M, Khanna R, Sahajwalla V, O'Kane P. The influence of ash impurities on interfacial reactions between carbonaceous materials and EAF slag at 1550°C. ISIJ International. 2009;**49**:329-336

Chapter 2

Functional Materials for Construction Application Based on Classical and Nano Composites: Production and Properties

Aleksandr Evhenovych Kolosov and
Elena Petryvna Kolosova

Additional information is available at the end of the chapter

http://dx.doi.org/10.5772/intechopen.73393

Abstract

At the present stage of polymeric material science, the physical and chemical modification of the surface of reinforcing fibers and liquid polymer binder is the basic direction in the development of functional polymeric composite materials (PCMs) for structural purposes. In this chapter, various aspects of the physical and chemical modification of the components of reactoplastic materials of structural design on the basis of classical and nano-modified (NM) PCMs are analyzed. The choice of the most effective types of carbon nanofillers for creating functional PCMs is exemplified by the example of carbon plastics. The main emphasis is made on ultrasonic processing as the dominant method of physical modification when obtaining PCMs. It is shown that such a physical modification is aimed at the intensification of many technological operations for the production of such materials, as well as at improving the physico-mechanical and operational characteristics of the resulting products and structures on their basis. The questions of designing the technological process for the production of functional classical and NM PCMs are briefly analyzed. The aspects of creation of NM carbonocomposites in which a continuous carbon fiber is combined with a binder in the volume of which the ultradisperse carbon nanoparticles are evenly distributed are considered. The prospects of production of functional hybrid PCMs based on reinforcing fabric with NM filler are shown. Features of obtaining functional NM carbono-composites with improved physico-mechanical and operational properties, in particular, with increased strength, electrical conductivity and crack resistance are described.

Keywords: reactoplast, functionality, production, carbon, nanotube, modification, hybrid, strength, electrical conductivity, crack resistance

1. Introduction

Polymeric composite materials (PCMs), combining low density, high elasticity modulus and strength, are now widely used in various fields of industry: aircraft building, automotive industry, construction, sports industry, medicine, etc. Modification of the surface of the reinforcing fiber and liquid polymer binder (PB) to improve the physico-mechanical and operational properties of the resulting classical PCMs and nano-modified (NM) PCMs is an actual task of polymer materials science [1, 2].

This task is realized both as a complex as well as separately by various methods of modification: physical—in the form of ultrasonic (US), chemical and combined physical and chemical. The aspects of designing the technological process for the production of functional classical PCMs and NMPCMs of structural design on the basis of reactoplastics are no less relevant [3]. Moreover, exactly US treatment is the dominant method of physical modification, which is simultaneously aimed at the intensification of many technological operations for the production of such materials, as well as improving the physico-mechanical and operational characteristics of the products and structures obtained [4].

A number of studies are devoted to the issues of preparation, enhancement of physico-mechanical and operational properties and features of the use of functional reactoplastic NMPCMs. In particular, the directions in which NMPCMs production technology is developing, including economic aspects of implementing their formation nanotechnologies, were described [5]. Among a wide range of means used to produce NMPCMs, it is preferable to use technical means implementing the method of low-frequency US cavitation [6]. The advisability of such choice is primarily due to the need for a uniform (homogeneous) distribution of nanoparticles introduced into the liquid oligomer. At the same time, this process is actively hampered by the physico-chemical nature of the nanoparticles, which are characterized by high surface energy.

This, in turn, causes the mutual attraction of nanoparticles, which leads to their coalescence and aggregation upon incorporation into the liquid oligomer. It was shown that the conditions necessary to create functional nanomaterials are small size and a distribution of carbon nanofiller particles as uniform as possible in the liquid polymeric matrix [7]. The efficiency of introducing the nanoparticles into the liquid polymer medium depends on not only the dose but also the mixing parameters [8].

One of the options for improving the physical and mechanical properties of carbon PCMs is the creation of carbon plastics combined filling [9]. This is accomplished by modifying the surface of a continuous carbon fiber and a liquid PB. The chemical modification of the last one is carried out by incorporating and subsequent uniform distribution in the bulk of the liquid PB of ultradispersed carbon nanoparticles. As the latter, for example, fullerenes, astralenes, CNTs and others are used.

Thus, the above brief analysis shows that the most relevant areas of research in the field of polymer nanotechnology in relation to functional nanocomposites are, in particular, the following:

- selection of the most effective types of carbon nanofillers for the development of functional PCMs using the example of carbon plastics;
- determination of the optimal concentration of nanoparticles in the polymeric matrix;
- choice of effective methods for dispersing nanofillers during the production of functional NMPCMs based on reactoplastics;
- creation of carbon plastics combined filling;
- production of functional hybrid PCMs (HPCMs) based on reinforcing fabric with NM filler;
- production of functional NM carbonic composites with increased electrical conductivity and crack resistance.

The above aspects are briefly presented in this chapter.

2. Effective methods and means of physical modification

2.1. The method of ultrasonic modification of liquid polymeric media

As the dominant method of physical modification of liquid polymer media and reinforced classical PCMs and NMPSMs of functional purpose, US low-frequency cavitation is used in most cases. The main parameters of this action are the frequency, amplitude, intensity, pressure, temperature and volume of the liquid medium (PB) being treated. The set of interdependent optimal parameters of cavitation processing, as a rule, is set experimentally in each specific case.

In the optimum, the resulting set of parameters of US cavitation processing leads to an increase in the physico-mechanical and operational properties of solidified oligomers and reinforced PCMs based on them [10]. The amount of hardening depends on the particular type of oligomer to be processed and can vary from 40 to 50% for classical hardened reactoplastics or may increase for several times (depending on the type of nano-modifier used) as compared to the initial composite for NMPCMs [8, 11].

The influence of the developed modes of low-frequency US cavitation treatment on the operational properties of reactoplastic PCMs was investigated in comparison with the known methods. An effective range of interrelated processing parameters has been found [11]. The obtained experimental results confirmed the prospects of realization of such a modification of liquid oligomers by the example of epoxy oligomers (EOs) and epoxy compositions (ECs).

It was found that such a modification is effective not only in the low-frequency, but also in the mid-frequency US ranges, both individually and in combination [12]. Variable overpressure during the US treatment is also a promising method. In particular, this is confirmed by the results of molding epoxy couplings with shape memory effect. An increase in intensity and a reduction in time was also established, both for a separate operation of sonification the liquid polymeric composition and for the manufacture of the entire product as a whole [13].

2.2. Ultrasonic modification during production of reinforced polymeric composites

The purpose of using US modification of reinforced PCMs is to achieve a range of positive results upon completion of such a modification.

The first positive result is the US activation of the surface and the structure of the reinforcing fibrous macrofiller to improve its wettability of the liquid EC. The second positive result is the degassing of the structure of the reinforcing macrofiller immediately before it is impregnated. The third positive result is an increase in the productivity (not less than 2–2.5 times) of operations of sonification, impregnation, dosed application of liquid EC and winding while maintaining the stability of the properties of the final PCM.

Another positive result is the stabilization of the content of the PB in the impregnated woven filler, with variation in the speed of its stretching in the impregnation and dosing operations [14]. Finally, the effective parameters of US treatment contribute to increasing the deformation-strength and adhesion characteristics of PCMs, to lower the level of residual stresses, to increase the durability and to reduce the cumulative hardening time [15].

As a result of practical use of the methods of US cavitation processing, the designs of the impregnation, dosing and winding units on the serial impregnating and drying equipment were improved. The above mentioned results once again confirm the choice of US treatment as the main method of physical modification of liquid (including polymeric) media and reinforced fibrous PCMs of functional purpose at the main stages of their production.

Despite the existence of a huge range of US cavitation processing tools, the technical means used for US modification of liquid polymeric media and reinforcing fillers based on them can be conditionally divided into US concentrators, speed transformers and radiating plates.

US concentrators (dispersants) are effectively used primarily for processing liquid polymeric media, including when nanomodifiers are introduced into them. Radiation plates are used mainly for processing impregnated woven fibrous fillers up to 2000 mm wide.

Despite on the difference in the objects of application, for both of the above mentioned types of US technical means it is necessary to determine the effective design and technological parameters [16]. Otherwise, the appearance of defective areas of the resulting final PCMs (both classical and NM) is possible.

In this case, during the treatment of impregnated tissue, the US cavitators are based on piezoceramic transducers with a radiating plate that undergoes bending vibrations [17]. In addition, it is necessary to eliminate the non-uniformity of bending vibrations of radiating rectangular plates by calculation-experimental methods [16, 17]. Otherwise, there is a high probability of obtaining defective PCMs.

2.3. Designing the technological process of ultrasonic production of polymeric composites

The tasks of designing the technology and equipment for the production of classical PCMs and NM functional PCMs are aimed at identifying and studying the interrelations between

the structural, mechanical and geometric parameters of products, on the one hand, and the technological factors of their production, on the other. For example, obtained analytically kinetic equations of longitudinal and transverse impregnation of oriented and woven fibrous fillers with liquid PBs make it possible to predict the impregnation time and the speed of broaching the fibrous filler through the impregnating bath, and also to design its dimensions [18]. Design of the optimal tension force of impregnated fibrous fillers in circumferential winding allows the study of experimental results on the influence of technological impregnation regimes on the strength of impregnated and cured fibrous fillers [19, 20].

Moreover, in order to minimize material and time costs, as a rule, the methodology of structural and parametric modeling of design and technological parameters of technology and equipment (tools) for sonification of liquid polymeric media and for producing reactoplastic PCMs is used [3]. In turn, the geometric parameters of the model of oriented classical PCMs, which are considered as structurally inhomogeneous media, are the basis for designing technological manufacturing parameters and predicting the stress-strain state of solidified classical PCMs [21–23]. **Figure 1** shows an innovative scheme for producing of unidirectional reactoplastic classical PCMs and NMPCMs for functional purposes using low-frequency US treatment.

For example, the investigated traditional structural scheme for impregnation and dosing of a polymer (epoxy) binder on a long fibrous filler using US modification (**Figure 1**) can be conveniently divided into such separate structured blocks: I—the block for sonification the EO and preparing an impregnation EC based on it; II—the block of "free" impregnation of oriented (woven) fibrous filler with liquid EC; III—the block of dosed application of liquid EC to impregnated fibrous filler.

The main stages of innovative production of unidirectional reactoplastic PCMs for functional purposes using US are as follows (**Figure 1**). Prior to the impregnation step, US treatment of the epoxy resin in reservoir 17 is carried out using an US concentrator 16. The US concentrator 16 is connected to a magnetostrictive transducer 15, which is powered by an US generator 14 (block I in **Figure 1**). Depending on the selected geometry of the US concentrator 16, a certain value of the amplitude A and intensity I_o of the US vibrations introduced into the liquid epoxy resin is obtained at the output. In the case of preparing a NM EC, for example, CNTs are added thereto. Controlled parameters of US processing are: time τ, temperature T, amplitude A and intensity I_o.

After US treatment of the epoxy resin, a hardener of epoxy resin enters the reservoir 17 from reservoir 18. Here, the epoxy resin is mixed with its hardener with the same US concentrator for a few seconds, resulting in an impregnating composition. Next, the tap 19 is opened and the impregnating composition is fed to the bath 1. After this, the dry long fibrous material 4 is rolled up from the bobbin 5, which, after passing the enveloping roll 6, enters the bath 1, where it is impregnated with the liquid PB 2, which has already been treated with US (block II in **Figure 1**). In this case, several structural forms of the placement of long fibers in the cross section of the impregnated filler, which affect the kinetics of the impregnation process, are possible.

After exiting the impregnation bath 1, a preliminary uncontrolled application of the PB 2 to the long fibrous material 4 is provided. This material in the dosing zone (block III in **Figure 1**)

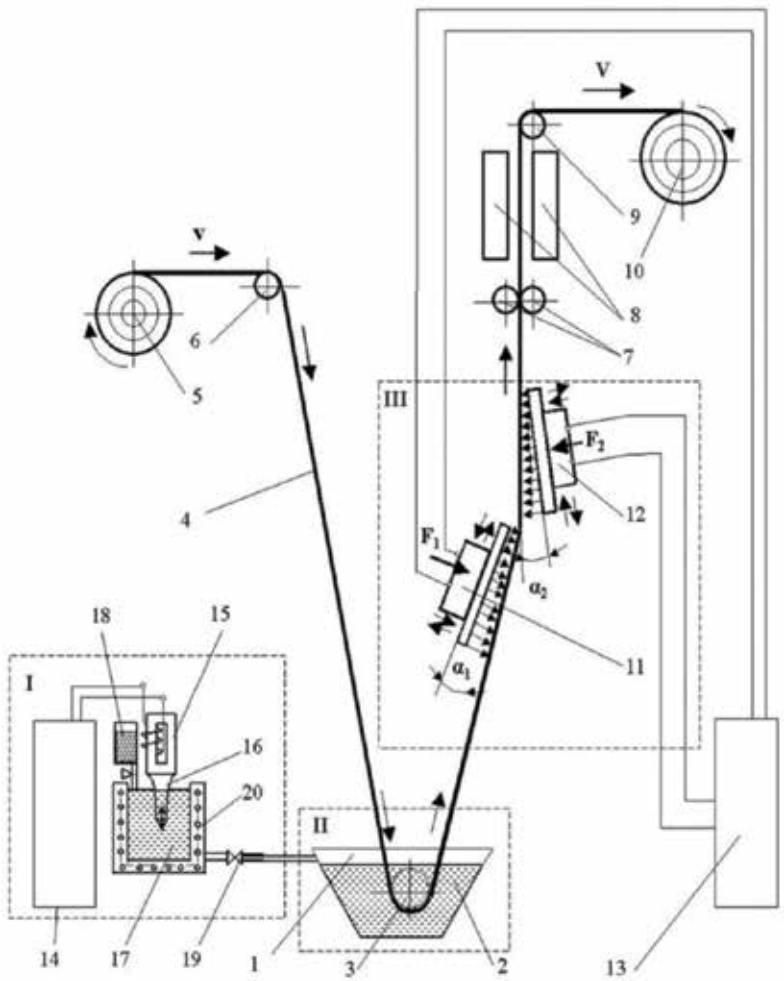

Figure 1. Scheme of impregnation and dosed deposition of PB on long-length fibrous material: 1—impregnating bath; 2—liquid PB; 3—envelope roll in impregnating bath; 4—long-measuring fibrous material; 5—bobbin with a dry fibrous material; 6, 9—enveloping rollers; 7—squeezing rollers; 8—drying chamber; 10—take-up bobbin; 11, 12—a pair of working US instruments (emitting US plates); 13, 14—US generators; 15—magnetostrictive transducer; 16—waveguide-concentrator US; 17—reservoir with epoxy resin; 18—reservoir with curing agent of epoxy resin; 19—the tap; 20—thermoregulating cell; F_1 and F_2 are the forces of pressing working tools 11 and 12 against the impregnated fibrous material; α_1 and α_2 are the slopes of the working tools 11 and 12 to the surface of the impregnated fibrous material; v—broaching speed.

is processed on both sides by US instruments in the form of US rectangular plates 11 and 12 emitting US having individual drives from the US generator 13. These plates 11 and 12 contact the material 4, which was impregnated and processed by the edge of the plate edge, with varying pressing forces F_1 and F_2, respectively. The US vibrations propagate both along the width and along the length of the plates 11 and 12. Moreover, the tools 11 and 12 are disposed with respect to each other along the length of the material 4, processed on both sides relative to it, and at different angles of inclination α_1 and α_2 to the plane of the material.

In turn, working US instruments 11 and 12 consist of several successively located structural elements of various shapes and sizes made of different materials.

Varying the content of the PB, uniformity of its distribution in the material, and removal of the excess PB are achieved by adjusting the angle of inclination α_1 and α_2 of the radiating plate to the surface of the material 4, by varying the power (intensity I_1 and I_2) applied to the transducers, and by dosing the pressing forces F_1 and F_2. The final spinning of the PB from the impregnated material is carried out by a means of squeezing the material made in the form of two rolls 7. The impregnated and squeezed material then enters the drying chamber 8, and after drying passes through the envelope roller 9 and is wound onto the take-up reel 10. When using the developed innovative technology and equipment, the dependence of the deposit on the speed of drawing the impregnated material is largely eliminated, as well as the degassing of the air from the structure of the impregnated material due to the contact US action.

Then, within the synthesis framework, only the above mentioned enlarged blocks I–III and their constituent structural elements are analyzed, as well as structural and technological interrelations between them. Implementation of the developed approaches to the use of effective US devices allows obtaining a wide range of practically defect-free classical PCMs and NM PCMs for functional purposes. Effective hardware for connection and repair of polyethylene pipelines using US modification and heat shrinking are studied in [24–28]. The epoxy-glue compositions and banding, fiberglass tape impregnated with epoxy compositions, thermistor couplings with shape memory and surface-treatment methods for polyethylene pipes are investigated. The results obtained in these studies are another example of the creation of functional materials for construction application based on classical reactoplastics and thermoplastics used in gas-pipeline repair.

3. Functionality of carbon plastics based on reactoplasts

A set of specific requirements to the constructional materials based on PCMs, which are used in highly loaded structural elements, are set [29, 30]. Among them are the simultaneous provision of high strength and rigidity; resistance to alternating dynamic loads; small mass; high long-term strength. No less important indicators are heat resistance and corrosion resistance, while ensuring a high degree of reliability of the designed construction as a whole. The above complex of requirements is satisfied, for example, by classical and NM PCMs in the form of carbon plastics based on thermoset (epoxy) matrices [31, 32].

For example, the spectrum of application of NMPCMs based on carbon fibers and HD modified with nanoparticles (CNTs) is highly loaded materials, products and structures intended primarily for use in chemical, shipbuilding, machine, engineering, building, aviation, rocket and aerospace and other industries [33–36]. The advantage of using carbon plastics in comparison with traditionally used metals, fiberglass and organic fibers, is that it provides increased compressive strength, high elasticity modulus and fatigue strength, low creep and dimensional stability of the molded article due to the low temperature coefficient of linear expansion. Not less important advantages are high indicators of chemical and radiation resistance,

as well as good workability (manufacturability) [37]. The above mentioned set of advantages also determines the advisability of processing carbon plastics on serial production equipment at low labor and energy costs.

It should be noted that in the CIS countries, a wide range of unidirectional structural carbon plastics for functional purposes was created (**Table 1**) [9, 31, 32].

In the CIS countries, aircraft component parts and units are usually manufactured by an autoclave solvent polymer impregnation processing technique [38]. However, foreign companies usually use nonsolvent processing technique. Molding without autoclave (e.g. infusion molding or vacuum and pressure impregnation) sufficiently decreases the PCM production costs.

In the reinforcement plane, the properties of the PCMs are determined mainly by the properties of the reinforcing material. And in the perpendicular plane, the properties of the PCM are largely limited by the strength characteristics of the PB and the adhesion value between the PB and the reinforcing filler. This often leads to the destruction crack initiation and propagation in the interlayer space of PCM under the influence of normal and tangential loads arising during the operation of products.

The growth of such cracks under the action of alternating, static and shock loads leads to a catastrophic destruction of PCM components. Therefore, the low impact strength of carbon composites significantly reduces the area of their possible application. The standard method for increasing the crack resistance is to introduce a thermoplastic polymer into the epoxide matrix which is soluble in it, for example, a polysulfone, whose concentration exceeds 20%

Physico-mechanical properties	**Structural carbon-fiber brand**					
	KMU-11 m	**KMU-31n**	**KMU-41**	**KMU-4e**	**KMU-5e**	**KMU-6-36**
Tensile strength $\sigma_t \cdot 10^{-1}$, MPa	80	75	70	100	80	70
Compression strength $\sigma_{cs} \cdot 10^{-1}$, MPa	60	60	60	100	80	70
Shear strength $\tau_s \cdot 10^{-1}$, MPa	5.9	5.5	5.5	8.0	6.0	5.7
Elasticity modulus $E \cdot 10^{-1}$, MPa	14,500	15,000	14,000	12,000	12,000	12,500
Fatigue strength $\sigma_{-1} \cdot 10^{-1}$ based on $I0^7$ cycles, MPa	50	45	50	70	55	50
Stress coefficient $K_{1c} \cdot 10^{-1}/0.31$, MN·m$^{3/2}$	—	68	126	—	—	94
Maximum operating temperature, °C	180	100	150	150	80	150

Table 1. The nomenclature of unidirectional carbon-fiber plastics for functional purpose [9, 31, 32].

(by weight) [38]. At the same time, the viscosity of the PB becomes extremely high, which makes this method unacceptable for the manufacture of PCM by infusion methods.

Especially emphasized should be the promising constructional NM carbon composite of brand VKU-18tr [39]. It is produced on the basis of the polymeric binding grade ENFB-2 M, an equiprobable fabric of Porcher Ind. (art. 3692). Nanoparticles of astralene of NTS brand in the amount of 0.5% of the mass fraction of the cured polymer matrix are used as the nanomodifier of the liquid PB. Carbon plastic of the brand VKU-18tr was compared with its closest analog in the form of carbon-plastic KMU-4-2 m-3692, obtained on the basis of the same components, but without the astralean nanoparticles.

The results of comparative tests of these carbon plastics are given in **Table 2**.

The results of **Table 2** indicate that the VKU-18tr NM carbon plastic surpasses the number of operating parameters of its analog material, for example, strength, including at higher temperatures. So, for example, at a temperature of 170°C, the strength of the VKU-18tr NM carbon plastic produced by compression is 54% higher. With an interlayer shifting, this excess is 32%, and with a bending, 20%. The same trend is observed with an increase in temperature: hardening at room temperature is from 10 to 15%, and at a temperature of 170°C it increases to 30–50%. Even more, as the temperature rises, the strength of the VKU-18tr NM carbon plastics increases under compression.

Property	**Reinforcement direction**	**Material**		**Improvement of carbon nanofiber properties, %**
		Carbon-fiber plastic VKU-18tr	**Carbon-fiber plastic KMU-4-2M-3692**	
Tensile strength, MPa	[0°]	780	750	4
	[90°]	600	550	8
	[0°, 90°, ±45°]	640	490	23
Tensile elasticity modulus, GPa	[0°]	65.4	64	—
	[0°, 90°, ±45°]	55.5	45	—
Shear strength, MPa	[0°]	768	700	10
	[90°]	660	600	10
	[0°, 90°, ±45°]	450	405	11
Interlayer shear strength, MPa	[0°]	46	42	10
Shear strength in sheet plane, MPa	[±45°]	93	82	13
Operating temperature, °C	—	170	120	42
Tropical stability after exposure in a tropical chamber for 3 mo., percent retention of compression properties	[0°, 90°, ±45°]	96	55	41

Table 2. Several parameters of VKU-18tr and KMU-4-2 M-3692NM carbon plastics for functional purpose [9, 39].

The above confirms the urgency of developing new, cost-effective and technologically advantageous methods for modifying the surface of carbon fiber and liquid PB. The ultimate goal of such a modification is to improve the physico-mechanical and operational properties of carbon composites.

4. Production of functional hybrid polymeric composite materials

One of the promising directions for improving the physico-mechanical and operational characteristics of elements of load-bearing unit made from reinforced reactoplastic PCMs is the creation of functional reactoplastic hybrid NMPCMs (HNMPCMs). The latter are obtained by incorporating nanoparticles into the structure of a liquid polymeric matrix and a reinforcing macrofiller [40, 41]. In investigations it was established that the nanomodification of the liquid PB, carried out with the help of optimal US action prior to impregnation of the reinforcing macronutrient, improves the processability of the PB and the strength of the solidified polymeric matrix [7, 37].

This, in turn, favorably affects on the hardening of the obtained NMPCMs, especially under the action of tensile loads [9]. At the same time, the nanomodification of only the liquid polymeric matrix does not have a significant effect on the strength characteristics of the PCM structural elements, the functional purpose of which is mainly in the perception of external force loads. This can be explained by the fact that when impregnating the reinforcing strands of the macrofiller with the NM liquid polymer matrix, the nanoparticles do not enter the interfiber space of the reinforcing macrofillers and filtering out on their boundaries.

Figure 2 shows a structural model of a functional HNMPCM, the reinforcing fabric of which contains fibers coated with CNTs [40]. The connection of CNTs grown on the surface of each individual fiber during interaction between parallel reinforcing fibers and transverse layers of reinforcing fabric is shown.

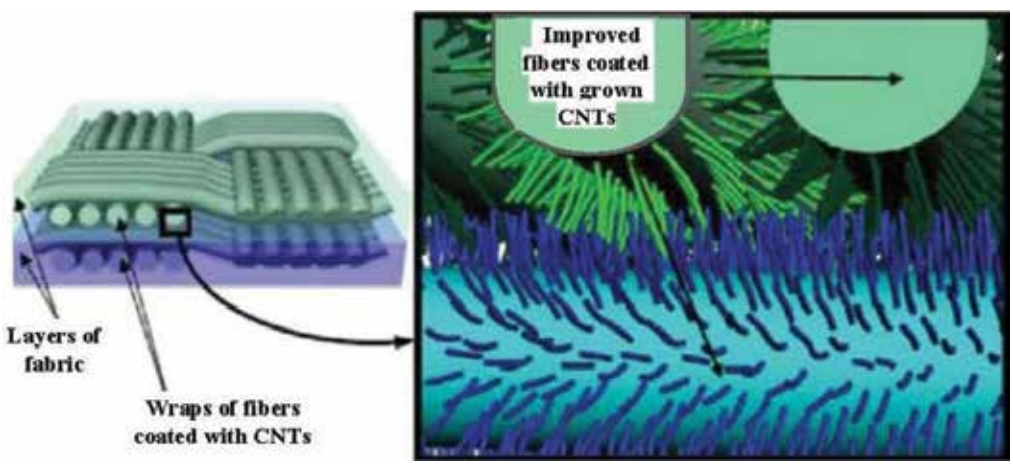

Figure 2. Scheme of a functional hybrid nanocomposite with grown CNTs on monofilaments [40].

4.1. Synthesis of carbon nanotubes on reinforcing macrofibers

The search for new efficient technologies has already led to original methods. One of them is growing of CNTs on monofilaments of reinforcing fabrics (**Figure 3**).

With this method, the classical technology of manufacturing composite products [40], practically is not changed, which is an undoubted advantage of the developed technology [41]. The principal possibility of growing CNTs on reinforcing fibers before their subsequent impregnation with a liquid PB was investigated. For the study, dry fiberglass and dry twill rope twill weave were used (type Twill of the brand: 3k, 2 × 2 Twill Weave Carbon Fiber Fabric, 5.7 Oz/Sq Yd, 50″ wide, .012″ thick and 3k, 2 × 2 Twill Weave). In **Figure 3a** and **b** shows the surface of the fiber before and after application of CNTs.

Growth of CNTs on carbon fibers was carried out by pyrolysis of gases (CVD process) [41]. The length of CNTs, as a rule, was much greater than the distance between the layers of tissue (~10 μm) and between the fibers in strands (~1–5 μm). CNTs grown on fiber reinforcing fibers were studied using a scanning electron microscope (SEM). It was found that the CNT grew uniformly and densely in the radial direction on the surface of each individual fiber in the reinforcing fabric (**Figure 3b**).

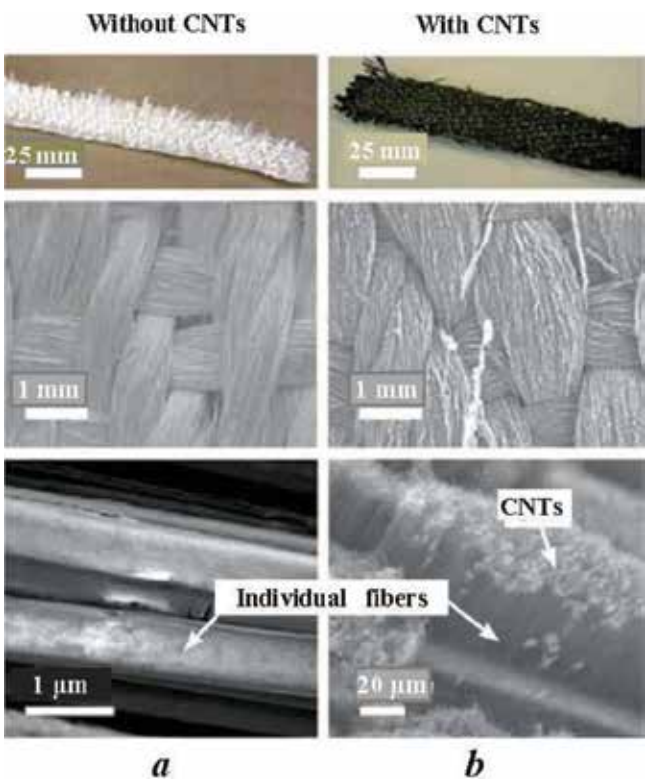

Figure 3. SEM image of glass fabrics and carbon fabrics used in laminate production [40]: a—without CNT; b—with CNTs grown along the radius on the surface of the fiber, as well as individual fibers coated with CNTs; resolution on the lower images of a and b ~20 μm.

Morphology (uniformity of growth, distribution along the fiber and throughout the laminate), the diameter of CNTs and the uniformity of their distribution were evaluated using a transmission electron microscope (TEM). The TEM analysis of multilayer photos showed that CNTs grown on fiber reinforcing fibers have an outer diameter of ~17 ± 2 nm and eight concentric layers (**Figure 4**).

As a result of impregnation with a polyester binder reinforcing NM fabric, a new structure is obtained—a HNMPCM, where nanoadditives are present not only in the polymeric matrix, but also in fibers. It is called free reinforced plastic (FFRP). When studying the wettability of CNTs with a reactoplastic polyester adhesive, it was found that CNTs are easily impregnated with such binding capillary method (free impregnation method) [41]. Improved adhesion between CNTs and reactoplastic material creates a strong functional nanocomposite for power purposes. Thus, due to the synthesis of CNTs directly on macrofibers, the solidified polymer fixes uniformly distributed CNTs on the surface of dry macrofibers, creating a functional nanocomposite of increased strength (the shear strength of HNMPCMs based on the polyester matrix increased by 60%).

It is known that one of the main problems during the process of making samples was the impregnation by PB of reinforcing woven layers, which contain single CNTs. Images obtained from optical and scanning electron microscopes demonstrate the presence of CNTs throughout the entire laminate section and the absence of differences between laminates with and without CNTs (**Figure 5**).

The PB under impregnation under the influence of vacuum completely impregnated all reinforcing macrofibers together with CNTs. The sections of the laminate without CNTs (**Figure 5c**) and with CNTs (**Figure 5d**) at the same scale indicate a qualitative structure and a uniform impregnation of the hybrid layers with a PB. This is confirmed by the absence of voids in the structure and the quasiregular distribution of the fibers after vacuum impregnation.

At the same time, the distance between macrofibers in the HNMPCM is slightly larger than in the base sample due to the expansion of the fibers by growing CNTs. Thus, the creation and

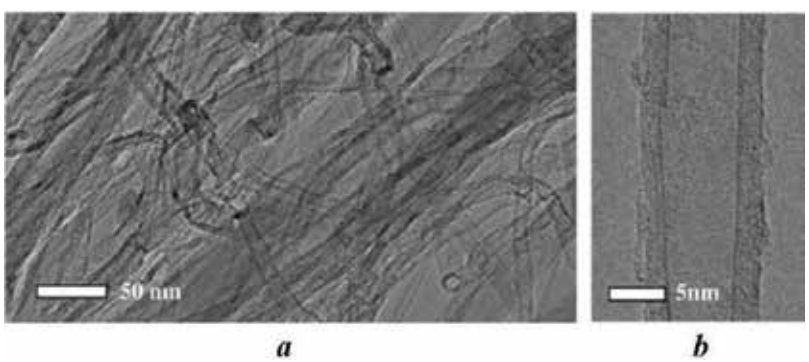

Figure 4. TEM images of CNTs grown on a carbon fiber with a low (a) image resolution and a single high-resolution CNT (b) (concentric layers in the CNT structure are shown) [41].

http://dx.doi.org/10.5772/intechopen.73393

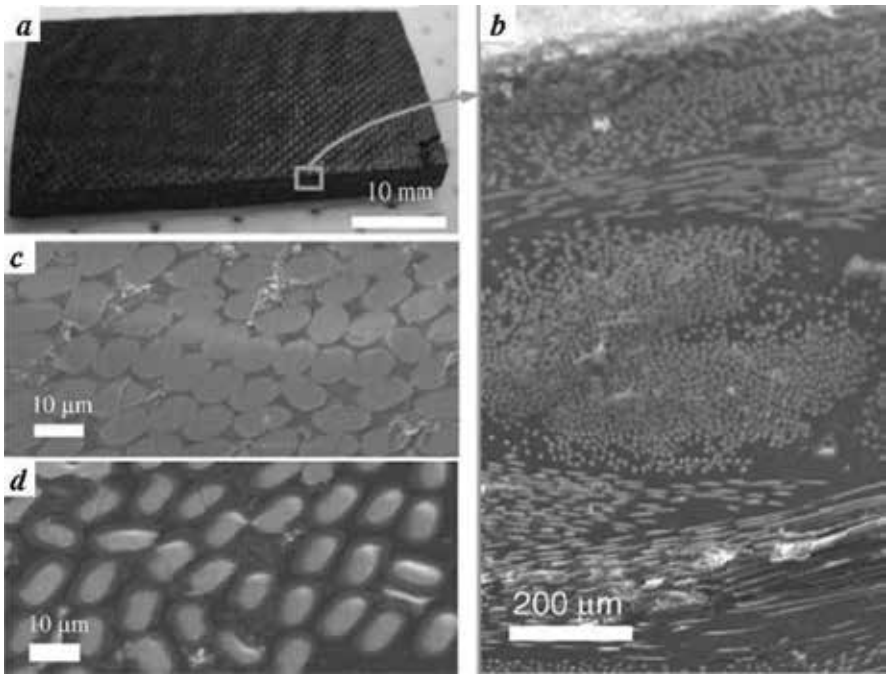

Figure 5. Hybrid composite samples based on a nanocomposite with a CNT content of 0.2% [41]: a—three-layer laminate after trimming; b—SEM image of intersecting tissue layers impregnated with a nanocomposite binder; c—SEM image of the section of composites without CNTs; d—cross section of reinforced CNT hybrid NMPCMs.

study of functional HNMPCMs has shown that the application of the method of gas-phase growth of CNTs ensures their uniform distribution on reinforcing macrofibers of the filler, and vacuum impregnation with a PB reliably binds CNTs with reinforcing macrofibers.

5. Production of functional nano-modified carbonocomposites with crack resistance

In the past 10 years in the CIS countries the possibility of using CNTs for additional reinforcement of PCM has been intensively studied. As a result of these studies, HNMPCMs are created, in which CNTs are contained along with a reinforcing macrofiller, carbon or glass fiber [33, 42]. These studies provide the basis for the creation of functional NM carbonocomposites with increased crack resistance. According to the data of the studies of a number of investigators, CNTs exert maximum influence on the value of the ultimate strength at interlayer shear and the fracture toughness of reinforced PCMs [43–45].

At the same time, the characteristics of PCM, which depend on the properties of the reinforcing filler (elasticity modulus and tensile strength), change slightly. Still, it should be noted that the results of the study of the effect of CNTs on the crack resistance of the HNMPCMs, obtained by various authors, differ significantly. The use of PB modified by CNTs in the

composition of the HNMPCM allows increasing the crack resistance coefficients G_{1c} and G_{2c} by an average of 15–40% [46–49]. At the same time, it is possible to obtain an increase in the crack resistance coefficient up to 120–180% if a thermoplastic polymer is incorporated into the PB together with the CNTs, which acts as a non-covalent CNT modifier [50, 51].

When using films based on a partially cured EC filled with CNT [40], or a mixture of CNT and thermoplastic polymer [52, 53], it is possible to increase the coefficient of crack resistance by 2–3 times. The resulting films were placed between the layers of the reinforcing filler. In addition, the crack resistance is affected by the method of obtaining HNMPCM [52]. In the first embodiment, the nanofiller was functionalized with silane groups. Before the winding on the reinforcing fiberglass, a PB (EC) modified with short CNTs and nanofibers was applied, after which the coefficient of crack resistance of the obtained monolithic HNMPCM sample was determined.

In the second variant of the winding, two separate plates were made on the basis of a modified PB, which were then glued together with a PB containing a functionalized nanofiller. The crack propagated along the gluing layer. Despite the practically identical composition of the modified binder, in the first case the crack resistance coefficients in the reinforcement direction G_{1c} and in the perpendicular direction G_{2c} increased by 5–14% compared to the initial values (monolithic plate based on the unmodified PB), and in the second by 79–109%, respectively. The influence of the degree of aggregation of CNTs and the type of functional groups covalently attached to their surface on the crack resistance of HNMPCM obtained by the vacuum forming method was investigated [38]. A binder based on an epoxy amine resin and an amine curing agent was used.

To regulate the rheological properties of the binder, an unsaturated polyester resin modifier and a radical polymerization initiator was used. The modification of the chemical structure occurred according to the type of interpenetrating polymer networks. The method of preparation of the concentrate (1.5% by weight) of CNTs "Taunit-M", covalently functionalized with carboxyl (CNT-COOH) and amide groups (CNT-CONH2) in the epoxy amine oligomer, is described by [54]. Four types of concentrates of functionalized CNTs (COOH-1, COOH-2, $CONH_2$-1 and $CONH_2$-2) were used in the epoxy amine resin, which differed in the types of functional groups and the degree of aggregate dispersion. The aggregate size in concentrates COOH-2 and $CONH_2$-2 was 3–20 μm, and in concentrates COOH-1 and $CONH_2$-1 does not exceed 3–5 μm. As the reinforcing filler, a uniform fabric firm Toray was used: weav-twill, thickness of the bundle 3k (3000 filaments).

Six layers of filler were used to assemble the pack, each of which was applied with a previously prepared binder in equal proportions in such a way that its mass fraction in the finished cured sample was 36–40%. It was found that the modification of the epoxy binder by carboxylated and amidated nanotubes leads to a decrease in the glass transition temperature T_g (maximum of 8°C). And with an increase in the degree of aggregation, the difference between the glass transition temperatures T_g in the modified functionalized CNT (FCNT) and the control sample decreases. The maximum hardening of the modified epoxy binder was 20%. The use of a binder modified with well-dispersed carboxylated nanotubes makes it possible to increase the value of the energy of interlayer destruction of carbon-plastic G_{IR} by 63% as compared to the initial sample. The likely reason for the increase in G_{IR} is the change in the propagation path of the crack in the modified FCNT samples from the HPCM.

For HNMPCMs prepared using a binder with uniformly distributed CNTs functionalized with amide groups, an increase in the G_{IR} value compared to the starting plastic is 41%. Aggregation of carboxylated FCNT leads to a decrease in the effect—an increase in the G_{IR} value is only 17%. **Figure 6** shows the results of a fractographic study of the surface of the HNMPCM after separation of the sample with a COOH-1 concentrator and a sample of reinforced plastic made using a SEM at various magnifications.

As can be seen from **Figure 6**, on a scale of up to 10 μm, the pattern of destruction of the initial and modified sample is practically the same. However, on a larger scale, there are significant differences: a large number of "pyramidal" formations are observed on the surface of a modified sample with FCNTs. In addition, the number of fibers destroyed during the stratification of the sample increases. It was found that when modifying the epoxy binders of the FCNT, the values of the elasticity modulus E and the tensile strength σ_t of the HNMPCM decrease on average by 35 and 25%, respectively. This is explained by a decrease in the volume fraction of the reinforcing fiber in the samples of HNMPCM (an average of 20%) compared to the control sample.

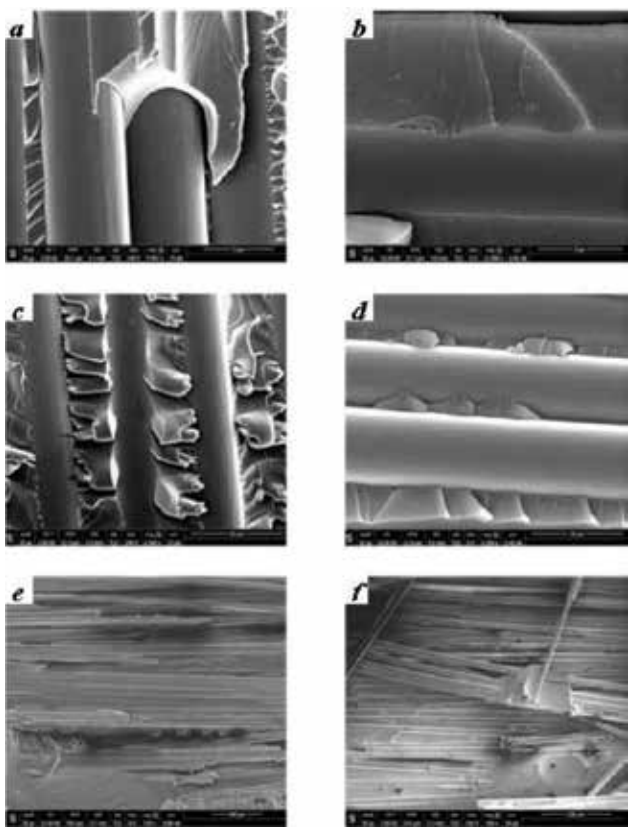

Figure 6. Results of fractographic investigation of the surface of the HNMPCM after separation, obtained with the help of SEM [38]: a, c, and e—control sample; b, d, and f—sample of HNMPCM with COOH-1 concentrate.

6. Production of structural electro conductive polymeric composites

In recent years, the efforts of researchers in the field of polymer nanotechnology are concentrated in the direction of the creation of functional constructional PCMs of a new type. In such PCMs, the CNTs themselves are used as the reinforcing element. In particular, one of the most important functions of such PCMs is a high level of electrical conductivity [55]. So, it is shown that the conductivity of the CNT-filled composites depends not only on CNTs type, concentration and polymer matrix composition, but also on the nanocomposite production method.

For example, for materials that can be manufactured by pressure die casting methods, the task of creating nanocomposites that combine a high level of functional and physico-mechanical properties can be solved by using multiphase polymer matrices and extruders. This is necessary to ensure a high level of shear stresses. In particular, the authors of the paper used the following method [56]. An array of vertically oriented CNTs that were grown on an alumina substrate was sheared off the substrate and then compressed in a direction perpendicular to the CNT orientation axis. Then the resulting deformed nanofiller was impregnated with ECs, which are used for the manufacture of PCM and cured.

It is shown that the electrical conductivity of such a deformed nanocomposite in the CNT orientation direction is 10 Sm/cm at a CNT concentration of about 6%. Other authors reached significantly larger values of the electro-physical and physico-mechanical characteristics [57]. In contrast to the method described in [56], they stretched an array of vertically oriented CNTs in a direction perpendicular to their growth. The resulting stretched sheets were impregnated with an EC by vacuum infusion. For PCM, obtained on the basis of 1750 stretched sheets oriented in mutually perpendicular directions, the following physico-mechanical and operational (electrical conductivity) characteristics were obtained: tensile strength of 117 MPa, elasticity modulus of 7.45 GPa, electrical conductivity of 2205 Sm/cm at concentration of CNTs at the level of 8%.

Other researchers demonstrated a different way of obtaining PCM with a high level of functional and physico-mechanical properties [58, 59]. It is declared that this method can be used in the future for large-scale industrial production. According to this method, an array of vertically grown CNTs (7–9 nm in size) was subjected to orientational stretching and impregnation with a solution of bismaleinimide resin (**Figure 7**).

The complex filament was collected by successively stacking several layers of oriented and impregnated nanotubes. From the obtained filaments, a prepreg was prepared, which was then pressed (the proportion of PCM being 50–55%).

Figure 8 shows a comparison of the dependence of the tensile strength of PCM on its elasticity modulus for materials reinforced with standard carbon fibers and CNTs.

□—high-strength plastics; ■—high-modulus plastics; •—developed plastics.

It was studied that such HNMPCMs due to the use of CNT as a reinforcing filler are characterized by a complex of high functional characteristics. In particular, the tensile strength is 3.8 GPa, elasticity modulus of 293 GPa and the electrical conductivity reaches 1230 Sm/cm. At

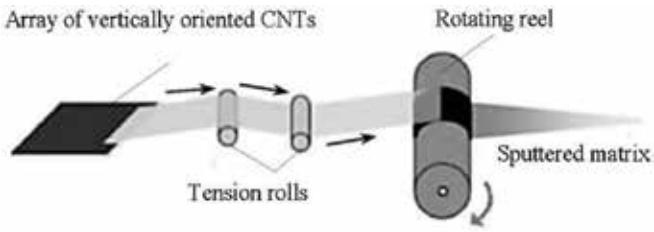

Figure 7. Scheme of the technological process of obtaining a complex filament from the CNT's array [58].

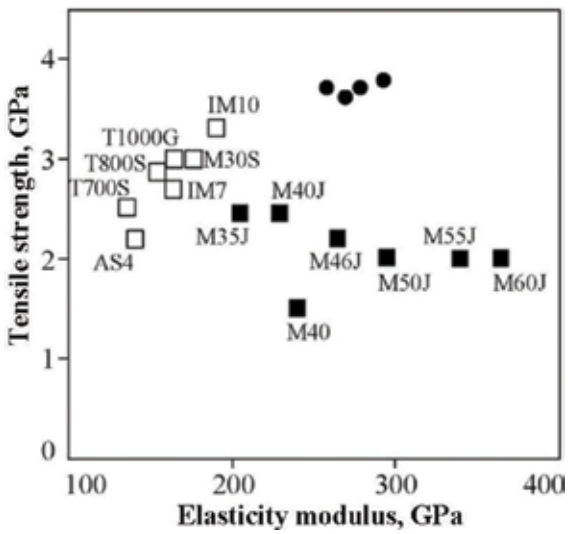

Figure 8. Comparative dependence of the tensile strength on the value of the elasticity modulus for materials reinforced with standard carbon fibers and CNTs [58].

the same time, during the production of such materials, it is advisable to use extruders in point of view of the need to obtain high shear stresses during the shaping of the such HNMPCMs.

Taking into account the fact that the density of the PCM is only 1.25 g/cm^3, this material is extremely promising for use in the design of aviation and space technology. Also, a high level of electrical conductivity ensures the stability of the resulting HNMPCM to the effect of a lightning discharge. In addition, one of the possible ways to impart electrical conductivity to classical PCM based on reinforcing fillers is the use of CNTs decorated with metal nanoparticles [55, 60].

Thus, based on the foregoing, it can be concluded that the electrical conductivity of nanocomposites with carbon nanotubes is influenced by: the type of nanotubes, the composition of the polymeric matrix, and the technologies for obtaining the NMPCMs, including US treatment for modifying liquid polymeric media [61]. The last one forms the distribution of CNTs by the bulk (volume) of the composite and affect the value of the contact resistance between CNTs. At the same time, the technology of obtaining composite materials from a stretched array of vertically oriented nanotubes makes it possible to produce functional PCMs with a record level of electrical conductivity and physico-mechanical properties.

7. Conclusions

The results of the studies described in this chapter confirm the effectiveness of physical, chemical and combined physico-chemical methods of modification as a basic direction of improving the technological and operational characteristics of classical PCMs and NM liquid polymer media and reinforced PCMs of functional purpose on their basis. The choice of the dominant method of physical modification of liquid polymer media and reinforced classical PCMs and NM PCMs of functional purpose in the form of US low-frequency cavitation has been experimentally confirmed.

The effective spectrum of interrelated regime parameters of US processing is characterized, which is established exclusively by an experimental method. The efficiency of creation of carbon plastics of combined filling is shown, as well as the prospects of creating HNMPCMs on the basis of reinforcing fabric with NM filler, which is used as CNT. Methods for obtaining functional NM carbonocomposites with improved physico-mechanical and operational properties, in particular, with increased strength, electrical conductivity and crack resistance are described. Potential applications of such materials are briefly described.

Further directions of research in the field of creation of reinforced PCMs on functional purpose are improving the properties of nanomodifiers used in the form of CNTs, improving the technology of de-agglomeration and subsequent alignment of nanocomposite components, and developing innovative methods for the synthesis of carbon plastics of combined filling and hybrid coal composites.

Author details

Aleksandr Evhenovych Kolosov[1]* and Elena Petryvna Kolosova[2]

*Address all correspondence to: a-kolosov@ukr.net

1 National Technical University of Ukraine, Igor Sikorsky Kyiv Polytechnic Institute, Kyiv, Ukraine

2 Faculty of Physics and Mathematics, National Technical University of Ukraine, Igor Sikorsky Kyiv Polytechnic Institute, Kyiv, Ukraine

References

[1] PJF H. Carbon nanotube composites. International Materials Review. 2004;**49**(1):31-43

[2] Kolosov AE. Prerequisites for using ultrasonic treatment for intensifying production of polymer composite materials. Chemical and Petroleum Engineering. 2014;**50**(1-2):11-17. DOI: 10.1007/s10556-014-9846-5

[3] Kolosov AE, Virchenko GA, Kolosova EP, Virchenko GI. Structural and technological design of ways for preparing reactoplastic composite fiber materials based on structural parametric modeling. Chemical and Petroleum Engineering. 2015;**51**(7-8):493-500. DOI: 10.1007/s10556-015-0075-3

[4] Kolosov AE, Sakharov AS, Sivetskii VI, Sidorov DE, Sokolskii AL. Substantiation of the efficiency of using ultrasonic modification as a basis of a production cycle for preparing reinforced objects of epoxy polymer composition. Chemical and Petroleum Engineering. 2012;**48**(5-6):391-397. DOI: 10.1007/s10556-012-9629-9

[5] Kolosov AE. Preparation of nano-modified reactoplast polymer composites. Part 1. Features of used nanotechnologies and potential application areas of nanocomposites (a review). Chemical and Petroleum Engineering. 2015;**51**(7-8):569-573. DOI: 10.1007/s10556-015-0088-y

[6] Kolosov AE. Preparation of reactoplastic nanomodified polymer composites. Part 2. Analysis of means of forming nanocomposites (patent review). Chemical and Petroleum Engineering. 2016;**51**(9-10):640-645. DOI: 10.1007/s10556-016-0100-1

[7] Kolosov AE. Preparation of reactoplastic nanomodified polymer composites. Part 3. Methods for dispersing carbon nanotubes in organic solvents and liquid polymeric media (review). Chemical and Petroleum Engineering. 2016;**52**(1-2):71-76. DOI: 10.1007/s10556-016-0151-3

[8] Kolosov AE. Preparation of reactoplastic nanomodified polymer composites. Part 4. Effectiveness of modifying epoxide oligomers with carbon nanotubes (review). Chemical and Petroleum Engineering. 2016;**52**(7-8):573-577. DOI: 10.1007/s10556-016-0235-0

[9] Kolosov AE. Preparation of reactoplastic nano-modified polymer composites. Part 5. Advantages of using nano-modified structural carbon-fiber composites (a review). Chemical and Petroleum Engineering. 2017;**52**(9-10):721-725. DOI: 10.1007/s10556-017-0259-0

[10] Karimov AA, Kolosov AE, Khozin VG, Klyavlin VV. Impregnation of fibrous fillers with polymer binders. 4. Effect of the parameters of ultrasound treatment on the strength characteristics of epoxy binders. Mechanics of Composite Materials. 1989;**25**(1):82-88. DOI: 10.1007/BF00608456

[11] Kolosov AE. Effect of low-frequency ultrasonic treatment regimes on reactoplastic polymer composite material operating properties. Chemical and Petroleum Engineering. 2014;**50**(3-4):150-155. DOI: 10.1007/s10556-014-9871-4

[12] Kolosov AE. Efficiency of liquid reactoplastic composite heterofrequency ultrasonic treatment. Chemical and Petroleum Engineering. 2014;**50**(3-4):268-272. DOI: 10.1007/s10556-014-9893-y

[13] Kolosov AE. Low-frequency ultrasonic treatment of liquid reactoplastic media with pressure variation. Chemical and Petroleum Engineering. 2014;**50**(5-6):339-342. DOI: 10.1007/s10556-014-9904-z

[14] Kolosov AE, Karimov AA, Khozin VG, Klyavlin VV. Impregnation of fibrous fillers with polymer binders. 3. Ultrasonic intensification of impregnation. Mechanics of Composite Materials. 1989;**24**(4):494-502. DOI: 10.1007/BF00608132

[15] Kolosov AE, Karimov AA, Repelis IA, Khozin VG, Klyavlin VV. Impregnation of fibrous fillers with polymeric binders. 6. Effect of parameters of ultrasound treatment on strength properties of wound fibrous composites. Mechanics of Composite Materials. 1990;**25**(4):548-555. DOI: 10.1007/BF00610711

[16] Kolosov AE, Sakharov AS, Sivetskii VI, Sidorov DE, Sokolskii AL. Method of selecting efficient design and operating parameters for equipment used for the ultrasonic modification of liquid-polymer composites and fibrous fillers. Chemical and Petroleum Engineering. 2012;**48**(7-8):459-466. DOI: 10.1007/s10556-012-9640-1

[17] Kolosov AE, Sivetskii VI, Kolosova EP, Lugovskaya EA. Procedure for analysis of ultrasonic cavitator with radiative plate. Chemical and Petroleum Engineering. 2013;**48**(11-12):662-672. DOI: 10.1007/s10556-013-9677-9

[18] Kolosov AE. Impregnation of fibrous fillers with polymer binders. 1. Kinetic equations of longitudinal and transverse impregnation. Mechanics of Composite Materials. 1988; **23**(5):625-633. DOI: 10.1007/BF00605688

[19] Kolosov AE, Repelis IA. Saturation of fibrous fillers with polymer binders. 5. Optimization of parameters of the winding conditions. Mechanics of Composite Materials. 1989;**25**(3):407-415. DOI: 10.1007/BF00614811

[20] Kolosov AE, Repelis IA, Khozin VG, Klyavlin VV. Impregnation of fibrous fillers with polymer binders. 2. Effect of the impregnation regimes on the strength of the impregnated fillers. Mechanics of Composite Materials. 1988;**24**(3):373-380. DOI: 10.1007/BF00606611

[21] Kichigin AF, Kolosov AE, Klyavlin VV, Sidyachenko VG. Probabilistic-geometric model of structurally inhomogeneous materials. Soviet Mining Science. 1988;**24**(2):87-94. DOI: 10.1007/bf02497828

[22] Kolosov AE, Klyavlin VV. Determination of the parameters of a geometric model of the structure of directionally reinforced fiber composites. Mechanics of Composite Materials. 1988;**23**(6):699-706. DOI: 10.1007/bf00616790

[23] Kolosov AE, Klyavlin VV. Several aspects of determination of the adequate model of the structure of oriented fiber-reinforced composites. Mechanics of Composite Materials. 1989;**24**(6):751-757. DOI: 10.1007/bf00610779

[24] Kolosov AE, Sakharov OS, Sivetskii VI, Sidorov DE, Pristailov SO. Effective hardware for connection and repair of polyethylene pipelines using ultrasonic modification and heat shrinkage. Part 1. Aspects of connection and restoration of polymeric pipelines for gas transport. Chemical and Petroleum Engineering. 2011;**47**:204-209. DOI: 10.1007/s10556-011-9447-5

[25] Kolosov AE, Sakharov OS, Sivetskii VI, Sidorov DE, Pristailov SO. Effective hardware for connection and repair of polyethylene pipelines using ultrasonic modification and heat shrinkage. Part 2. Production bases for molding of epoxy repair couplings with shape memory. Chemical and Petroleum Engineering. 2011;**47**:210. DOI: 10.1007/s10556-011-9448-4

[26] Kolosov AE, Sakharov OS, Sivetskii VI, Sidorov DE, Pristailov SO. Effective hardware for connection and repair of polyethylene pipelines using ultrasonic modification and heat shrinkage. Part 3. Analysis of surface-treatment methods for polyethylene pipes connected by banding. Chemical and Petroleum Engineering. 2011;**47**:216. DOI: 10.1007/s10556-011-9449-3

[27] Kolosov AE, Sakharov OS, Sivetskii VI, Sidorov DE, Pristailov SO. Effective hardware for connection and repair of polyethylene pipelines using ultrasonic modification and heat shrinkage. Part 4. Characteristics of practical implementation of production bases developed using epoxy-glue compositions and banding. Chemical and Petroleum Engineering. 2011;**47**:280. DOI: 10.1007/s10556-011-9460-8

[28] Kolosov AE, Sakharov OS, Sivetskii VI, Sidorov DE, Pristailov SO. Effective hardware for connection and repair of polyethylene pipelines using ultrasound modification and heat shrinking. Part 5. Aspects of thermistor couplings and components used in gas-pipeline repair. Chemical and Petroleum Engineering. 2011;**47**:285. DOI: 10.1007/s10556-011-9461-7

[29] Chiganova GA, Chiganov AS. Structure and properties of ultrafine diamond powder produced by detonation synthesis. Inorganic Materials. 1999;**35**(5):480-484

[30] Puzyr AP, Bondar VS, Bukayemsky AA, et al. Physical and chemical properties of modified nanodiamonds. In: Gruen D, Shenderova OA, AYa V, editors. Syntheses, Properties and Applications of Ultrannaocrystalline Diamond, NATO Sci. Ser. II, Math., Phys., Chem. Vol. 192. Springer, Kluwer Academic Publishers B.V.; 2005. pp. 261-270

[31] Gunyaev GM, Sorina TG, Khoroshilova IP, Rumyantsev AF. Structural epoxide carbon-fiber plastics. Aviation Industry. 1984;**12**:41-45. https://viam.ru/public/files/1984/1984-199127.pdf

[32] Anan'eva ES, Markin VB. Potential application of carbon-fiber plastics with combined filling in aerospace technology. Polzunov Vestnik. 2009;**4**:223-226

[33] Gunyaev GM, Kablov EN, Aleksashin VM. Modifying of constructional carbon plastics with carbon nanoparticles. Russian Chemistry Journal. 2010;**54**(1):3-11

[34] Ponomarev AN. Nanotechnology and nanostructured materials. Industriya. 2002;**1**:12

[35] Gunjaev GM. In: Shalin RE, editor. Polymer Matrix Composites. London: Chapman & Hall; 1995. pp. 92-129

[36] Il'chenko SI, Gunyaev GM, Aleksashin VM, et al. Carbon fulleroid nanoparticles: Effect on structure and properties of epoxide carbon-fiber plastics. Nanotekhnika. 2005;**3**:18-28

[37] Kolosov AE. Production of High Quality Traditional and Nano-Modified Reactoplastic Polymer Composites. Kiev: BPI BPK Polilekhnika; 2015. 227 p

[38] Bolshakov VA, Solodilov VI, Korokhin RA, Merkulova YI, Dyachkova TP. Research of crack resistance of polymeric composite materials fabricated by infusion using various concentrates on the basis of modified CNT. Proceedings of VIAM. 2017;**7**:79-89. DOI: 10.18577/2307-6046-2017-0-7-9-9

[39] Gunyaev GM, Chursova LV, Komarova OA, et al. Structural polymer carbon nanocomposites—A new direction in materials science. Vse Mater. 2011;**12**:2-9

[40] Stepanishev NA. Nanocomposites. The problem of filling. M. Plastiks. 2010;**4**(86):23-27 http://www.plastics.ru/pdf/Stepanischev_04_2010.pdf

[41] Stepanishchev NA, Tarasov VA, Boyarskaya RV, et al. Strength of fibrous composites with nanomodified filler. Herald of the Bauman Moscow State Technical University. Ser. Mechanical Engineering. 2013;**3**:122-132

[42] Kablov EN, Kondrashov SV, Yurkov GY. Perspectives of use of carbon-containing nanoparticles in binding for polymeric composite materials. Russian Nanotechnologies. 2013;**8**(3-4):24-42

[43] Bekyarova E, Thostenson ET, Yu A, et al. Functionalized single-walled carbon nanotubes for carbon fiber-epoxy composites. Journal of Physical Chemistry C. 2007;**111**:17865-17871

[44] Gojny FH, Wichmann MHG, Fiedler B, Bauhofer W, Schulte K. Influence of nano-modification on the mechanical and electrical properties of conventional fiber-reinforced composites. Composites: Part A. 2005;**36**:1525-1535

[45] Yokozeki T, Iwahori Y, Ishibashi M, et al. Fracture toughness improvement of CFRP laminates by dispersion of cup-stacked carbon nanotubes. Composites Science and Technology. 2009;**69**:2268-2273

[46] Davis DC, Whelan BD. An experimental study of interlaminar shear fracture toughness of a nanotube reinforced composite. Composites: Part B. 2011;**42**:105-116

[47] Almuhammadi K, Alfano M, Yang Y, Lubineau G. Analysis of interlaminar fracture toughness and damage mechanisms in composite laminates reinforced with sprayed multi-walled carbon nanotubes. Materials and Design. 2014;**53**:921-927

[48] Guan AJ, Mirjalili V, Zhang Y, et al. Enhancement of mechanical performance of epoxy/carbon fiber laminate composites using single-walled carbon nanotubes. Composites Science and Technology. 2011;**71**:1569-1578

[49] Mujika F, Vargas G, Ibarretxe J, et al. Influence of the modification with MWCNT on the interlaminar fracture properties of long carbon fiber composites. Composites: Part B. 2012;**43**:1336-1340

[50] Mirjalili V, Ramachandramoorthy R, Hubert P. Enhancement of fracture toughness of carbon fiber laminated composites using multi wall carbon nanotubes. Carbon. 2014; **79**:413-423

[51] Fenner JS, Daniel IM. Hybrid nanoreinforced carbon/epoxy composites for enhanced damage tolerance and fatigue life. Composites: Part A. 2014;**65**:47-56. https://doi.org/10.1016/j.compositesa.2014.05.023

[52] White KL, Sue HJ. Delamination toughness of fiber-reinforced composites containing a carbon nanotube/polyamide-12 epoxy thin film interlayer. Polymer. 2012;**53**:37-42

[53] Ye Z, Bakis CE, Adair JH. Effects of carbon nanofiller functionalization and distribution on interlaminar fracture toughness of multi-scale reinforced polymer composites. Carbon. 2012;**50**:1316-1331

[54] Merkulova YI, Kondrashov SV, D'Yachkova TP, Marakhovskii PS, Yurkov GY. Effect of carbon nanotubes dispersed in binder on properties of epoxy nanocomposite. Russian Journal of Applied Chemistry. 2015;**88**(11):1848-1854

[55] Kondrashov SV, Shashkeev KA, Popkov OV, Solovyanchik LV. Perspective technologies for obtaining of functional materials of structural purpose on the basis of nanocomposites with CNTs (review). Proceedings of VIAM. 2016;**3**(39):54-64. DOI: 10.18577/2307-6046-2016-0-3-7-7

[56] Garcia EJ, Saito DS, Megalini L, Hart AJ, Guzman de Villoria R, Wardle BL. Fabrication and multifunctional properties of high volume fraction aligned carbon nanotube thermoset composites. Journal of Nano Systems & Technology. 2009;**1**(1):1-11

[57] Cheng Q, Wang J, Jiang K, Li Q, Fan S. Fabrication and properties of aligned multiwalled car bon nanotube-reinforced epoxy composites. Journal of Materials Research. 2008;**23**(11):2975-2983

[58] Wang X, Yong ZZ, Li QW, Bradford PD, Liu W, Tucker DS, Cai W, Wang H, Yuan FG, Zhu YT. Ultrastrong, stiff and multifunctional carbon nanotube composites. Materials Research Letters. 2013;**1**(1):19-25

[59] Wang C, Guo Z-X, Fu S, et al. Polymers containing fullerene or carbon nanotube structures (review). Progress in Polymer Science. 2004;**29**:1079-1141

[60] Kondrashov SV, D'yachkova TP, Bogatov VA, et al. Use of carbon nanotubes to increase the heat resistance of epoxide binders. Perspekt. Mater. 2013;**2**:17

[61] Kolosov AE. Low-frequency ultrasonic treatment as an effective method for modifying liquid reactoplastic media. Chemical and Petroleum Engineering. 2014;**50**(1-2):79-83. DOI: 10.1007/s10556-014-9859-0

Chapter 3

Design, Fabrication and Application of Multi-Scale, Multi-Functional Nanostructured Carbon Fibers

Yang Liu, Chao Zhang and Xinyu Zhang

Additional information is available at the end of the chapter

http://dx.doi.org/10.5772/intechopen.74215

Abstract

To further improve and upgrade the existing functions of carbon fibers, and to endow the carbon fiber with new and desired functions, the most effective and economic way is to create nanostructures on the carbon fiber surface. The carbon fibers with nanostructures grown on the surface, or namely nanostructured carbon fibers, not only maintain the intrinsic high strength, light weight, high thermal conductivity of carbon fiber, but also obtain significant functional enhancements in mechanical properties, interfacial bonding and electrocatalytic property. Different kinds of nanostructures, such as nanoparticles, nanorods, nanotubes, nanosheets, and nanoflowers, are controllably grown on the surface of carbon fibers by using various kinds of techniques, including chemical vapor deposition (CVD), laser ablation, microwave treatment, and hydrothermal process. These multiscale, multifunctional nanostructured carbon fibers not only add new and interesting branches to the carbon fiber family, but also pave the way for the application of carbon fibers in next-generation fiber-reinforced composite, energy storage device and green energy production.

Keywords: surface growth, carbon fiber, nanostructures, fiber-reinforced composite, electrocatalyst

1. Introduction

Owning to its high mechanical strength, light weight and one-dimensional morphology, carbon fiber has become one of the most important materials in fabricating structural components and load-bearing parts, and has found wide-spread applications from the fields of automotive, sports, to aircrafts and aerospace shuttles. Perceived by its name, carbon fiber is composed of the elemental carbon (C). Different from graphite, which is composed of sheets of carbon

atoms (graphene sheets) that parallelly stack on each other, the carbon fibers are composed of graphene sheets that twisted, folded and crumbled upon each other. Therefore, carbon fibers would have extremely high tensile strength and stiffness as compared to graphite. Carbon fibers are majorly produced from the precursors such as polyacrylonitrile (PAN), rayon and petroleum pitch [1]. In a typical process, the precursors are spun and drawn to form filament yarns, which are subsequently subject to the pre-oxidation, thermal carbonization and graphitization processes. After the thermal carbonization process, the precursor filament yarns are converted to carbon filament yarns with high carbon contents (~92–99%). The carbon filament yarns produced from the carbonization process (1500–2000°C) generally exhibit high tensile strength while the ones produced from the graphitization process (2500–3000°C) generally exhibit high elastic modulus [2].

Due to its high mechanical strength, high modulus, thermal conductivity and low thermal expansion, carbon fibers are widely used in the high technology sectors, such as aerospace and nuclear engineering, where high performance under high damping, high temperature and corrosive environment is required [3]. However, in general engineering sectors and transportation, the application of carbon fiber is restrained by the cost and production rates, and it only appears in limited parts of the products, where high strength and light weight are needed. The final properties of carbon fibers are highly dependent on their precursors and different types of carbon fiber can be produced based on the specific requirements of application. For example, the carbon fiber produced from PAN has the highest tensile strength (**Table 1**), which is suitable for the high technology applications. On the other, the carbon fiber produced from cellulose may have lower tensile strength accompanied with low cost, which is suitable for general engineering applications (**Table 2**) [4].

The properties of carbon fibers can be further improved by the growth of nanostructured materials on their surfaces, a process commonly known as "whiskerization" [5–7]. Techniques such as chemical vapor deposition, hydrothermal process and electrochemical deposition are usually employed to accomplish the nanostructure growth [8–10]. During the growth process, the nanostructures are directly formed on the surface layer of the carbon fibers, either through the pre-deposited "seed layer" or hydrophobic interaction. After the growth process, the as-grown nanostructures and the carbon fiber substrates integrate and form free-standing, binder-free multi-scale composites. Depending on the properties of the as-grown nanostructures, the applied functions of carbon fiber can be greatly enhanced and extended.

Precursor	Tensile strength (GPa)	Tensile modulus (GPa)	Elongation at break (%)
PAN	2.5-7.0	230-400	0.6-2.5
Mesophase pitch	1.5-3.5	200-800	0.3-0.9
Rayon	≈ 1.0	≈ 50	≈ 2.5

Table 1. Mechanical properties of PAN, pitch and rayon based carbon fibers [3].

Precursor Material	Diameter	Strength [GPa]	Modulus [GPa]	Elongation [%]
lyocell	7.5	0.9		
rayon	7.5	0.81		
lyocell		0.49	37.6	1.4
lyocell filled with 5 wt% carbon black		0.57	48.3	1.2
rayon		0.82	79.2	
lyocell		0.94	99.7	
lyocell		1.07	96.6	
lyocell		0.40		
rayon "Ural"		0.5–1.2	100	
hydrated cellulose		1.65	97	
rayon		0.944	54.3	1.76
rayon		1.535	59.8	2.57
viscose rayon		0.6	50	
cellulosic fiber		2–4		
cellulose fiber		0.2–0.44		3.0
sisal fiber		0.8	25	

Table 2. Mechanical properties of cellulose based carbon fibers [4].

For example, growth of carbon nanotubes or zinc oxide nanowires on the carbon fiber surface can significantly increase the tensile strength (133%) and interfacial strength (113%) of the fiber-reinforced composite prepared by using these carbon fibers [11, 12]. By growing metal oxide or metal dichalcogenide nanostructures on carbon fiber surface, the electrochemical catalytic and capacitive properties of carbon fibers can be substantially enhanced [13, 14]. Upon integrating the intrinsic high electrical and thermal conductivity, high mechanical strength and chemical inertness of carbon fibers with the nanostructured materials of high electrochemical activity, ideal bi-functional (anode and cathode) electrodes for metal-air batteries and water-splitting cells can be readily realized, which further extends the applications of carbon fiber to energy storage and green energy [15, 16]. This chapter will focus on the state-of-the-art design and growth of functional nanostructures on carbon fiber surface, as well as their advanced applications.

2. Nanostructures grown on carbon fiber for fiber-reinforced composites

Due to its excellent mechanical, thermal and chemical properties, carbon fibers are widely used for the fabrication of fiber-reinforced composites (FRC), forming high-performance structures and components for high-technology applications. However, the most frequent occurring cases for the failure of FRC known as fiber pull-out and delamination are caused by the internally weak bonding between the fibers and the polymeric matrix [17, 18]. In this regard, growth of secondary nanostructures on the surface of carbon fibers to improve the interfacial bonding

between the fibers and matrix has been proposed [19, 20]. In order to obtain the desired enhancement in the interfacial bonding strength, three main factors should be considered, including: (i) the as-grown nanostructures should have intrinsically good mechanical properties, proper size range and high surface area, which can significantly increase the interfacial area between the fiber and matrix, as well as providing good anchoring strength; (ii) the nanostructures should be directly grown on the surface of carbon fibers to avoid the involvement of binders, as binders could affect the mechanical strength of the final composites; (iii) the process of growth should not deteriorate the intrinsic mechanical properties of carbon fibers.

2.1. Growth of nanocarbons

Due to their intrinsic affinity to the surface of carbon fibers, carbon nanomaterials (nanocarbons) have been grown on carbon fiber for the FRC application. For example, carbon nanotubes (CNTs) grown on carbon fibers are speculated to improve the interfacial bonding in FRC due to the high mechanical strength, high surface area and good substrate adhesion [21]. Extensive research efforts have been devoted to grow CNTs on carbon fibers while the diameter, length and crystallinity of the as-grown CNTs can be effectively controlled [22–25]. Techniques of chemical vapor deposition (CVD) are widely applied to grow CNTs on carbon fiber surface (**Figure 1**). In a typical process, the carbon fibers are firstly cleaned and desized in organic solvents by sonication, and then immersed in the catalyst solution at elevated temperature for absorbing and loading of the metal catalysts. Metals, such as iron (Fe), nickel (Ni), cobalt (Co), are the major catalysts used for the growth of CNTs [27, 28]. After the immersion and the subsequent drying process, the surface of carbon fiber is densely loaded with small metal particles, as shown in **Figure 2**. Afterwards, the metal-loaded carbon fibers are placed in a quartz tube furnace, which are subsequently heated in the presence of hydrogen (H_2) and carbon source mixed stream (e.g., benzene, ethylene, acetylene) to accomplish the CNT growth. The flow rate of total gas streams is typically in the range between 100 mL min^{-1} and 300 mL min^{-1}, and inert gas protection is required during the heating and cooling steps.

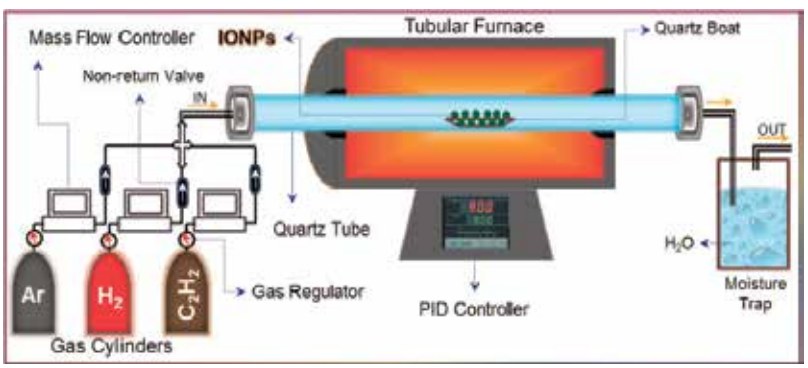

Figure 1. Schematic illustration of the CVD process for growing CNTs [26].

http://dx.doi.org/10.5772/intechopen.74215

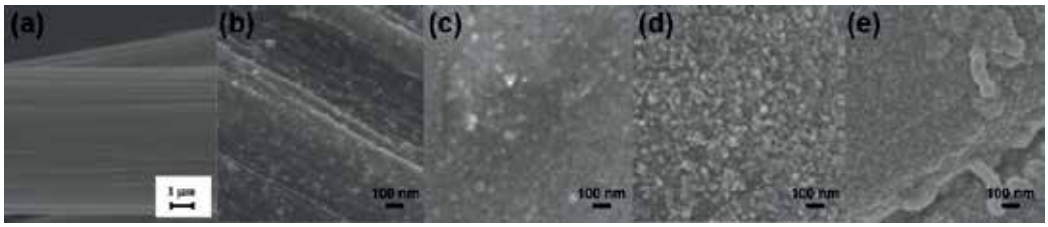

Figure 2. Scanning electron microscopy (SEM) images of (a) bare carbon fiber surface [11] and (b-c) Ni particle-loaded carbon fiber surface with increasing concentrations of the catalyst solution [24].

The as-grown CNTs exhibit long and curved shapes which wrapped around the longitudinal axis of the carbon fibers randomly, as shown in **Figure 3**. The morphology of the as-grown CNTs can be controlled by a wide-range of parameters including types of catalyst, catalyst concentration, gas flow rate, growth time and temperature. A brief summary of the relationship between the carbon fiber morphology and these parameters is provided in **Table 3**. Amongst these parameters, the catalyst concentration is speculated to play a major role since all the morphological related parameters (e.g., diameter, length, density) can be effectively tuned by it (**Figure 4**). It should be noted that there exists a proper range for tuning the growth parameters of CNTs, and beyond this range CNTs may not be properly grown [30]. Other than CNTs, carbon nanofibers (CNFs) can also be grown on the surface of carbon fiber by using the same chemical vapor deposition (CVD) procedures [31–33]. Different from CNTs, the CNFs is characterized as long nanofibers with solid core, and they would generally have higher aspect ratios than CNTs. It is speculated that by increasing the time of CVD the CNTs can be further grown into CNFs, as shown in **Figure 5** [34].

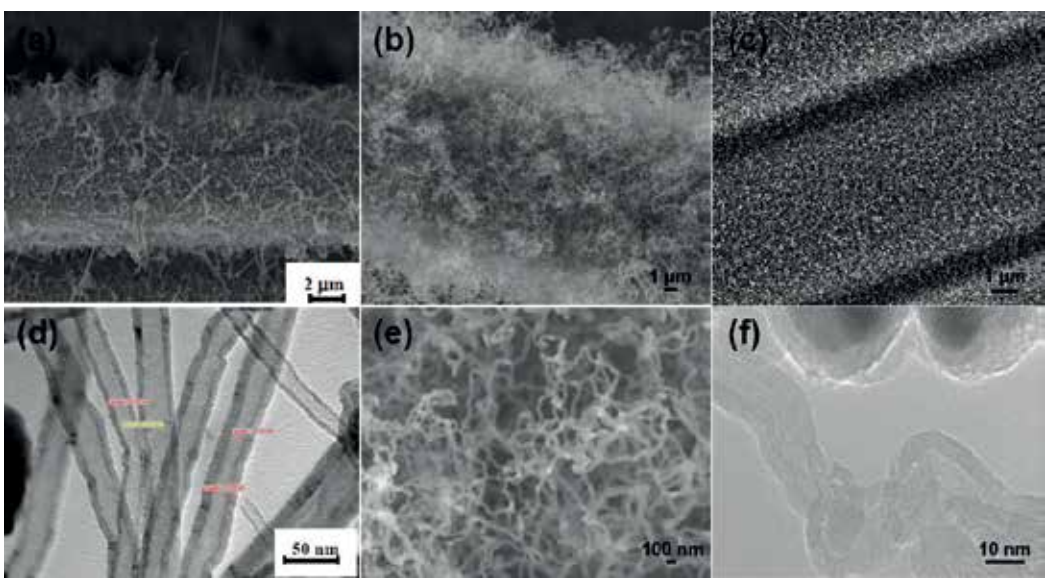

Figure 3. SEM and TEM images of CNTs grown on carbon fiber by using (a, d) Fe based catalyst [11], (b, e) Co based catalyst [22], and (c, f) Ni based catalyst [29].

Parameters	Diameter	Length	Thickness
Catalyst concentration	−	+	+
Temperature	-	+	-
Time	−	+	+
Flow rate	−	+	+

Table 3. Correlation between the morphology of CNTs and growth conditions. (+) represents in direct proportion while (−) represents in inverse proportion.

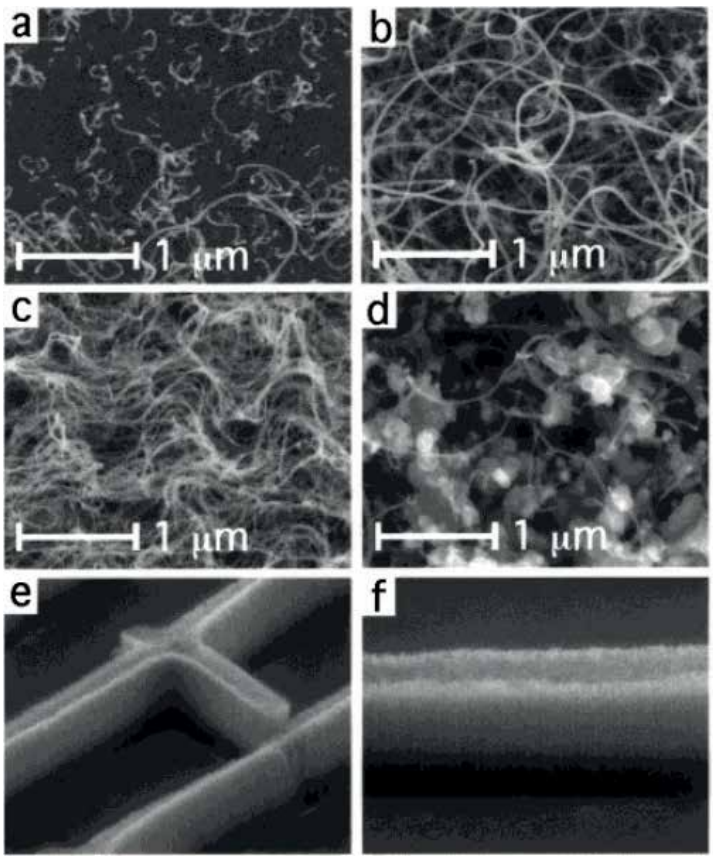

Figure 4. Pattern films of CNTs grown by increasing catalyst concentrations: (a) 10 mM, (b) 25 mM, (c) 40 mM, (d) 70 mM; (e, f) 50 mM $Fe(NO_3)_3 \bullet 9H_2O$. Aligned CNTs grown perpendicular to the substrate surface can be observed in (e) and (f) with a width of 10 μm and height of 20 μm [30].

2.2. Growth of nanostructured metal oxides

Besides CNT and CNFs, metal oxide nanostructures are also grown on carbon fibers to improve their interfacial bonding strength, respectively [35–37]. The hydrothermal method is widely used to grow metal oxide nanostructures, as illustrated in **Figure 6**. Compared with the growth of nanocarbons, growing metal oxide nanostructures on carbon fibers by the

http://dx.doi.org/10.5772/intechopen.74215

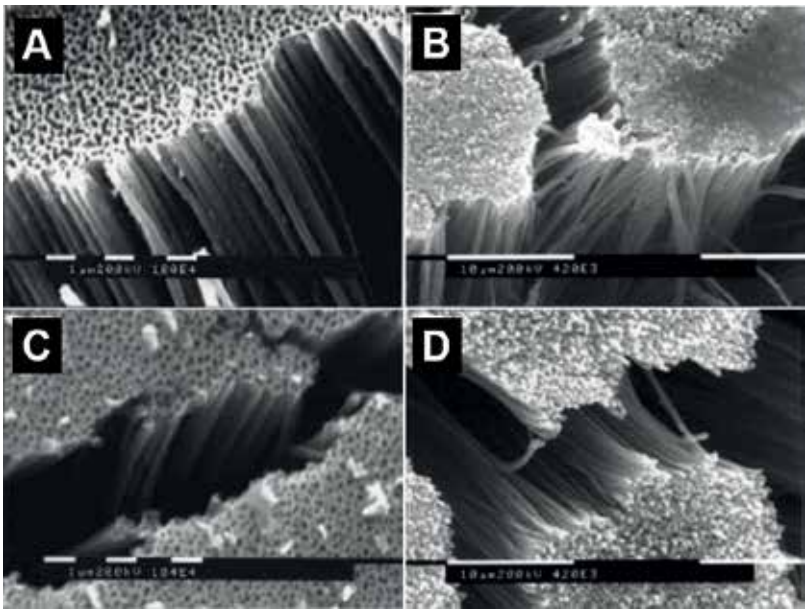

Figure 5. SEM images of the CVD-grown (a, C) CNTs and (B, D) CNFs obtained from 10 min and 40 min at 900°C, respectively [34].

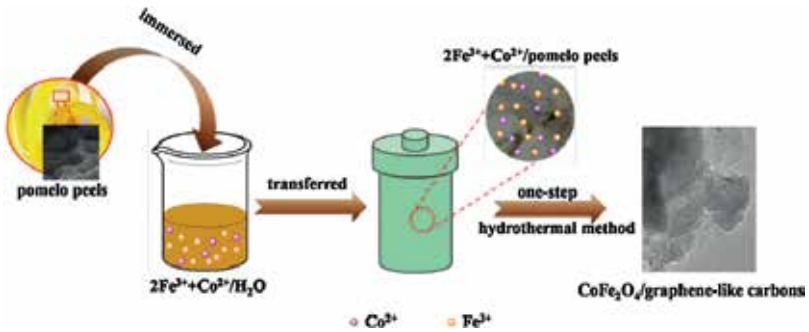

Figure 6. Schematic illustration of a typical hydrothermal process that used for the synthesis of metal oxide [42].

hydrothermal method may obtain the advantages including: (i) higher degree of morphological control over the as-grown nanostructures can be achieved on the carbon fiber surface. In other words, higher structural uniformity and higher growth density can be readily achieved for the as-grown metal oxide nanostructures; (ii) the growth process of metal oxides is simpler and requires less instrumentation, the material and energy consumption are also less comparing with the thermal CVD process; (iii) by using the same growth protocol, different types of nanostructured metal oxides can be grown on the surface of carbon fibers. However, CNTs and CNFs grown by thermal CVD may still possess the pros including: (i) higher theoretically predicted improvement in the interfacial strength for FRC; (ii) higher surface area of the as-grown nanostructures, and (iii) better affinity or adhesion to the carbon fiber substrate [38].

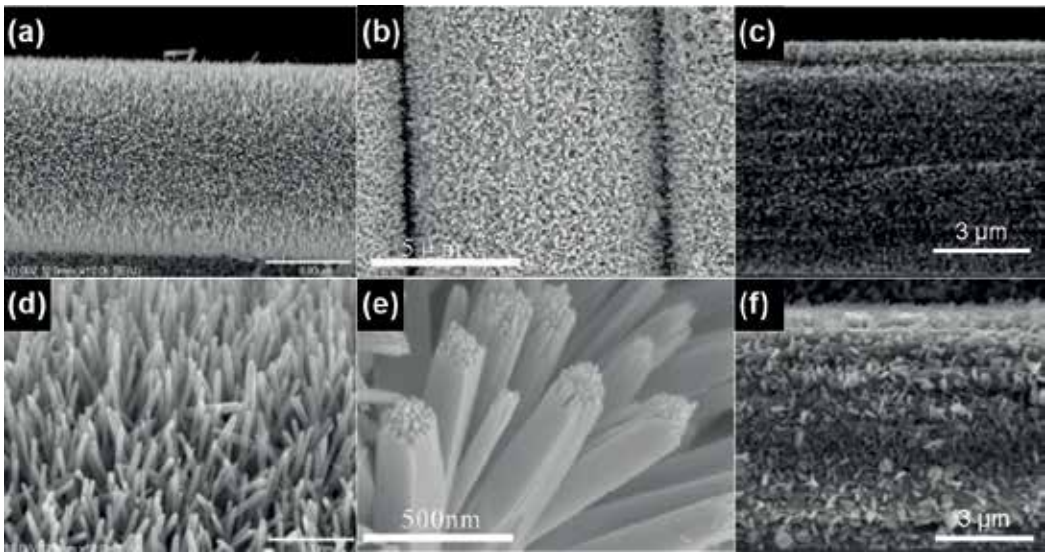

Figure 7. SEM images of metal oxide nanostructures grown on carbon fiber by using hydrothermal method: (a, d) ZnO nanowires, (b, e) TiO_2 nanorods and (c, f) CuO nanowires [12, 36, 37]. The CuO nanowires in (c) were synthesized from 10 mM seeding solution while the nanowires in (f) were synthesized from 50 mM seeding solution.

Given the remarkable advantages of growing metal oxide nanostructures for FRC application, extensive research efforts have been made to investigate their growth process as well as their functional performance in FRC [39–41].

During the hydrothermal process, the metal oxide "seeds" are firstly deposited on the surface of carbon fiber by immersing the carbon fibers in the solution of metal salts. Afterwards, the seed-loaded carbon fibers are annealed at elevated temperature in atmospheric pressure, in order to improve the adhesion between the seeds and the fibers. Then the treated carbon fibers are immersed in a "growth solution" which contains the metal salts and organic polyamines (e.g., hexamethylenetetramine, HMTA). The growth process is then proceeded by heating the solution in a glass beaker at elevated temperature on a hotplate. Or a stainless-steel autoclave can be used if higher temperature and pressure are needed. The zinc oxide (ZnO) and copper oxide (CuO) nanowires, titanium dioxide (TiO_2) nanorods synthesized by using the hydrothermal method are shown in **Figure 7**. Similar to the growth of nanocarbons, structural control over the as-grown metal oxide nanostructures can be achieved by tuning the concentration of the "seeding solution," loading quantity of the metal oxide "seeds," as well as the time of growth (**Figure 7c** and **f**).

2.3. Mechanical properties of carbon fibers with surface-grown nanostructures

The carbon fibers with carbon or metal oxide nanostructures grown on the surface are eventually subject to the mechanical testing, in order to reveal their functional performance in enhancing the interfacial bonding strength within the FRC and the mechanical strength of the whole FRC.

Materials	Tensile strength (MPa)	Modulus (GPa)	Interfacial shear strength (MPa)	Maximum increment (%)	Reference
CNT-CF	27	1.07		133% in tensile strength	[11]
ZnO NW		3.34	33.87	113% in shear strength	[12]
CNF	23.9–24.8	0.75–0.79			[33]
CNT				17% in fracture toughness	[23]
CuO NW				42.8% in tensile strength	[36]
TiO_2 NR	200.5			45% in tensile strength	[37]
ZnO NW				209.5% in loss factor	[43]
ZnO NR				50% in loss factor	[44]
CNT				300% in conductivity	[45]
CNT				510% in conductivity	[46]
CNT				56% in loss factor	[47]
CNT				69% decrease of crack propagation	[48]
CNT			18.1	45% in shear strength	[49]
CNT				127% in impact energy dissipation	[50]
CNT				30% in shear strength	[51]
SiO_2 NP			52	44% in shear strength	[52]
Graphene				173% in shear strength	[53]

Table 4. Mechanical properties of carbon fiber with different nanostructured materials grown on its surface. NW refers to nanowires while NR and NP refer to nanorods and nanoparticles, respectively. The "shear strength" shown in table refers to interfacial shear strength.

In a typical process, the carbon fibers are chopped into smaller fibers with less dimensions (length $\leqq$ 2 mm), which are subsequently mixed or blended with the matrix materials, such as epoxy and polypropylene. The mixtures are then cast in a mold with applied pressure and subsequently solidified by either curing or compression molding to form the FRC. Mechanical testing, including tensile strength, modulus, shear strength and compressive strength, are applied to the nanostructured carbon fiber reinforced polymer composites (CFRC) and the representative results are shown in **Table 4**. It is found that the as-grown CNTs and CNFs are capable of increasing the mechanical strength of the whole CFRC to a great extent, while the metal oxide nanowires can significantly improve the interfacial strength between the carbon fiber and polymer matrix.

3. Nanostructures grown on carbon fibers for energy storage and green energy electrodes

Similar to the growth of metal oxides, secondary nanostructures composed of the compounds of transition metals and non-metals can also be grown on the surface of carbon fiber to extend

its range of application to energy storage and green energy electrodes. The intrinsically high electrical and thermal conductivity, chemical inertness and flexibility make carbon fiber an ideal electrode substrate for the fabrication of high-performance hybrid electrodes that are capable of catalyzing targeted electrochemical reactions in harsh conditions effectively, efficiently and stably. The state-of-the-art research has been focused on using the carbon fiber hybrid electrodes in supercapacitors, lithium-ion batteries and water-splitting [54–56]. To accomplish the requirements for these applications, various types of hybrid catalysts have been grown on the surface of carbon fibers either by electrochemical deposition or electrodeless deposition. However, most of these materials can be categorized as the hybrids of transition metals and non-metals, including MnO_2, MoS_2, NiP, FeS_2, $CoSe_2$, $NiCo_2S_4$, etc., [54–59]. Similar to the growth of metal oxides, the hydrothermal method is widely adapted for growing the hybrid electrode catalysts. Other methods, such as in-situ redox process and thermal annealing, are also used to grow the hybrid catalysts [60, 61]. However, in order to obtain hybrid catalysts with desired elemental composition, additional steps such as vulcanization, selenization and phosphorization are required. The representative SEM images of the hybrid catalysts grown on carbon fibers are shown in **Figure 8**.

Based on their elemental composition, the applications of the as-grown hybrid catalysts can be categorized as supercapacitor, lithium-ion battery and water-splitting. For example, the metal oxides (e.g., MnO_2) are well-suited for supercapacitors and metal dichalcogenides (e.g., MoS_2) with layered structures are suitable for lithium-ion batteries, while metal phosphorus based catalysts (e.g., NiP) are suitable for water splitting. The carbon fiber-based hybrid electrodes demonstrate high electrocatalytic performance in these applications, as shown in **Table 5**.

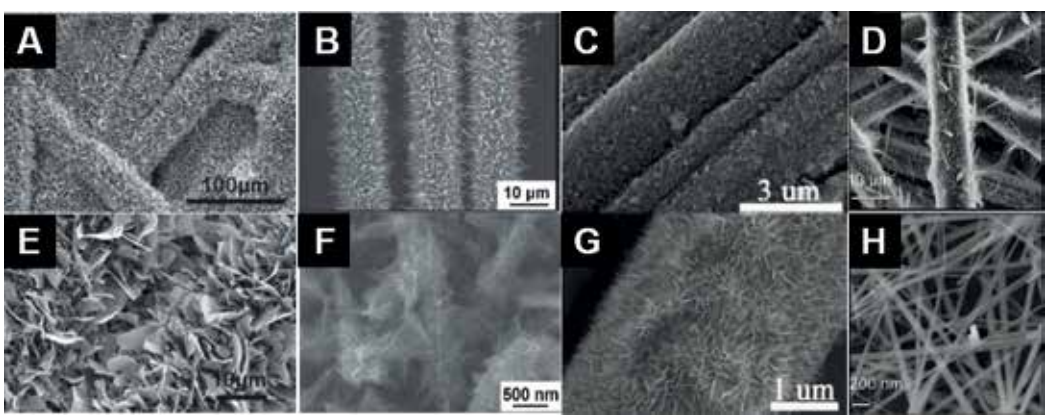

Figure 8. SEM and magnified images of hybrid nanostructured catalysts on the surface of carbon fibers: (A, E) NiP nanoflakes; [56] (B, F) whisker-like MnO_2 arrays; [62] (C, G) MoS_2 nanosheets; [61] (D, H) Co_3O_4 nanonet [63].

Materials	Applications	Performance	Reference
$NiCo_2S_4$ nanotube	Supercapacitor	Discharge areal capacitance of 2.86 F cm^{-2} at 4 mA cm^{-2}	[54]
FeS_2	Lithium battery	Discharge density of 1300 Wh kg^{-1}	[55]
NiP	Water splitting	250 mV OP for 100 mA cm^{-2} cathodic current density; 0.3 V OP for OER current of 50.4 mA cm^{-2}	[56]
PPy-MnO_2	Supercapacitor	69.3 F cm^{-3} at 0.1 A cm^{-3}; 6.16 × 10^{-3} Wh cm^{-3} at 0.04 W cm^{-3}	[57]
MoS_2 nanofilm	Water splitting	216 mV OP for 100 mA cm^{-2} cathodic current density	[58]
$CoSe_2$ NP	Water splitting	180 mV OP for 100 mA cm^{-2} cathodic current density	[59]
MnO_2	Supercapacitor	Volume capacitance of 2.5 F cm^{-3}; energy density of 2.2 × 10^{-4} Wh cm^{-3}	[60]
MoS_2 NS	Lithium-ion battery	Discharge capacity of 971 mA h g^{-1}	[61]
MnO_2 arrays	Supercapacitor	Capacitance of 274.1 F g^{-1} at 0.1 A g^{-1}	[62]
Co_3O_4 nanonet	Supercapacitor	Capacitance of 1124 F g^{-1} at 25.34 A g^{-1}	[63]
MnO_2	Supercapacitor	Capacitance of 467 F g^{-1} at 1 A g^{-1}	[64]
CuO NF	Supercapacitor	Capacitance of 839.9 F g^{-1} at 1 mV s^{-1}; energy density of 10.05 Wh kg^{-1} and power density of 1798.5 W kg^{-1}	[65]
Nickel copper hydroxide	Supercapacitor	770 F g^{-1} at 5 mA cm^{-2}; energy density of 33 Wh kg^{-1} at a power density of 170 W kg^{-1}	[41]
WP NR	Water splitting	230 mV OP for 100 mA cm^{-2} cathodic current density	[66]

Table 5. Applications and performance of different hybrid nanostructured catalysts grown on carbon fiber. OP refers to overpotential, while NS refers to nanosheets, NF refers to nanoflowers.

4. Conclusion and future work

The growth of nanostructured materials on the surface of carbon fibers can significantly improve the interfacial mechanisms of the carbon fiber-based composites as well as introducing additional advanced functions to the carbon fiber substrate. The growth of one dimensional nanocarbons and nanostructured metal oxides on carbon fibers results in greatly enhanced tensile strength, interfacial shear strength, impact resistance and damping when being used in fiber reinforced composites. On the other, by growing hybrid nanostructured catalysts on carbon fibers, high performance electrodes with outstanding electrocatalytic properties can be facilely prepared, which further extends the applications of carbon fiber-based electrodes to supercapacitors, lithium-ion batteries and water splitting cells. In order to further improve the functional performance of the carbon fibers grown with surface nanostructures, future research in the related fields should pay attention to tailor the morphology and composition, as well as the orientation, spacing and thickness of the as-grown nanostructure.

Acknowledgements

The authors gratefully acknowledge the financial support from Sun Yat-sen University and Auburn University.

Conflict of interest

The authors declare no conflict of interest.

Author details

Yang Liu[1]*, Chao Zhang[1] and Xinyu Zhang[2]

*Address all correspondence to: liuyang56@mail.sysu.edu.cn

1 Sun Yat-sen University, Guangzhou, China

2 Auburn University, Auburn, Alabama, USA

References

[1] Park SJ, Heo G. Precursors and Manufacturing of carbon Fibers. In: Carbon Fibers. Springer Series in Materials Science. Vol. 210. Dordrecht: Springer; 2015. pp. 31-66

[2] Frank E, Hermanutz F, Buchmeiser MR. Carbon fibers: Precursors, manufacturing, and properties. Macromolecular Materials and Engineering. 2012;**297**:493-501

[3] Chand S. Carbon fibers for composites. Journal of Materials Science. 2000;**35**:1303-1313

[4] Frank E, Steudle DLM, Ingildeev D, Spörl DJM, Buchmeiser MR. Carbon fibers: Precursor systems, processing, structure, and properties. Angewandte Chemie, International Edition. 2014;**53**:5262-5298

[5] Egashira M, Katsuki H, Ogawa Y, Kawasumi S. Whiskerization of carbon beads by vapor phase growth of carbon fibers to obtain sea urchin-type particles. Carbon. 1983;**21**:89-92

[6] Kowbel W, Bruce C, Withers JC, Ransone PO. Effect of carbon fabric whiskerization on mechanical properties of C-C composites. Composites Part A: Applied Science and Manufacturing. 1997;**28**:993-1000

[7] Vishkaei MS, Salleh MAM, Yunus R, Biak DRA, Danafar F, Mirjalili F. Effect of short carbon fiber surface treatment on composite properties. Journal of Composite Materials. 2010;**45**:1885-1891

[8] Felisberto M, Tzounis L, Sacco L, Stamm M, Candal R, Rubiolo GH, Goyanes S. Carbon nanotubes grown on carbon fiber yarns by a low temperature CVD method: A significant enhancement of the interfacial adhesion between carbon fiber/epoxy matrix hierarchical composites. Composites Communications. 2017;**3**:33-37

[9] Huang F, Yan A, Sui Y, Wei F, Qi J, Meng Q, He Y. One-step hydrothermal synthesis of Ni_3S_4@MoS_2 nanosheet on carbon fiber paper as a binder-free anode for supercapacitor. Journal of Materials Science: Materials in Electronics. 2017;**28**:12747-12754

[10] Wu MS, Guo ZS, Jow JJ. Highly Regulated electrodeposition of needle-like manganese oxide nanofibers on carbon fiber fabric for electrochemical capacitors. Physical Chemistry C. 2010; **114**:21861-21867

[11] Suraya AR, Sharifah-Mazrah SMZ, Yunus R, Azowa IN. Growth of carbon nanotubes on carbon fibres and the tensile properties of resulting carbon fibre reinforced polypropylene composites. Journal of Engineering Science and Technology. 2009;**4**:400-408

[12] Lin Y, Ehlert G, Sodano HA. Increased interface strength in carbon fiber composites through a ZnO nanowire interphase. Advanced Functional Materials. 2009;**19**: 2654-2660

[13] Sassin MB, Chervin CN, Rolison DR, Long JW. Redox deposition of nanoscale metal oxides on carbon for next-generation electrochemical capacitors. Accounts of Chemical Research. 2013;**46**:1062-1074

[14] Liu Y, Ren L, Zhang Z, Qi X, Li H, Zhong J. 3D Binder-free $MoSe_2$ nanosheets/carbon cloth electrodes for efficient and stable hydrogen evolution prepared by simple electrophoresis deposition strategy. Scientific Reports. 2016;**6**:22516

[15] Liu Q, Wang Y, Dai L, Yao J. Scalable fabrication of nanoporous carbon fiber films as bifunctional catalytic electrodes for flexible Zn-Air batteries. Advanced Materials. 2016; **28**:3000-3006

[16] Du S, Ren Z, Zhang J, Wu J, Xi W, Zhu J, Fu H. Co_3O_4 nanocrystal ink printed on carbon fiber paper as a large-area electrode for electrochemical water splitting. Chemical Communications. 2015;**51**:8066-8069

[17] Sakai M, Matsuyama R, Miyajima T. The pull-out and failure of a fiber bundle in a carbon fiber reinforced carbon matrix composite. Carbon. 2000;**38**:2123-2131

[18] Chen WC. Some experimental investigations in the drilling of carbon fiber-reinforced plastic (CFRP) composite laminates. International Journal of Machine Tools & Manufacture. 1997;**37**:1097-1108

[19] Tang LG, Kardos JL. A review of methods for improving the interfacial adhesion between carbon fiber and polymer matrix. Polymer Composites. 1997;**18**:100-113

[20] Thostenson ET, Li WZ, Wang DZ, Ren ZF, Chou TWJ. Carbon nanotube/carbon fiber hybrid multiscale composites. Journal of Applied Physics. 2002;**91**:6034-6037

[21] Thostenson ET, Ren Z, Chou TW. Advances in the science and technology of carbon nanotubes and their composites: A review. Composites Science and Technology. 2001;**61**:1899-1912

[22] Zhao J, Liu L, Guo Q, Shi J, Zhai G, Song J, Liu Z. Growth of carbon nanotubes on the surface of carbon fiber. Carbon. 2008;**46**:365-389

[23] Liu Z, Wang J, Kushvaha V, Poyraz S, Tippur H, Park S, Kim M, Liu Y, Bar J, Chen H, Zhang X. Poptube approach for ultrafast carbon nanotube growth. Chemical Communications. 2011;**47**:9912-9914

[24] Dey NK, Hong EM, Choi KH, Kim YD, Lim JH, Lee KH, Lim DC. Growth of carbon nanotubes on carbon fiber by thermal CVD using Ni nanoparticles as catalysts. Process Engineering. 2012;**36**:556-561

[25] Greef ND, Zhang L, Magrez A, Forro L, Locquet JP, Verpoest I, Seo JW. Direct growth of carbon nanotubes on carbon fibers: Effect of the CVD parameters on the degradation of mechanical properties of carbon fibers. Diamond and Related Materials. 2015;**51**:39-48

[26] Atchudan R, Perumal S, Edison TNJ, Pandurangan A, Lee YR. Synthesis and characterization of graphenated carbon nanotubes on IONPs using acetylene by chemical vapor deposition method. Physica E: Low-dimensional Systems and Nanostructures. 2015;**74**:355-362

[27] Homma Y, Kobayashi Y, Ogino T, Takagi D, Ito R, Jung YJ, Ajayan PM. Role of transition metal catalysts in single-walled carbon nanotube growth in chemical vapor deposition. The Journal of Physical Chemistry. B. 2003;**107**:12161-12164

[28] Hofmann S, Blume R, Wirth CT, Cantoro M, Sharma R, Ducati C, Havecker M, Zafeiratos S, Schnoerch P, Oestereich A, Teschner D, Albrecht M, Knop-Gericke A, Schlogl R, Robertson J. State of transition metal catalysts during carbon nanotube growth. Journal of Physical Chemistry C. 2009;**113**:1648-1656

[29] Tehrani M, Boroujeni AY, Luhrs C, Phillips J, Al-Haik MS. Hybrid composites based on carbon fiber/carbon nanofilament reinforcement. Materials. 2014;**7**:4182-4195

[30] Kind M, Bonard JM, Forro L, Kern K. Printing gel-like catalysts for the directed growth of multiwall carbon nanotubes. Langmuir. 2000;**16**:6877-6883

[31] Lim S, Yoon SH, Shimizu Y, Jung H, Mochida I. Surface Control of activated carbon fiber by growth of carbon nanofiber. Langmuir. 2004;**20**:5559-5563

[32] Tzeng SS, Hung KH, Ko TH. Growth of carbon nanofibers on activated carbon fiber fabrics. Carbon. 2006;**44**:859-865

[33] Ghaemi F, Ahmadian A, Yunus R, Ismail F, Rahmanian S. Effects of thickness and amount of carbon nanofiber coated carbon fiber on improving the mechanical properties of nanocomposites. Nanomaterials. 2016;**6**:6

[34] Che G, Lakshmi BB, Martin CR, Fisher ER, Ruoff RS. Chemical vapor deposition based synthesis of carbon nanotubes and nanofibers using a template method. Chemistry of Materials. 1998;**10**:260-267

[35] Ehlert GJ, Galan U, Sodano HA. Role of surface chemistry in adhesion between ZnO nanowires and carbon fibers in hybrid composites. ACS Applied Materials & Interfaces. 2013;**5**:635-645

[36] Deka BK, Kong K, Seo J, Kim D, Park YB, Park HW. Controlled growth of CuO nanowires on woven carbon fibers and effects on the mechanical properties of woven carbon fiber/polyester composites. Composites: Part A. 2015;**69**:56-63

[37] Fei J, Zhang C, Luo D, Cui Y, Li H, Lu Z, Huang J. Bonding TiO_2 array on carbon fabric for outstanding mechanical and wear resistance of carbon fabric/phenolic composite. Surface and Coating Technology. 2017;**317**:75-82

[38] Steiner SA. Carbon Nanotube Growth on Challenging Substrates: Application for Carbon-Fiber Composites. Cambridge, Massachusetts, USA: Massachusetts Institute of Technology; 2012

[39] Sheveleva IV, Zemskova LA, Voit AV, Kuryavyi VG, Sergienko VI. Study of the formation and electrochemical properties of nickel oxide-carbon fiber composites obtained in the presence of surfactants. Russian Journal of Electrochemistry. 2011;**47**:1220-1226

[40] Abdurhman AAM, Zhang Y, Zhang G, Wang S. Hierarchical nanostructured noble metal/metal oxide/graphene-coated carbon fiber: In situ electrochemical synthesis and use as microelectrode for real-time molecular detection of cancer cells. Analytical and Bioanalytical Chemistry. 2015;**407**:8129-8136

[41] Zhang L, Gong H. A cheap and non-destructive approach to increase coverage/loading of hydrophilic hydroxide on hydrophobic carbon for lightweight and high-performance supercapacitors. Scientific Reports. 2015;**5**:18108

[42] Dong N, He F, Xin J, Wang Q, Lei Z, Su B. A novel one-step hydrothermal method to prepare $CoFe_2O_4$/graphene-like carbons magnetic separable adsorbent. Materials Research Bulletin. 2016;**80**:186-190

[43] Malakooti MH, Hwang HS, Sodano HA. Morphology-controlled ZnO nanowire arrays for tailored hybrid composites with high damping. ACS Applied Materials & Interfaces. 2015;**7**:332-339

[44] Skandani AA, Masghouni N, Case SW, Leo DJ, Al-Haik M. Enhanced vibration damping of carbon fibers-ZnO nanorods hybrid composites. Applied Physics Letters. 2012;**101**:073111

[45] Pozegic TR, Anguita JV, Hamerton I, Jayawardena KDGI, Chen JS, Stolojan V, Ballocchi P, Walsh R, Silva SRP. Multi-functional carbon fibre composites using carbon nanotubes as an alternative to polymer sizing. Scientific Reports. 2016;**6**:37334

[46] Pozegic TR, Hamerton I, Anguita JV, Tang W, Ballocchi P, Jenkins P, Silva SRP. Low temperature growth of carbon nanotubes on carbon fibre to create a highly networked fuzzy fibre reinforced composite with superior electrical conductivity. Carbon. 2014;**74**:319-328

[47] Tehrani M, Safdari M, Boroujeni AY, Razavi Z, Case SW, Dahmen K, Garmestani H, Al-Haik MS. Hybrid carbon fiber/carbon nanotube composites for structural damping applications. Nanotechnology. 2013;**24**:155704

[48] Romhany G, Szebenyi G. Interlaminar fatigue crack growth behavior of MWCNT/carbon fiber reinforced hybrid composites monitored via newly developed acoustic emission method. Express Polymer Letters. 2012;**6**:572-580

[49] Aziz S, Rashid SA, Rahmanian S, Salleh MA. Experimental evaluation of the interfacial properties of carbon nanotube coated carbon fiber reinforced hybrid composites. Polymer Composites. 2015;**36**:1941-1950

[50] Boroujeni AY, Tehrani M, Nelson AJ, Al-Haik M. Effect of carbon nanotubes growth topology on the mechanical behavior of hybrid carbon nanotube/carbon fiber polymer composites. Polymer Composites. 2016;**37**:2639-2648

[51] Bekyarova E, Thostenson ET, Yu A, Kim H, Gao J, Tang J, Hahn HT, Chou TW, Itkis ME, Haddon RC. Multiscale carbon nanotube–carbon fiber reinforcement for advanced epoxy composites. Langmuir. 2007;**23**:3970-3974

[52] Qin W, Vautard F, Askeland P, Yu J, Drzal L. Modifying the carbon fiber–epoxy matrix interphase with silicon dioxide nanoparticles. RSC Advances. 2015;**5**:2457

[53] Chi Y, Chu J, Chen M, Li C, Mao W, Piao M, Zhang H, Liu BS, Shi H. Directly deposited graphene nanowalls on carbon fiber for improving the interface strength in composites. Applied Physics Letters. 2016;**108**:211601

[54] Xiao J, Wan L, Yang S, Xiao F, Wang S. Design hierarchical electrodes with highly conductive $NiCo_2S_4$ nanotube arrays grown on carbon fiber paper for high-performance pseudocapacitors. Nano Letters. 2014;**14**:831-838

[55] Zhu Y, Fan X, Suo L, Luo C, Gao T, Wang C. Electrospun FeS_2@carbon fiber electrode as a high energy density cathode for rechargeable lithium batteries. ACS Nano. 2016;**10**:1529-1538

[56] Wang X, Li W, Xiong D, Petrovykh DY, Liu L. Bifunctional nickel phosphide nanocatalysts supported on carbon fiber paper for highly efficient and stable overall water splitting. Advanced Functional Materials. 2016;**26**:4067-4077

[57] Tao J, Liu N, Ma W, Ding L, Li L, Su J, Gao Y. Solid-state high performance flexible supercapacitors based on polypyrrole-MnO_2-carbon fiber hybrid structure. Scientific Reports. 2013;**3**:2286

[58] Wang H, Lu Z, Xu S, Kong D, Cha JJ, Zheng G, Hsu PC, Yan K, Bradshaw D, Prinz FB, Cui Y. Electrochemical tuning of vertically aligned MoS_2 nanofilms and its application in improving hydrogen evolution reaction. Proceedings of the National Academy of Sciences of the United States of America. 2013;**110**:19701-19706

[59] Kong D, Wang H, Lu Z, Cui YJ. $CoSe_2$ nanoparticles grown on carbon fiber paper: An efficient and stable electrocatalyst for hydrogen evolution reaction. American Chemical Society. 2014;**136**:4897-4900

[60] Xiao X, Li T, Yang P, Gao Y, Jin H, Ni W, Zhan W, Zhang X, Cao Y, Zhong J, Gong L, Yen W, Mai W, Chen J, Huo K, Chueh Y, Wang Z, Zhou J. Fiber-based all-solid-state flexible supercapacitors for self-powered systems. ACS Nano. 2012;**6**:9200-9206

[61] Wang C, Wan W, Huang Y, Chen J, Zhou H, Zhang X. Hierarchical MoS_2 nanosheet/active carbon fiber cloth as a binder-free and free-standing anode for lithium-ion batteries. Nanoscale. 2014;**6**:5351

[62] Luo Y, Jiang J, Zhou W, Yang H, Luo J, Qi X, Zhang H, Yu DYW, Li CM, Yu T. Self-assembly of well-ordered whisker-like manganese oxide arrays on carbon fiber paper and its application as electrode material for supercapacitors. Journal of Materials Chemistry. 2012;**22**:8634

[63] Yang L, Cheng S, Ding Y, Zhu X, Wang ZL, Liu M. Hierarchical network architectures of carbon fiber paper supported cobalt oxide nanonet for high-capacity pseudocapacitors. Nano Letters. 2012;**12**:321-325

[64] Cakici M, Reddy KR, Alonso-Marroquin F. Advanced electrochemical energy storage supercapacitors based on the flexible carbon fiber fabric-coated with uniform coral-like MnO_2 structured electrodes. Chemical Engineering Journal. 2017;**309**:151-158

[65] Xu W, Dai S, Liu G, Xi Y, Hu C, Wang X. CuO nanoflowers growing on carbon fiber fabric for flexible high-performance supercapacitors. Electrochimica Acta. 2016;**203**:1-8

[66] Pu Z, Liu Q, Asiri AM, Sun X. Tungsten phosphide nanorod arrays directly grown on carbon cloth: A highly efficient and stable hydrogen evolution cathode at all pH values. ACS Applied Materials & Interfaces. 2014;**6**:21874-21879

Chapter 4

3D Woven Composites: From Weaving to Manufacturing

Hassan M. El-Dessouky and Mohamed N. Saleh

Additional information is available at the end of the chapter

http://dx.doi.org/10.5772/intechopen.74311

Abstract

Manufacturing near-net shape preforms of fibre-reinforced composites has received growing interest from industry. Traditionally, a preform was made from 2D fabrics, but recently, it has been shown that 3D textiles can be used with success; with weaving being the predominant technology for carbon fibre composites. In 3D weaving, weft, warp and binder fibres run across, along and through the fabrics in the X, Y and Z directions, respectively. Producing a unitised single-piece fabric and subsequently reducing the takt time required for rapid composite manufacturing are two of the main advantages of using 3D woven preforms. Weaving of 3D fabrics, manufacturing of 3D composites, physical characterisation and mechanical testing of infused composites samples are discussed in this chapter. Finally, a large automotive composite made of single-piece 3D woven preform was manufactured and presented for demonstration.

Keywords: 3D woven composites, carbon fibre, manufacturing, mechanical properties, resin transfer moulding (RTM)

1. Introduction

Two-dimensional (2D) laminated composites are characterised by their in-plane high specific stiffness and strength [1]. However, many real life applications are exposed to out-of-plane loading conditions that make it impossible to resort to the 2D laminates as the proper solution. Wind turbine blades, stringers and stiffeners in aircraft, pressure vessels and construction applications are some examples of applications in which out-of-plane loading conditions are imposed on the structure. Thus, the need for composite materials with enhanced through-thickness "out-of-plane" properties has emerged. This need requires replacing

2D laminated composites with three-dimensional (3D) textile structures. The "enhanced out-of-plane properties" is not the only advantage of 3D composites. The delamination resistance, due to the z-binder existence, enhances the impact performance and damage tolerance of such material systems [2]. In addition, using textile technology can be utilised to manufacture near-net-shape preforms. So, it reduces the manufacturing/machining cost and time even further. Although various techniques exist for manufacturing 3D textile preforms, the most widely used nowadays is weaving due to its high production rate along with the ability to produce various 3D woven structures [1]. In terms of the energy consumption required for textile production, it depends very much on the type of the yarn and the weaving pattern. For example one of the published studies entitled "Material Intensity of Advanced Composite Materials" [3], reported that the average figure for the electricity consumption is approximately 0.11 kWh per m^2 for glass fibres and 0.214 kWh/m^2 for carbon fibres.

Generally, 3D woven composites can be divided into two main groups depending on how deep the binder penetrates through the fabric. If it penetrates all the way through the thickness it is referred to as through-thickness (TT) interlock (see **Figure 1a, c**) while it is classified as layer-to-layer (LTL) if the binder only holds adjacent layers (see **Figure 1b**). Then this classification is further divided according to the interlacing angle of the structure. The first category is the angle interlock (AI) in which the interlacing angle between the binder and weft yarns can have any value except 90° (**Figure 1c**). The second category is a special case of the first one. The orthogonal interlock (ORT) (**Figure 1a**) occurs when the interlacing angle between the binder and weft yarns is equal to 90° [1].

The weave pattern used during the weaving process can also affect the classification of 3D woven composites. For instance in the case of ORT weave, the frequency of the z-binder sweeping the top and bottom surfaces of the weave can vary from plain (**Figure 2a**) to twill (**Figure 2b**) or satin (**Figure 2c**) pattern. This will directly affect the unit-cell size, degree of crimp, elastic response and damage/delamination resistance as highlighted previously in [4–6].

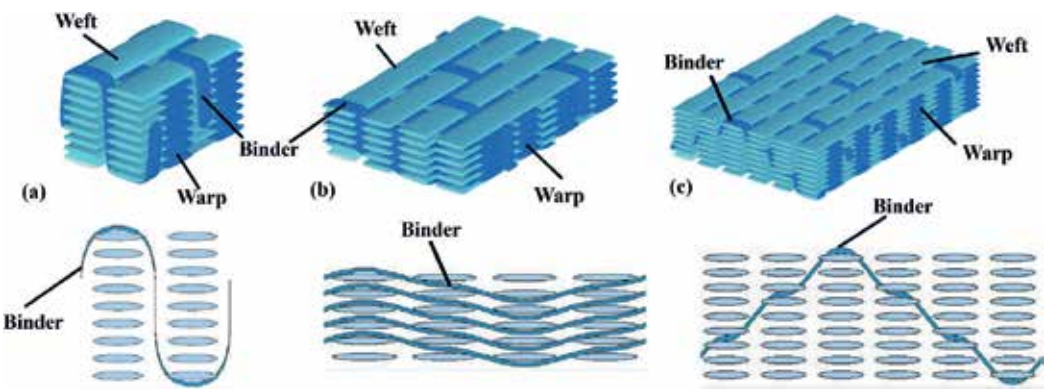

Figure 1. Types of 3D woven composites based on the binder path: (a) ORT, (b) LTL and (c) AI [4].

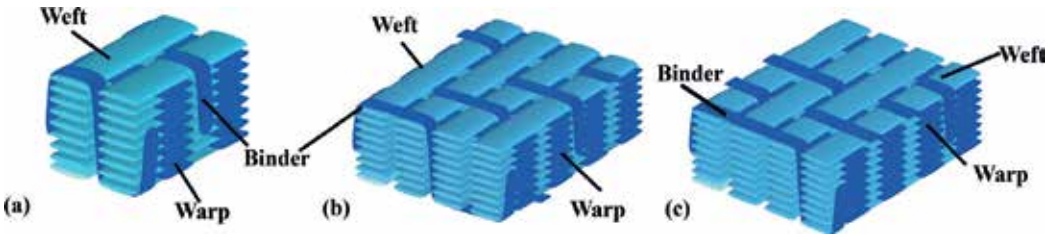

Figure 2. Examples of possible weave binding patterns for ORT: (a) plain, (b) twill and (c) satin [4].

The applications of 3D woven composites have been growing tremendously in industry recently [7–9]. In applications that require load transfer around a bend such as curved beams, T-joints and brackets, 3D woven AI and LTL architectures have been utilised [10]. The main advantages observed for these architectures are that they have better interlaminar shear and radial stress resistance. In addition, McClain [2] reported successfully using 3Dwoven AI and LTL architectures in truss beams with integrated off-axis stiffeners. Applications [2] in which continuous fibres are required for joining skin and stiffening elements as well managed to utilise those previously highlighted architectures, and consequently overcoming the need for bonding or fastening composite parts which is one of the major challenges facing 2D laminated composite nowadays. 3D woven LTL composites have been utilised in the automotive industry [11–13]. Not only LTL and AI woven composites have managed to find their way into industry, but also their ORT woven counterparts. For example, Bayraktar et al. [11] reported using ORT woven composites to replace high-strength steel beams. Hemrick et al. [14] reported the use of ORT woven composite in ultra-light weight heat exchangers in the automotive industry. The concept utilises the high thermal conductivity of ORT woven composites due to the through-thickness binding yarns creating a conduction path for the heat to dissipate. Moreover, ORT woven composites have been successfully employed in the LEAP project to manufacture engine casings and fan blades for A-320-neo, 737-MAX and Comac C-919 [15].

Considering the environmental impact, the technique presented in this study can be used to weave recycled carbon fibre yarns. There are commercially available yarns produced from recycled short carbon fibre. However, from structural and strength point of view, these yarns are not recommended to be used as the principal reinforcing material in FRP composites. They can still be used as a secondary material. For instance, along the warp direction in a weaving process, continuous carbon fibre yarns can be used as the principal material while the recycled carbon fibre yarns can be used as a secondary material along the weft direction depending on the loading experienced by the structural component.

In this chapter, a case study on manufacturing a complex automotive part from 3D composite is discussed. Considering the fabric drapeability and conformity, one of the most common 3D woven architectures, LTL weave is considered in this study. The design and weaving of three weave patterns of LTL: plain, twill and satin weaves (LTL-PW, LTL-TW and LTL-SW) are presented. Flat composite panels are manufactured using resin transfer moulding (RTM). The quality and integrity of the manufactured composite samples are physically characterised

through optical microscopy, density measurements, voids content and fibre volume fraction analysis. To observe the differences in mechanical properties between the different LTL weave designs, composite samples are mechanically tested to failure using tensile and flexure 3-point bending tests. The possibility of manufacturing a large and complex automotive component of multi-weave (LTL-PW, LTL-TW & LTL-SW) composite is demonstrated.

2. Experimentation

2.1. Weave design

Recently developed weave-design software (EAT-3D Module) for composite structures is used to design LTL plain, twill and satin weaves; each of which contains five warp and five weft layers. All weaves were designed with the same drafting plan to weave fabrics with the same loom setup and change weave designs within the same piece of fabric to produce a multi-weave preform. **Figure 3** demonstrates the schematic of the three different fabrics, with the warp yarns highlighted in blue, the weft yarns are in red and the through thickness binders are shown in green.

A Dornier double-rapier FT-Dobby loom was used in this study. The machine was commissioned to weave conventional 2D fabrics, but it has been recently modified to weave 3D structures (See **Figure 4**). A creel of 912 positions was loaded with T300-6 k carbon fibre bobbins to warp the loom. The creel is equipped with central tension control to alter the tension of warp and binder during the weaving process. **Figure 4** shows the setup of weaving machine (loom & creel) used to weave the 3D weave designs mentioned above. Considering the configuration of the automotive demonstrator (750 × 700 × 2 mm) and the creel number of ends (912) available, the densities in the warp and the weft were set up to 12.66 ends/cm and 21.00 picks/cm respectively. The unbalanced fabric sett or density allows better handle-ability, stability and transferability of woven preforms that is not achievable in the case of the balanced sett.

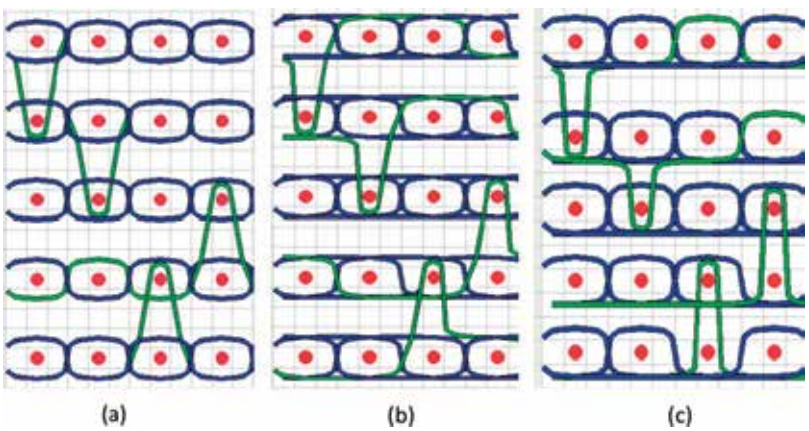

Figure 3. Schematic cross-sections of weaves designed: (a) LTL-PW, (b) LTL-TW and (c) LTL-SW.

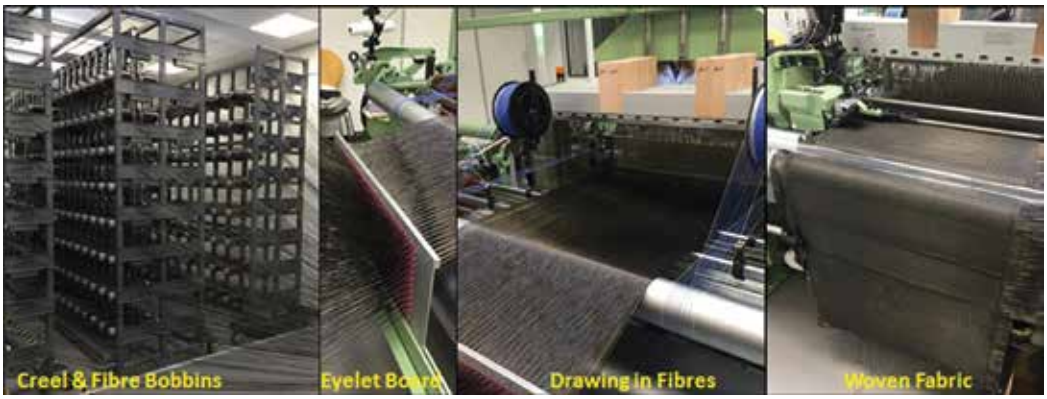

Figure 4. Weaving setup.

All fabrics produced have approximately the same areal density (~1350 gsm) to ensure fibre volume fraction (~50%) in the final composite.

2.2. Composite panels manufacturing

A resin transfer moulding (RTM) tool of 320 × 310 mm was used to manufacture flat composite panels. Gurit T-Prime 130-1 epoxy was used and mixed at: 100/27 by wt% of resin/hardener. The density of the cured resin was measured to be 1.156 g/cm^3. The laminate thickness was designed to be 1.5 mm. Heater pads were positioned on the outside of the tool to heat it. The tool was preheated to 80°C. Prior to injecting the resin, it was degassed in a degassing chamber for 30 min, and then placed in a pressure pot. The resin was injected at 2 bars of pressure, and −1 bar of vacuum was attached to the outlet tube. When the resin had fully wetted the preform the outlet pipe was clamped, the pressure was left on for a further 15 min to ensure the entire mould had an even pressure and compaction and that any air bubbles would shrink to reduce voids in the final composite. The panels were left to cure in the mould for 1 hour at 80°C after the outlet pipe was clamped.

2.3. Physical characterisation of composite samples

2.3.1. Density, fibre volume fraction and void content

In order to examine the quality and integrity of the manufactured composite, physical characterisation of the RTM panels was conducted. The fibre-volume fraction (V_f) analysis was carried out in accordance with ASTM D 3171 standard [16]. A minimum of 6 specimens were cut from random locations from the cured laminates resulting in total of 18 specimens for the three different architectures. According to the ASTM standard, the minimum weight of each specimen has to be 1 g to be able to determine the void content, so specimens' weight in this study was approximately 1.2 g. The density of the specimens was determined, before the burn-off, using AccuPyc II 1340 Gas Pycnometer from micromeritics. Then, the furnace was adjusted at 600°C and the burn-off duration for each specimen was approximately 25 min. The calculation of fibre, matrix and voids content (%) is depicted as follows:

$$V_f = \left(M_f / M_i\right) \times \left(\rho_c / \rho_r\right) \times 100 \quad (1)$$

$$V_m = \left(M_i - M_f\right) / M_i \times \left(\rho_c / \rho_r\right) \times 100 \quad (2)$$

$$V_v = 100 - \left(V_f + V_m\right) \quad (3)$$

where M_i is the initial mass of specimen before burn-off, g, M_f is the final mass of specimen after burn-off, g, ρ_r is the density of the reinforcement/fibre, g/cm^3, ρ_c is the density of the composite specimen, g/cm^3, ρ_m is the density of the matrix, g/cm^3, V_f is the fibre volume percentage, V_m is the matrix volume percentage, V_v is the voids volume percentage.

Table 1 lists the V_f analysis results. The volume of voids (V_v) in all composites was found to be negative. This can be attributed to the experimental error during the V_f analysis, which suggests that the manufactured panels for all 3D woven fabrics were free from voids. Optical microscopy images support this observation as discussed later in this section.

2.3.2. Optical microscopy

Using two-part epoxy compound the composite specimens (20 × 20 mm) were cured in 30 mm diameter resin blocks. The polishing procedure was as follows: silicon carbide SiC-220 for 20 s and SiC-1200 for 2 min until flat, 9-μ (MD-Plan) for 4 min, 3-μ (MD-Dac) for 4 min and OP-S for 2.5 min plus 1 min on water to clean OP-S off. Rotation speed was 150 rpm and applied force per sample was 30 N. Alicona-IFM-G4 microscope was used to optically scan the polished sections and optical images were captured for illustration.

Figure 5 depicts the optical cross-sections of the three composite laminates across weft direction (top image) and across warp direction (bottom image); (a) LTL-PW, (b) LTL-TW, and (c) LTL-SW. The arrangement of weft, warp and binder tows is marked (see **Figure 5**) for clarification.

To further investigate the composite's integrity, wettability and porosity, **Figure 6** shows a selection of the zoomed-in optical images taken from the cross-sections displayed in **Figure 5** for the three LTL weaves plain, twill and satin respectively. The optical cross-sections were captured along the warp (left) and weft (right) directions. No voids were observed which suggests that the binding yarns behaved as channels for the resin to follow during the

Property/weave	LTL-PW	LTL-TW	LTL-SW
Density (g/cm^3)	1.438 ± 0.005	1.456 ± 0.017	1.464 ± 0.006
V_f (%)	46.51 ± 0.66	48.12 ± 1.05	48.71 ± 0.46
V_v (%)	−0.06 ± 0.35	−0.70 ± 0.96	−1.24 ± 0.40

Table 1. Results of the fibre volume fraction analysis.

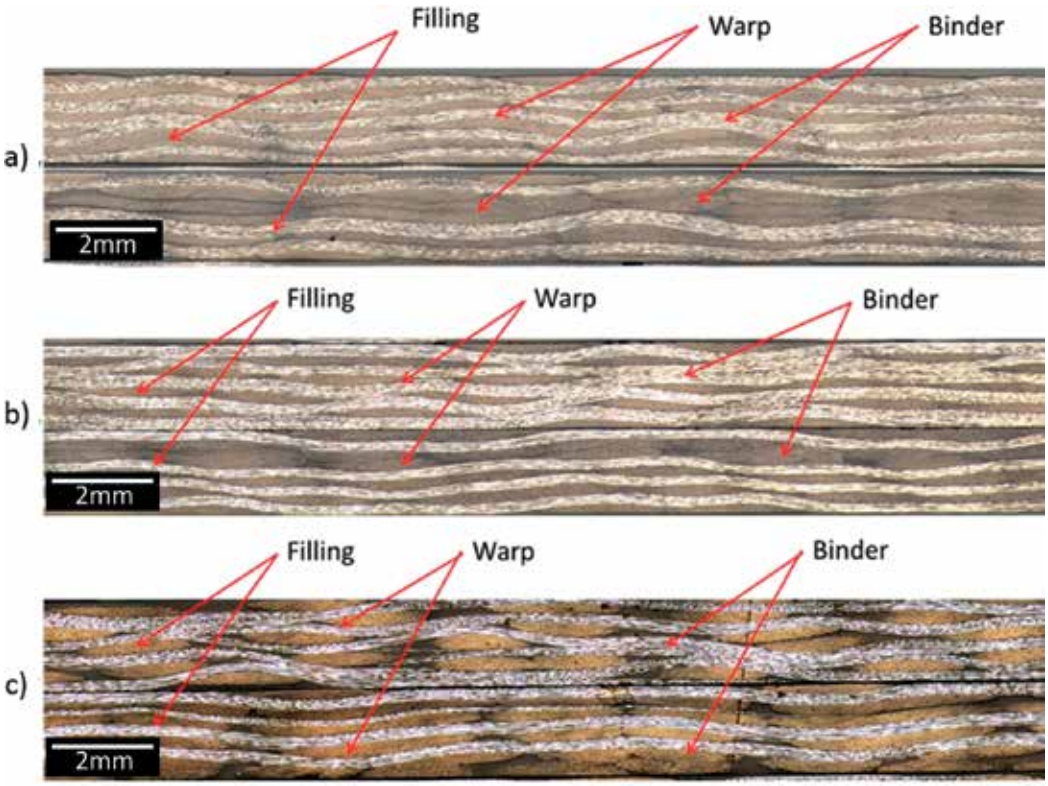

Figure 5. Optical cross-sections of the composite laminates at a low magnification: (a) LTL-PW, (b) LTL-TW and (c) LTL-SW.

infusion process. On the other hand, the existence of binding yarns in 3D woven architectures creates resin rich areas (RRA) in the cured composite. RRA, present between yarns, have been reported as one of the drawbacks of using 3D woven composites as they allow cracks to propagate quickly and cause failure at specific locations in the fabric architecture upon loading [17].

2.4. Mechanical testing

Mechanical testing was carried out to observe the differences in mechanical properties between the different weave designs. The composite laminates manufactured by RTM were mechanically tested to failure using tensile and flexure 3-point bending tests at AMRC Advanced Structural Testing Centre (ASTC). These two tests were chosen to represent some of the different loading conditions that a composite part may experience to during its commercial use. All the tests were carried out in the warp and weft direction as each direction exhibits different properties due to the fibre counts and orientations in each direction. Six specimens were tested for each direction to assure repeatability. All the specimens had a thickness of approximately 1.5 mm.

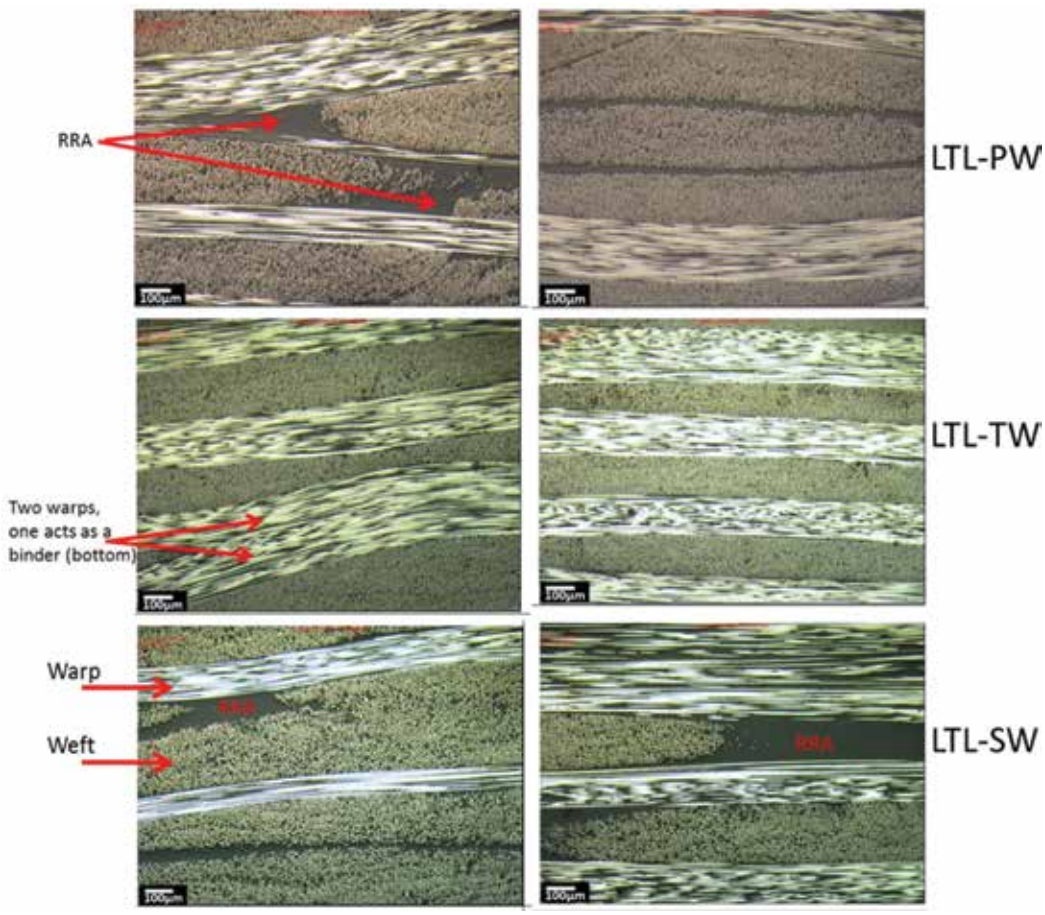

Figure 6. A selection of optical cross-sections of the composite samples at a higher magnification across the weft (left) and warp (right) directions.

In the tensile and flexural results a general observation is the modulus and strength results in the weft direction are significantly higher in comparison to the warp direction for all the fabrics. This could be attributed to two main reasons; (i) the directional V_f whereby the V_f in the weft direction is almost double the V_f in the warp direction, (ii) the warp yarns experience higher crimp due to the interlacement points between the layers making them susceptible to localised stress leading to premature localised damage and ultimate failure. These reasons are further highlighted in the following sections in the summary tables for the modulus and strength results.

2.4.1. Tensile testing

Following ASTM D3039, tensile tests were carried out. **Figure 7** shows the tensile stress–strain graphs for each material including the test setup. The graphs show the repeatability of the test

in each direction. The warp specimens are highlighted as solid lines and the weft specimens as dashed lines.

Tables 2 and **3** summarise the tensile results in the warp and weft direction along with the directional V_f. In both the warp and weft direction the LTL-PW composite performed the least in strength and modulus. Within the plain weave fabric the yarns are undergoing constant undulation. This undulation creates more interlacement points within the fabric which affects the modulus in the linear elastic regime and during the tensile extension the interlacing points create localised stress affecting the ultimate strength.

The LTL-SW demonstrated the highest modulus in the warp and weft directions. This is due to the directional V_f which is higher in the LTL-SW compared to the other weaves as it contains the least amount of crimp.

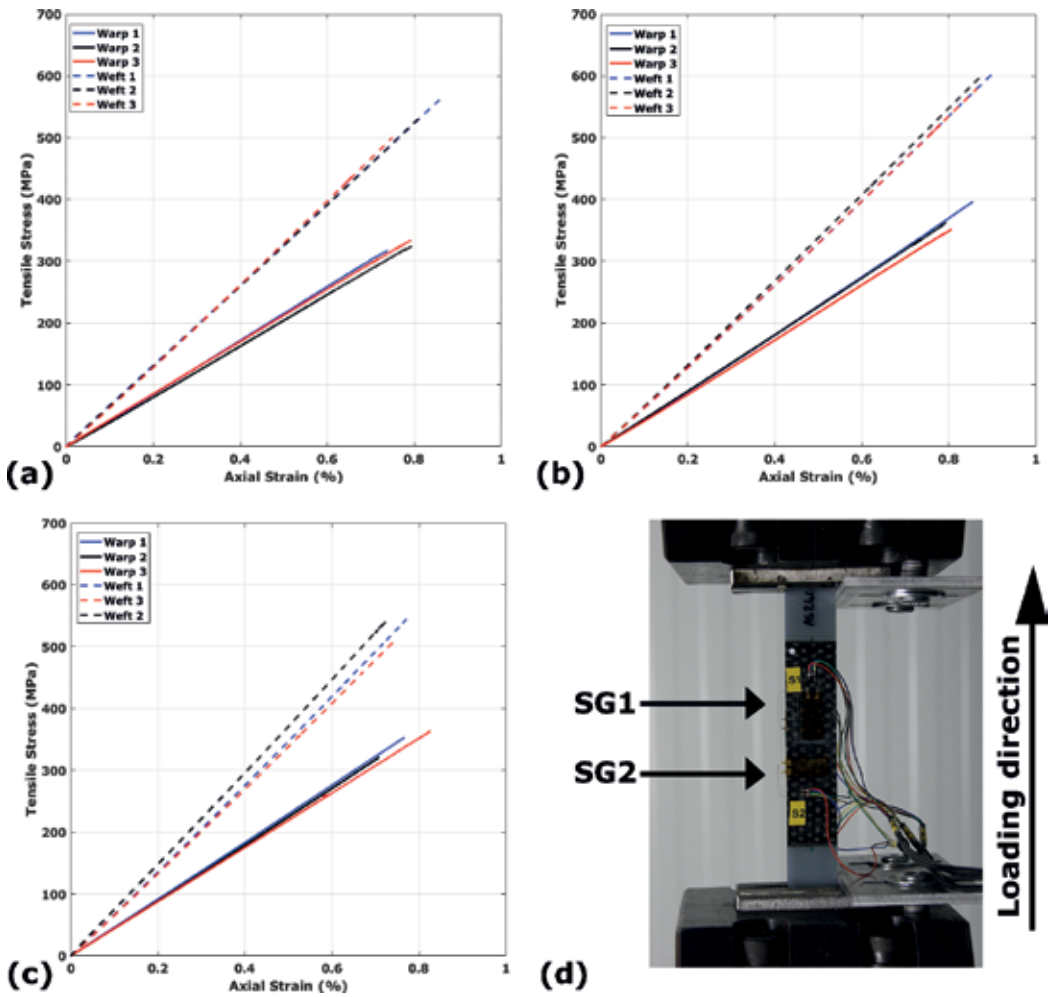

Figure 7. (a–c) Tensile stress–strain graphs: (a) LTL-PW, (b) LTL-TW, (c) LTL-SW and (d) test setup.

Warp direction	V_f (%)	Modulus (GPa)	Tensile strain (%)	Tensile strength (MPa)
LTL-PW	17.50 ± 0.25	41.25 ± 1.49	0.83 ± 0.08	335.26 ± 15.24
LTL-TW	18.11 ± 0.39	44.20 ± 0.98	0.80 ± 0.04	359.56 ± 22.45
LTL-SW	18.33 ± 0.17	51.52 ± 9.56	0.69 ± 0.11	345.47 ± 15.80

Table 2. Tensile results in the warp direction.

Weft direction	V_f (%)	Modulus (GPa)	Tensile strain (%)	Tensile strength (MPa)
LTL-PW	29.01 ± 0.41	63.46 ± 3.18	0.82 ± 0.05	525.86 ± 24.08
LTL-TW	30.01 ± 0.65	67.74 ± 2.38	0.84 ± 0.06	582.89 ± 32.78
LTL-SW	30.38 ± 0.29	70.99 ± 2.54	0.79 ± 0.07	575.11 ± 65.96

Table 3. Tensile results in the weft direction.

The failure strain of the fibre used (12 k-T300) is 1.5%. The measured failure strain from the test was 50% lower due to the interlacing nature between warp and weft yarns within the fabrics. It is possible that higher localised stress/strain than measured was experienced, at the interlacements or the matrix RRA, causing failure of the coupons. Saleh et al. [6] used a digital image correlation system during tensile testing which showed areas where interlacement points occurred to experience high strain values near failure of the coupon.

2.4.2. Flexure testing

Using ASTM D7264, 3 point bending flexure tests were carried out. The flexure stress–strain curves of all the tested architectures are represented in **Figure 8** along with the test setup. In the graphs the warp results are plotted as solid lines and the weft results as dashed lines. The graphs show good repeatability between the repeats in each direction. As expected, all specimens behave in a linear elastic manner up to failure as they are loaded along the fibre direction, in either the warp or weft direction.

Tables 4 and **5** summarise the flexural properties obtained in correspondence with the V_f in both directions, warp and weft.

The flexural modulus of composite materials is a function of the composite lay-up/ stacking sequence. More precisely, it is a function of how far the aligned plies with the loading direction are from the mid-plane of the cured laminate as well as the volume fraction in this specific direction. Ideally for isotropic materials, the flexure modulus should not differ from the tensile modulus for the same material such as metals, however practically this is not the case especially in the case of fibre reinforced polymers because of their orthotropic nature. Thus, flexure testing is not ideal for determining the modulus and it is recommended that the tensile modulus is used over the flexural modulus.

As a general remark, the main difference between the flexure test and the tensile test in this study is that the tested specimen in the case of flexure testing experiences both tensile and

http://dx.doi.org/10.5772/intechopen.74311

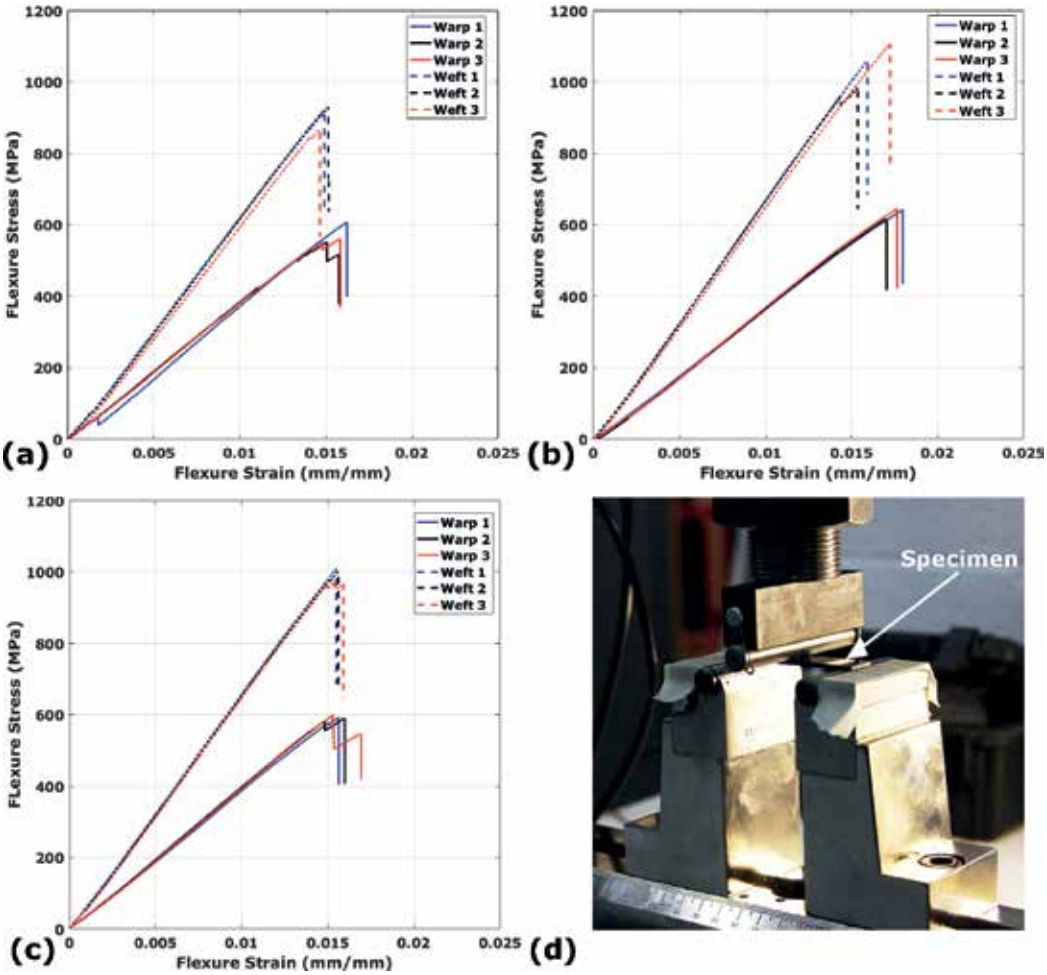

Figure 8. (a-c) Flexure stress–strain graphs: (a) LTL-PW, (b) LTL-TW, (c) LTL-SW and (d) test setup.

compressive stresses in the lower and the upper surfaces respectively due to the nature of the imposed loading condition. So, it is not straight forward to determine the reason behind final fracture as it might be a mixed mode. It seems there is a trend in the obtained results, but it is difficult to justify this behaviour without carrying out a detailed damage propagation investigation by different techniques such as X-ray CT, optical microscopy or acoustic emission techniques.

Warp direction	V_f (%)	Modulus (GPa)	Flexural strain (%)	Flexural strength (MPa)
LTL-PW	17.50 ± 0.25	35.58 ± 5.19	1.53 ± 0.10	574.07 ± 30.31
LTL-TW	18.11 ± 0.39	33.99 ± 2.91	1.73 ± 0.10	644.88 ± 51.72
LTL-SW	18.33 ± 0.17	35.16 ± 2.18	1.56 ± 0.02	573.27 ± 37.43

Table 4. Flexural results in the warp direction.

Weft direction	V_f (%)	Modulus (GPa)	Flexural strain (%)	Flexural strength (MPa)
LTL-PW	29.01 ± 0.41	57.48 ± 2.46	1.48 ± 0.02	902.30 ± 19.58
LTL-TW	30.01 ± 0.65	62.84 ± 2.14	1.54 ± 0.10	996.42 ± 64.00
LTL-SW	30.38 ± 0.29	61.49 ± 2.44	1.53 ± 0.09	968.21 ± 65.16

Table 5. Flexural results in the weft direction.

3. Composite demonstrator manufacturing

The use of 2D fabrics in composite preforming applications is well established but there are two major deficiencies, the lack of reinforcement through thickness and labour cost, which drive the interest towards using 3D woven preform in high volume manufacturing such as automotive. Therefore, an automotive floor section made of 3D woven fabric is selected to be demonstrated. Traditionally such component (**Figure 9a**) was made of three discrete 2D preforms leading to some drawbacks such as: (i) preforms overlap, (ii) discontinuous fibres along the component, (iii) interlaminar delamination and (iv) labour time consuming. Considering the complex geometry of the demonstrator and to overcome the drawbacks of 2D fabrics, a drapeable and single –piece 3D woven preform is required to conform well to the intricate features of the demonstrator. The LTL architecture could be a suitable solution.

The fabric designed and produced for the generic automotive part was made up of 5 zones; each zone was made of a specific weave to suit the conformity of the area on the mould. For areas requiring high conformity (**Figure 9b**, zone 3), a satin weave was considered. The area (**Figure 9b**, zone 2) requires a medium conformity, so a twill weave was suggested. Whereas an area with low conformity (**Figure 9b**, zone 1) a plain weave was nominated. The preform of varying drapeable weave allows the fabric to conform to the mould and prevents the fabric from wrinkling.

The RTM mould of the generic automotive part was designed and manufactured from aluminium (**Figure 10**) and used to perform RTM injections of the fabric woven. The parts were injected from one inlet in the top half of the mould and four outlet points were positioned in each corner, on the bottom of the mould.

To preform and cut the 3D multiweave fabric, a template was used to hold the fabric in the correct position and shape whilst the fabric was cut. This method prevented the fabric from moving whilst being cut. Once the fabric was cut it was crucial not to move the fabric to prevent the fabric from fraying and distortion.

As with the flat panels, Gurit T-Prime 130-1 resin and hardener was used. The parts were injected at room temperature and placed in the oven after injection to cure at 80°C. During the injection −1 bar of vacuum was applied to the outlet, whilst the resin at the inlet was under pressure. At 2 bar of pressure the mould took 25 min for the resin to exit all the outlets and

http://dx.doi.org/10.5772/intechopen.74311

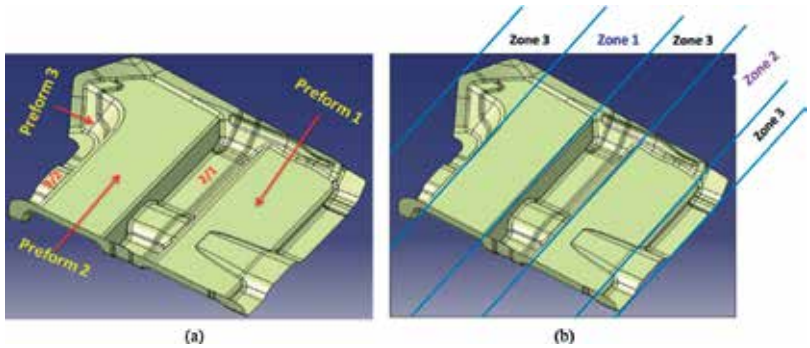

Figure 9. CAD of generic automotive component, (a) the use of three types of 2D preforms and (b) the use of a single 3D woven preform.

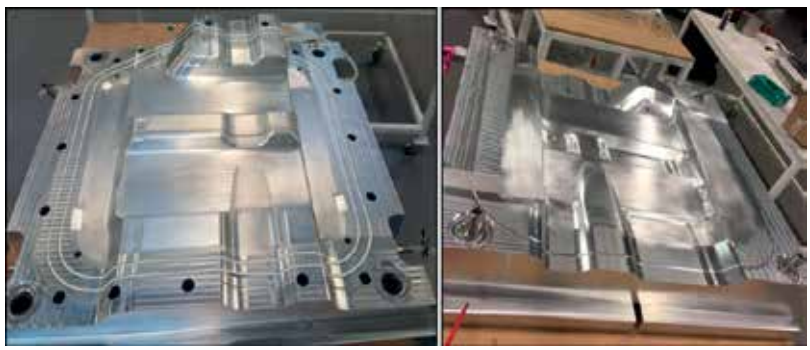

Figure 10. RTM mould: Male (left) and female (right) tools.

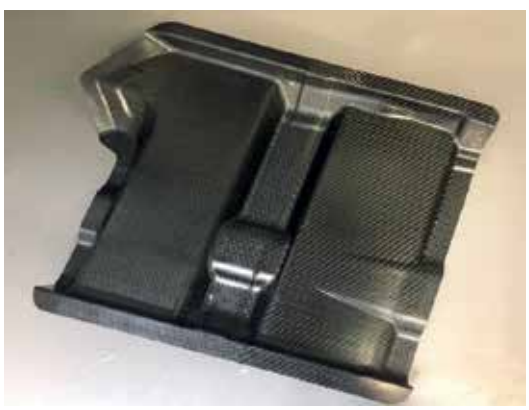

Figure 11. Automotive composite RTM cured part.

the pressure and inlet was left open for a further 30 min. Whereas at 3.5 bar of pressure the mould took 12 min for the resin to exit all the outlets and the pressure and inlet was left open for a further 22 min.

One of the successful RTM parts is demonstrated in **Figure 11**. Further investigations of the cured composite component are required to assess the quality of the RTM part and to determine the fibre volume fraction and voids content alongside with optical scans.

4. Conclusion

A standard loom equipped with a cost-effective shedding system, Dobby not Jacquard, was successfully used to weave 3D complex architectures. The density measurements and optical microscopy revealed that the RTM composite laminates made were voids free.

In the mechanical testing, the tensile and flexural results showed that the modulus and strength to be significantly higher in the weft direction. It is believed the difference is due to differences in the directional V_f and that the warp yarns experiencing significantly higher crimp. The LTL plain fabric exhibited the lowest mechanical properties due to the constant undulation and cross over points between the yarns in the fabric. It is thought that the cross over points created areas of high localised stress leading to earlier failure of the composite coupons. The LTL twill and satin fabric performed fairly similar to each other. The two fabrics had the same amount of cross over points (interlacing) between the warp and the weft, which was less than the plain woven fabric. Due to less crossover points in the fabrics, there were less areas of localised stress allowing the coupons to withstand higher loads.

Final fabric was woven with multiple zones made up of different weave patterns. The different zones corresponded to different areas on the generic automotive part to suit the varying conformity of the part. The fabric conformed well to the RTM tool and successful part was demonstrated.

5. Current limitations and future trends

There are still some limitations in the process of 3D weaving of carbon fibre for manufacturing composites. Two of the main limitations are the heavy tow weaving and the fibre orientation. Heavy tows more than 24 k are difficult to weave using conventional weaving machines. Moreover, fundamentally in weaving, the warp yarns run in one direction (x-direction) while the weft yarns run in the transverse direction (y-direction). Thus, it is quite challenging if different orientations for yarns are required to produce a multiaxial or off axis fabrics for instance. There are some research-scale weaving looms that are customised to produce biased 3D weaving but yet is commercialised to date.

Currently, 3D weaving represents an automated process which can provide through thickness reinforced composites at high laydown rates using fibrous materials in their least value added form. It therefore offers the ability to add functionality, reduce cost and hit rate requirements for high volume manufacture of composites compared to traditional 2D approaches. These benefits exist in the woven fabric itself, but to mechanically convert this fabric into a useable preform for a composite moulding operation, a number of solutions are required such as

thickness tapering, stabilisation & edge trimming. These additional processes add extra flexibility by moving the manufacturer from a weaver of fabric to a producer of composite preforms tailored to match performance specifications, therefore adding significant extra value. Current add-on processes often involve a number of slow manual operations to convert the fabric into a preform and, in many cases, also distort or damage it. Thus, the ultimate goal of weaving of 3D woven fabrics development is to achieve integrated manufacturing process via automation to overcome the slow manual operations in the composites' supply chain.

Acknowledgements

Authors would like to acknowledge the collaboration with the UK Catapult centres Manufacturing Technology Centre (MTC), National Composites Centre (NCC) and Warwick Manufacturing Group (WMG). Special thanks to AMRC composite centre staff involved: Alice Snape, Jody Turner, Hannah Tew and Richard Scaife.

Conflict of interest

The authors declare that they have no conflict of interest.

Author details

Hassan M. El-Dessouky[1,2,3]* and Mohamed N. Saleh[1]

*Address all correspondence to: hassanoptics@yahoo.com

1 Composites Centre, AMRC with Boeing, University of Sheffield, UK

2 Department of Fashion and Textiles, University of Huddersfield, UK

3 Physics Department, Mansoura University, Egypt

References

[1] Ansar M, Xinwei W, Chouwei Z. Modeling strategies of 3D woven composites: A review. Composite Structures. 2011;**93**:1947-1963. DOI: 10.1016/j.compstruct.2011.03.010

[2] Mcclain M, Senior R, Organic TE, Composites M. Overview of recent developments in 3D structures. Albany Engineered Composites. 2012:1-12

[3] Stiller H. Material Intensity of Advanced Composite Materials. Wuppertal: Wuppertal Institute for Climate, Environment and Energy; 1999

[4] Saleh MN, Soutis C. Recent advancements in mechanical characterisation of 3D woven composites. Mechanics of Advanced Materials and Modern Processes. 2017;**3**. DOI: 10.1186/s40759-017-0027-z

[5] Saleh MN, Wang Y, Yudhanto A, Joesbury A, Potluri P, Lubineau G, et al. Investigating the potential of using off-Axis 3D woven composites in composite joints' applications. Applied Composite Materials. 2016;**24**:377-396. DOI: 10.1007/s10443-016-9529-9

[6] Saleh MN, Yudhanto A, Potluri P, Lubineau G, Soutis C. Characterising the loading direction sensitivity of 3D woven composites: Effect of z-binder architecture. Composites. Part A, Applied Science and Manufacturing. 2016;**90**:577-588. DOI: 10.1016/j.compositesa.2016.08.028

[7] McHugh C. Creating 3-D, One Piece, Woven Carbon Preforms Using Conventional Weaving and Shedding. SAMPE Conf. vol. 45; 2009. pp. 33-41

[8] McHugh C. The Manufacture of One Piece Woven Three Dimensional Carbon Fiber Nodal Structures. SAMPE Conf.; 2010

[9] Chen X, Chen X, Taylor LW, Tsai L. An overview on fabrication of three- dimensional woven textile preforms for composites. Textile Research Journal. 2011;**81**:932-944. DOI: 10.1177/0040517510392471

[10] Redman C, Bayraktar H, Mcclain M. Curved Beam Test Behavior of 3D Woven Composites. SAMPE Conf; 2014

[11] Bayraktar H, Ehrlich D, Goering J, Mcclain M, Composites AE, Hampshire N, et al. 3D Woven Composites for Energy Absorbing. 20th Int. Conf. Compos. Mater., Copenhagen; 2015. pp. 19-24

[12] EL-Dessouky H, Snape A, Tew H, Scaife R, Modi DK, Kendall K, et al. Design, weaving and manufacture of a large 3d composite structure for automotive applications. 7th World Conf. 3D Fabr. their Appl. 3D Fabr. their Appl; 2016

[13] El-Dessouky HM, Snape AE, Turner JL, Saleh MN, Tew H, Scaife RJ. 3D weaving for advanced composite manufacturing: From research to reality. SAMPE. 2017;**2017**

[14] Hemrick JG, Lara-Curzio E, Loveland ER, Sharp KW, Schartow R. Woven graphite fiber structures for use in ultra-light weight heat exchangers. Carbon N Y. 2011;**49**:4820-4829. DOI: 10.1016/j.carbon.2011.06.094

[15] Jewell J, Kennedy R, Menard A. Full-scale LEAP Fan Blade-Out Rig Test Yields Outstanding Results; Advanced LEAP Fan Endurance Test Complete. CFM Power Flight; 2011

[16] ASTM-D3171. Standard test methods for constituent content of composite materials. ASTM International. 2010;**15**:1-6. DOI: 10.1520/D3529M-10.2

[17] Mahadik Y, Brown KAR, Hallett SR. Characterisation of 3D woven composite internal architecture and effect of compaction. Composites. Part A, Applied Science and Manufacturing. 2010;**41**:872-880. DOI: 10.1016/j.compositesa.2010.02.019

Chapter 5

Building Hierarchical Micro-Structure on the Carbon Fabrics to Improve Their Reinforcing Effect in the CFRP Composites

Feng Xu, Xusheng Du and Helezi Zhou

Additional information is available at the end of the chapter

http://dx.doi.org/10.5772/intechopen.74706

Abstract

Nano-fibers grafted on carbon fibers (CFs) has been of one of the most popular methods used for the carbon fibers surface treatment, which could significantly influence the interfacial properties between polymer matrix and carbon fibers in composites. This chapter demonstrated three novel carbon fibers surface treatment methods, they are carbon nanotubes (CNTs) grafted on CFs using catalysts formed in an ethanol flame, carbon fiber forests (CFFs) by carbon fiber surface brushing and abrading and ZnO nanowire grown onto CFs though a facile hydrothermal method respectively. Based on metal catalyst particles or dopamine-based functionalization formed onto the nano-fiber/CF interface, a good interfacial bonding strength between the nano-fiber and CFs was observed by an instrumented tip of an atomic force microscope and further improvement of interfacial shear strength with epoxy as measured by the single fiber pull out/microbond test was realized. The hierarchical micro-fibers on CF fabrics were then utilized to fabricate the laminates to characterize anti-delamination capacity (the mode I and mode II interlaminar fracture toughness) of these composite laminates, wherein carbon fiber fabrics were grafted with CNTs, short CFs and ZnO nanowires respectively.

Keywords: CNTs forests, ZnO nanowires, interfacial bonding, anti-delamination

1. Introduction

Carbon fiber reinforced polymer (CFRP) composite laminates have been widely used in weight-critical structures, such as aircraft, spacecraft, and racing cars, due to their excellent mass-specific mechanical properties. However, poor interlaminar toughness has become an

important limiting factor in practical structural applications. To overcome the deficiencies in through-thickness strength, lots of techniques were developed to improve the interlaminar fracture toughness of CFRP composites by toughening the resin with various reinforcements [1]. Although toughened bulk resins exhibit higher toughness value, they only provide limited improvement on the delamination resistance in the CFRP composites in most cases due to the limitation by the carbon fibers [2]. Moreover, some processing problems were inevitably caused by the increasing viscosity of the resin due to the presence of high content of fillers. The challenge remains, therefore, to develop a new solution to facilitate practical applications of such composites as reliable and robust structural material.

The building up of hierarchical multi-scale reinforcement for CFRP composites by directly attaching or in situ growing micro-structure onto the fiber surface has been demonstrated as an efficient method for improving reinforcing properties of the composites. Moreover, grafting micro-structure onto carbon fibers (CFs) has been shown to improve the interfacial load transfer in polymer composites by fiber pull-out and fiber fragmentation tests [3]. Two major interfacial interactions, that is, micro-fiber/polymer and micro-fiber/CF, are believed to contribute to the improved mechanical properties. The advantages of this technique over the ones of attaching the preformed micro-structure mentioned above could be better dispersion, higher density, and even orientation control in the composites.

This chapter proposes a comprehensive and systematic view of improving the reinforcing effect in the CFRP composites by three typical hierarchical micro-structures including CNTs on CFs, CFFs on CFs and ZnO NWs on CFs. Firstly, we will demonstrate that the simple method allows the CNTs to be readily grafted onto CF mats for interfacial strength and fracture toughness enhancement. The objective of this work was to grow CNT effectively on carbon fabrics by a simple flame synthesis method and to characterize their effects on the interfacial properties and fracture toughness of the CFRPs. Next, we review our recent work on the toughness improvement of carbon fiber/epoxy composites by brushing and abrading of the woven fabrics. At last, we propose a novel dopamine-based functionalization method to improve the interfacial adhesion between ZnO NWs and CFs. Carbon fiber was modified with dopamine, and then ZnO nanowires were grown onto the modified carbon fibers by a facile hydrothermal method. The chapter concludes with a summary and comparison of existing toughening methods.

2. Hierarchical carbon nanotubes forests on carbon fibers

Carbon fiber is a multifunctional reinforcement for FRPs due to its light weight, good chemical and thermal stability, high electrical and thermal conductivity, and mechanical properties as well. It is suitable to be used as fiber substrate for in situ growing CNTs as its high thermal stability can withstand the temperatures for the process. Therefore, the building up of the hierarchical carbon reinforcement can be also achieved by in situ growing CNTs onto CFs and it was demonstrated to be an efficient way to interfacial improvement of carbon fiber reinforced composites (CFRPs) [4]. CNTs could be directly applied onto the fiber surface by

http://dx.doi.org/10.5772/intechopen.74706

the spreading of CNT powder [5] or CNT-solvent paste [6], and transferring CNT arrays [7]. Grafting of CNTs onto CFs could also be achieved by the chemical reaction between the pre-modified functional groups on the surface of both CNTs and CFs [8]. The electrophoresis technique could also been employed [9], where CNTs were uniformly deposited on the surface of carbon fabric from the CNT dispersion in an electric field. Among the various in situ growing CNTs methods, chemical vapor deposition (CVD) could be the most utilized method for growing CNTs onto CFs [10], even though it is an energy intensive batch process and requires costly reagents and equipment. Great interfacial improvement and good adhesion between CNTs deposit by CVD and CFs has been demonstrated [11].

Comparing with CVD methods, the flame growth of CNTs onto CFs is developed very recently and the strong adhesion of in situ flame synthesized CNTs onto CF was demonstrated by direct measurement of the force for peeling single CNT from CF [12]. These imply possible interfacial improvement of the CFRPs by the flame growth of CNTs onto CFs. On the other hand, the oxygen-functional groups have been proved to be formed on the surface of the flame synthesized CNTs [13], and their existence was believed to be an advantage of the flame synthesized CNTs over the conventional CNTs by CVD. In addition, for the method of in situ growing CNTs onto CFs, a great challenge is to prevent the mechanical degradation of the CFs by the intense heating using normal CVD techniques (usually above 700°C and tens of mins or even more), as evident mechanical degradation of the fiber has been observed [14]. In the view of commercial application, it is highly desirable that the mechanical properties of CFs in the hierarchical carbon structure are retained.

2.1. The preparation and characterization of flame synthesized CNTs onto CF

The growth of CNTs was performed by Du et al. [12, 13] though inserting the CF mats with $NiCl_2$ catalyst into the core of the flame, where the temperature is about 500–700°C. Both tip growth mechanism and root growth mechanism are found to be involved in the flame growth process. The CNT growth time is several minutes and the process is adopted in an open environment. Compared to the optical image of bare carbon fabric (**Figure 1a**), entangled CNTs uniformly grown on the surface of the CFs and SCF can be observed in SEM image (**Figure 1b**). By analysis of the CNTs scratched from CF mats and dispersed them in ethanol,

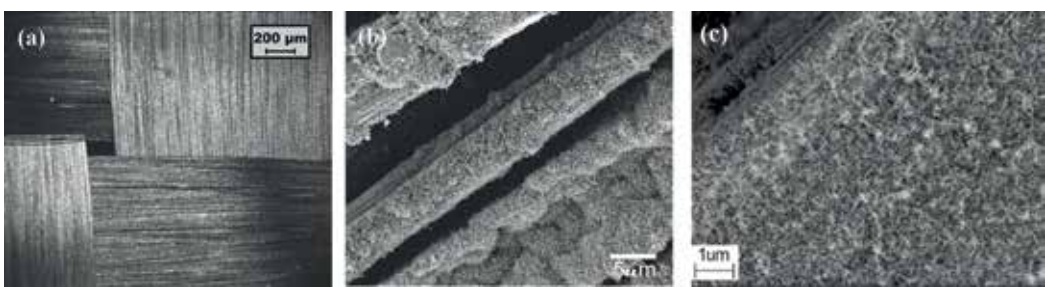

Figure 1. (a) Optical image of carbon fabric [13]; (b) SEM image of CNT/CF growth for 3 min [13]; (c) SEM image of CNT/SCF growth for 3 min [18].

the length of most CNTs growth 3 min are observed to be roughly 1–2 μm, much larger than the ones growth for 1 min (always <500 nm). Another synthesized CNTs onto CF system is based on short carbon fibers (SCFs), which were prepared by cutting plain woven carbon fiber fabrics. The diameter and average length of SCFs were about 7 μm and 750 (±200) μm, respectively. Then, CNTs grew on the SCF surface by the ethanol flame synthesis method for 3 min, and their morphology is displayed in **Figure 1(c)**.

Moreover, the single fiber tensile testing results indicates the growth of CNTs on the surface of the fiber does not result into any evident decrease in fiber tensile strength, demonstrating the advantage of our flame growth method over those previous reports with other techniques, where the tensile performance decreased more or less [14].

2.2. Interfacial shear strength

The concept of in situ growing CNTs on the surface of CFs has been introduced to increase the interfacial shear strength of CFs in the matrices [4]. The growth of the CNTs on the surface of CFs leads to the formation of two interfaces: one between the CF and CNT and a second between the CNT and polymer matrix. Outstanding adhesion between CNTs deposit by CVD and CFs has been demonstrated [4]. According to the single fiber fragmentation test, there was a dramatically increase in the interfacial shear strength after the CNTs grafted onto CFs [15]. The bonding of CNTs to CF was so strong that the failure occurred within the CF surface rather than the interface and the outlayers of CFs were even peeled off during the fracture process [16]. In a recent work, the strong adhesion of in situ flame synthesized CNTs to CF substrate was demonstrated by measurement of the force for peeling single CNT from CF [12]. This demonstrates a good possibility for increased interfacial shear strength and fracture toughness of the CFRPs by the flame growth of CNTs onto carbon fabric reinforcement.

Typical pull-out load versus displacement of the single fiber pull-out test for CF grafted with CNTs for 3 min was shown as **Figure 2a** conducted by Du et al. [17], where the load increases

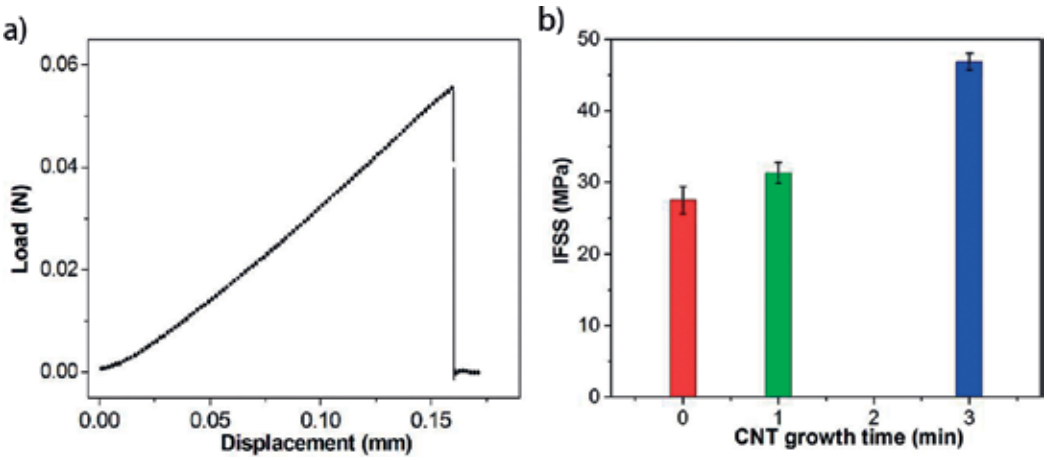

Figure 2. (a) The pull-out load versus the displacement [17]; (b) the interfacial shear strength versus CF with CNT growth in different time [17].

almost linearly with the displacement until the peak load is reached, followed by a sudden drop to zero, indicating the instantaneous debonding of the fiber-matrix interface. As shown in **Figure 2b**, the modification with CNTs significantly increases the IFSS by 70.5% with the interface of CNT growing for 3 min, however, the modification with CNTs growing for 1 min has no significant effect on the enhancement of the interfacial properties. The results here demonstrate that the interfacial properties can be significantly promoted and controlled by tuning the factors of flame growth CNTs. It is expected that the enhanced IFSS measured with the single fiber pull-out test could transform into the improved the fracture toughness properties of the lamina.

2.3. Interlaminar fracture toughness

Typical energy release rate as a function of the crack growth (*R*-curves) for CF grafted with CNTs growing for 3 min is shown in **Figure 3a**, conducted by Du et al. [13]. It can be clearly seen that the modification with CNTs lead to significantly increased fracture toughness. For the lamina with CNTs growing for 3 min onto carbon fabrics, the average G_{IC} increases by 67% comparing with those with bare carbon fabrics. Similar research on the effect of the grafting of CNTs onto CFs on the mode I fracture toughness of laminates shows a ~46% increase of G_{IC} after the CNTs growing onto carbon plain woven by CVD [10]. From the SEM image (**Figure 3b**, **c**) [13] of the mode I fracture surface of laminate reinforced with bare CF and CNT/CF, it can be found that there exists improved interfacial adhesion between the fiber and matrix after the flame growth of CNTs onto carbon fabrics. The increased interfacial adhesion results into the cohesive failure of the matrix. This indicates that the CNTs have strong bonding with the CFs.

Similarly, as shown in **Figure 4a**, the modification of the carbon fabrics by in situ flame growth of CNTs also shows great effect on the mode II fracture toughness of the lamina. The average G_{IIC} of the lamina, increases from 1.40 kJ/m^2 for the bare carbon fabrics to 2.22 kJ/m^2 for the ones modified with CNTs growing for 3 min, or a ~60% increase [13]. After the modification with CNTs, the zipper-like patterns can still be observed in the area with CF bundles parallel to the crack propagation, as shown in **Figure 4b**. It can be observed that the grafting of CNTs increase the number of zipper-like patterns (**Figure 4c**), which corresponds to a clear increase in G_{IIC} in the laminate with the insert crack.

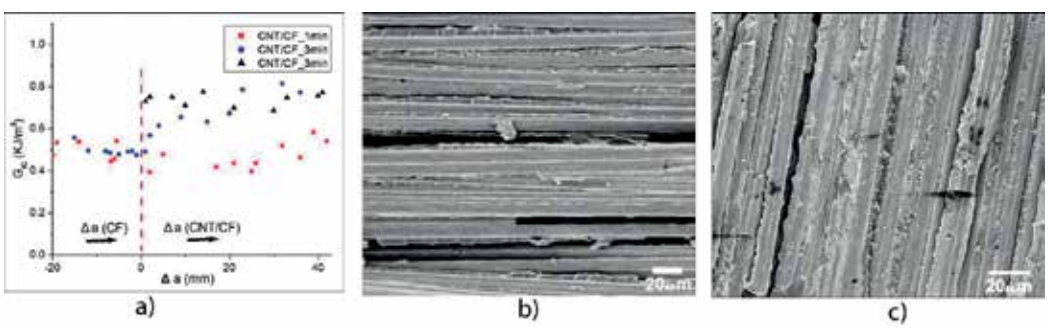

Figure 3. (a) Typical R-curve for mode I interlaminar fracture of the laminate; (b) SEM image of the mode I fracture surface of laminate reinforced with CF baseline and (c) the CNT/CF [13].

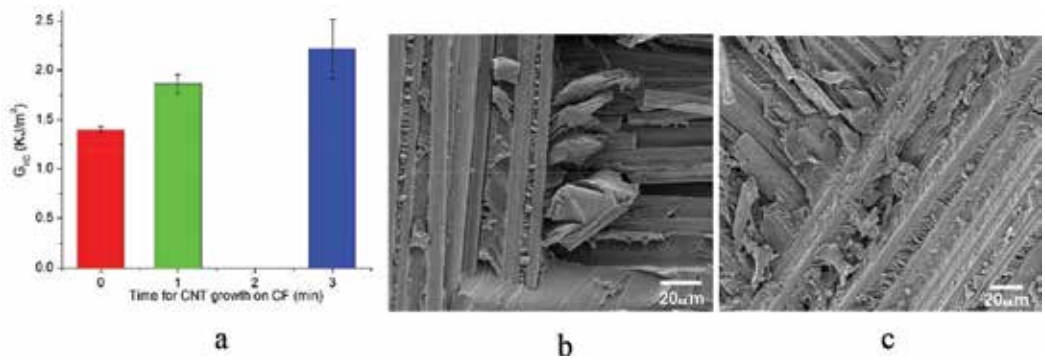

Figure 4. (a) The mode II interlaminar fracture toughness of the laminate, G_{IIC} versus CNT growth time; (b) SEM image of the mode II fracture surface of laminate reinforced with CF baseline and (c) the CNT/CF [13].

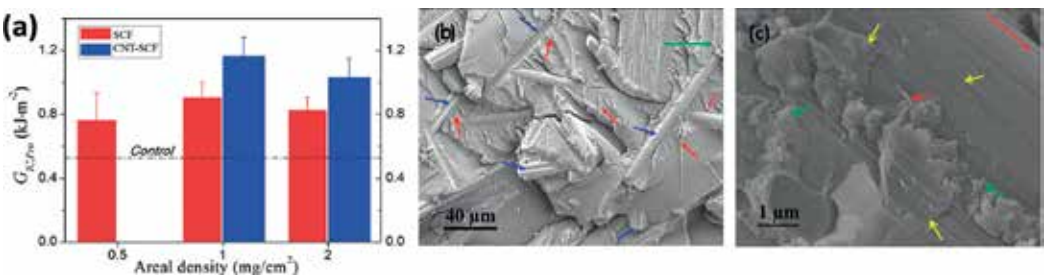

Figure 5. (a) The mode I interlaminar fracture toughness of the laminate; (b) SEM image of the mode I fracture surface of laminate reinforced with SCF and (c) the CNT-CF-SCF [18].

The influences of SCF and CNT-SCF interleaves on mode I interlaminar fracture initiation G_{IC} of CFRP laminates are also discussed in our previous work [18]. As **Figure 5a** shown, the materials tested were: (a) CFRP without any interleave (control), CFRP with (b) SCF or (c) CNT-SCF interleaves of areal density 0.5, 1.0 and 2.0 mg/cm^2. The experimental results showed that, compared to the control, SCF interleaves with areal density of 1.0 mg/cm^2 did not have much effect on G_{IC}, Ini (0.48 vs. 0.51 kJ/m^2); however, the CNT-SCF interleaves with areal density of 1.0 and 2.0 mg/cm^2 increased G_{IC}, In of the control by 0.14 and 0.31 kJ/m^2 to 0.62 and 0.79 kJ/m^2, respectively, hence confirming the higher toughening effect afforded by the CNTs adhered onto the epoxy matrix. Compared with characteristic brittle fracture of epoxy between adjacent CFs in the control CFRP laminates as shown in **Figure 3b**, **Figure 5b** shows clearly rugged and multi-planar fractures typified by brittle failure of epoxy with intense river marks around both debonded and dislodged SCFs lying more or less flat on the fracture surface. Moreover, as **Figure 5c** shown, clusters of CNTs may break or pull-out when the lowly embedded SCFs are debonded from the matrix leaving behind residual holes on the track. This action provides extra toughening of CNT-SCF interleaves due to CNT bridging and pull-out that are absent in SCF-interleaves.

Comparisons of G_{IC} of typical CNT-modified CFRPs in the literatures are given in **Table 1**. As the table shown, it can be seen that the enhancement of G_{IC} value of laminated composites modified by flame synthesis method in Du's work [13] is a little larger than the laminated

CNT grafted region	Test method	Toughness improvement	Ref
Growing CNT by CVD	DCB	46% (Mode-I)	[10]
Growing CNT by flame synthesis method	DCB	67% (Mode-I)	[13]
CNT grafted short carbon fibers	DCB	125%(Mode-I)	[18]

Table 1. Improvements in the fracture toughness of typical CNT-modified CFRPs.

composites modified by CVD method [10], which is possibly due to the better adhesion of in situ flame synthesized CNTs onto CF [12]. Moreover, flame synthesized CNTs grafted short carbon fibers interleaved laminated composites shows the remarkable toughness improvement among the CNT-modified CFRPs, this is because the hierarchical short carbon fibers interleave contribute the toughness improvement additionally.

3. Hierarchical short carbon fiber forests on carbon fibers

Up to now, there is limited report on the enhancement of the interfacial properties between fabric and matrix in laminates by increasing the surface roughness of fabric directly. In this section, fuzzy fabrics were prepared with a simple fabric surface brushing and abrading method. With this method, the carbon fiber forests (CFFs) will be fabricated in situ on the surface of the continuous woven carbon fabrics. In the CFRP composite reinforced with the modified fabrics, the CFF is expected to be distributed uniformly in the epoxy rich area in the interlayer of the laminates and acts as interleaf. Moreover, different from the previous interleaving method with additional materials being put into the interlayer, one of the advantages of our in situ produced CFF interleaves is that they adhered well to the fabrics as some fibers of them root in the carbon fabrics, which is believed to provide better delamination resistance. And its 'green' manufacturing process is much more cost-effective, chemical-free, and environmental friendly.

3.1. The morphology and characterization of short carbon fiber forests

The carbon fiber forests were fabricated through a brushing and abrading process on one side face of woven carbon fiber cloth. **Figure 6** exhibited the evolution of the morphology of fiber fabrics after different brushing and abrading times, respectively.

As shown in **Figure 6a**, the carbon fiber bundles in the original plain woven carbon fabrics are continuous and interweaving across each other, and the fabric surface texture is clean and tidy. As the abrading times increase, the broken carbon fibers are increased, and correspondingly, the fabric surface texture become more defective and rougher(**Figure 6b–c**). Moreover, it can be seen that broken carbon fibers are uniformly and randomly distributed on the surface of the fabrics and form a fiber forest. No fiber bundles/aggregation separated from the fabrics was observed. These indicate that the original fiber bundles were partially damaged and some broken carbon fibers in the bundles tend to stand up from the in-plane of the carbon fabrics.

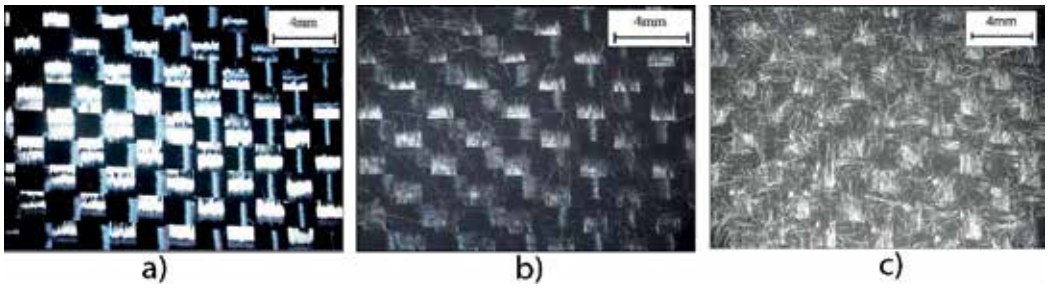

Figure 6. The surface morphology of (a) original carbon fabric; (b) carbon fabric abraded by 5 times; and (c) carbon fabric abraded by 30 times [32].

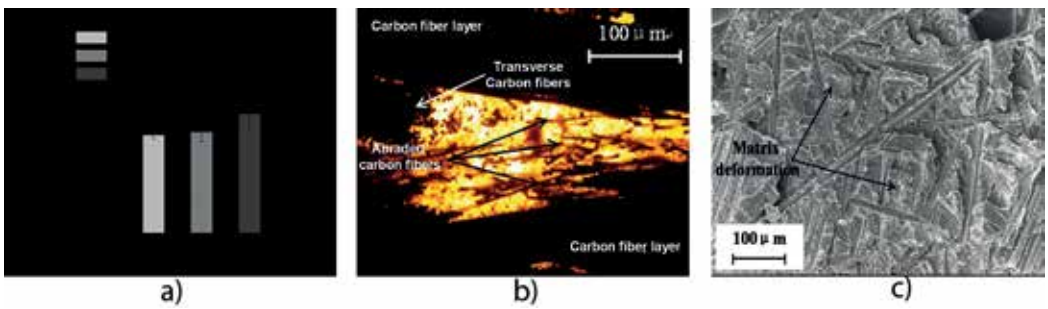

Figure 7. (a) Toughness of CCFs toughened laminate; (b) the optical images of the mid-layer of laminates interleaved by CFF;(c) the mode I fracture surface morphology of CFF interleaved CFRP composites [32].

3.2. Interlaminar fracture toughness of CFRP composite laminates with hierarchical short carbon fiber

As shown in **Figure 7a**, the delamination resistance of the modified laminates depends on the brushing times. The fracture toughness of the composites increased slightly and slowly over that of the baseline composite with the increasing abrading times from 5 to 20. When the abrading time was further increased to 30 times, the significant increase of the mode I fracture toughness of CFRP composite occurred, where GIC is increased by 62.4% for composites interleaved with one layer of CFF. Further improvements of the delamination resistance up to 83.2% can be achieved by the modification of both plies with CFF on their surface. These provide versatile designs of the laminate structure with the enhanced interlaminar fracture toughness in certain inter-layers. The significant improvement of the delamination resistance by 30 abrading times implies that the establishment of the effective 3D fiber network in the interlayer, which resists the crack opening efficiently. **Figure 7b** shows the morphology of CFF in the interlayer of CFRP composite. It is observed that carbon fibers in the interlayer of composite were random distributed, and the tips of some carbon fibers were separated from surrounding fiber bundles and randomly exposed out of the matrix region in the interlayer. Such a CFF structure was expected to interlock/ intersect each other in the narrow matrix region in the interlayer and formed a interwoven network structure, which potentially help to retard the crack propagation efficiently. To better understand the mechanism of the CFF

Reinforcement material for laminate	Test method	Fracture toughness increment (%)	Ref
SCF tissue	DCB	−5 to 28	[21]
CNT-SCF tissue	DCB	98–125	[18]
CNT forests by flame	DCB	67	[13]
CNT forests by CVD	DCB	31–61	[10]
CFF by brushing method	DCB	62.4	[32]

Table 2. Improvement on the interlaminar fracture toughness of CFRPs with various reinforcements.

interleaved CFRP composites, the fracture surfaces of samples after DCB test was studied by SEM (**Figure 7c**), where one could see that carbon fibers in the CFF were separated from the original carbon fiber bundles and randomly distributed in the fracture surface. The toughness enhancement of the fiber reinforced composites could be attributed to observed several generally accepted mechanisms, including fiber breakage, fiber-matrix debonding, fiber pull-out and matrix plastic deformation.

Table 2 gives some literature results on the mode I interlaminar fracture toughness for CFRP composites modified by various hierarchical short fibers such as SCFs [18], Kevlar fibers [19] and CNTs [13]. It can be seen that the enhancement of G_{IC} value of CFRP composites modified by brushing method is obviously among the best results, and there is no additional interleaving materials for the CFRP composite as the CFF is created in situ by the surface brushing and abrading of the fabrics themselves. Although both the CFF and SCF tissue are composed of carbon fibers, they display different morphology in CFRP composite. The carbon tissues were composed of chopped short carbon fibers with ~15 mm in length [20], which were mainly aligned in the in-plane direction of the laminates. In contrast, CFFs in the interlayer are expected to be distributed randomly in 3D directions, which demonstrates efficient crack bridging for toughness improvement. Furthermore, the morphology of well-adhesion of CFF interleaves to the fabrics in the CFRP composite revealed in **Figure 7b** is superior to the SCF tissue interleaves [18], in which SCF was additionally inserted into the interlayer of carbon fabrics without any bonding force to adjacent fabric plies.

4. Multifunctional ZnO nanowires grown on carbon fibers

Because of their unique magnetic, piezoelectric and optical properties, ZnO nanowires have been widely used in energy and environment applications [21–25]. Carbon fiber, which has been extensively used in light-weight structures, is a good support for ZnO because of its excellent electrical properties and flexibility to hybrid material, therefore, the established ZnO nanowire-carbon fiber hybrid materials can be used in highly wearable and stretchable supercapacitors, flexible piezoelectric generators and quantum dot-sensitized solar cells. The preparation, multi-functionality and application of ZnO nanowire-carbon fiber hybrid materials were mainly investigated in most previous studies, and few efforts were made to characterize the mechanical properties of this hybrid material. Actually, the mechanical properties, particularly,

the interfacial adhesion strength between the carbon fiber and ZnO NWs, play a key role in their application. For example, the ZnO NWs may easily fall off the carbon fiber in service if the interfacial adhesion between carbon fibers and ZnO NWs is relatively weak, which may lead to degradation of the material performance and possible material failure in further. So it is critical to investigate the interaction between ZnO NWs and carbon fibers and further clarify the adhesion mechanism.

CF/ZnO NWs has intrinsically poor interfacial adhesion because of insufficient functional groups on the CF surface that connects with ZnO, the current chemical oxidative methods including acid or plasma treatments are utilized to introduce the functional groups onto the CF surface to improve the CF/ZnO NWs interfacial adhesion, but oxidation functionalization can etch the fiber substrate and thus decrease the CF strength, which is undesirable for all applications. To address this problem, we [26] recently introduces Polydopamine (PDA) onto the CF surface to bond with the ZnO NWs, because PDA owns a robust chelating capability toward metal ions and can act as nucleation sites to form a metal oxide-PDA core/shell structure, the experimental results showed uniform and vertical aligned ZnO nanowires are well grown in the CF surface modified by PDA. In fact, the formed PDA layer has many functional groups such as quinone, carboxyl, catechol, amino and imino groups, which formed the main interaction, namely, the coordination between the catechol groups and the Zn^{2+} ion, this interaction gradually promotes the ZnO seed layer, from which ZnO NWs are nucleated and grow on the PDA-modified CF.

4.1. Pull-out force and strength of ZnO NW from CF

The adhesion strength between ZnO NWs and CF modified by PDF is the key factor to evaluate the PDA bonding effect between ZnO NWs and CF. Thus, it is necessary to measure the adhesion force between ZnO NWs and CF. Similar work has been done by Sodano et al., who have investigated the interaction between ZnO and graphite [27]. They applied a ZnO nanoparticle coated AFM tip close to the surface of highly oriented pyrolytic graphite to study the interaction between ZnO and carbon substrate. Although their method can, to some degree, reflect the interaction between ZnO and graphite substrate, real adhesion force between ZnO and carbon fibers cannot be measured. So it is necessary to develop a concise and direct method to measure the adhesion force and adhesion strength between CF and ZnO NWs. Recently, we [26] measured the pull-off force of ZnO NW from CF though a nanomanipulator equipped with a sensitive force measurement system inside the SEM chamber. **Table 3** gives the pull-out force and adhesion strength between bare or PDA-modified CFs

Hierarchical CFs	ZnO NW diameter (nm)	Pull-out force (N)	Adhesion strength (MPa)
CF/ZnO	300	1.65 ± 0.3	23.32 ± 4.56
CF/ZnO	700	8.7 ± 0.55	22.61 ± 3.68
CF/PDA/ZnO	300	4.2 ± 0.89	59.41 ± 5.32
CF/PDA/ZnO	700	27.5 ± 1.75	71.45 ± 8.54

Table 3. Pull-off (adhesion) force and adhesion strength between ZnO NW and CFs.

and ZnO NWs with different diameters of ZnO NW [26]. It can been seen that the pull-off force between PDA-modified CF and ZnO NW is much larger than that between bare CF and ZnO NW for a given ZnO NW diameter, which indicates great pull-out force improvement between CF and ZnO NW when PDA is introduced. Similar increase for the adhesion strength is also observed.

4.2. Interfacial strength of ZnO NW grafted CFRP composite

The interfacial shear strength (IFSS) of carbon fiber/epoxy composites was characterized by Zheng et al. [26] using the single fiber microbond tests. The results show average IFSS of bare CFRP is improved by 47% after ZnO growth owing to the mechanical interlock leaded by the penetration of stiff ZnO NWs into the epoxy resulting in an increased bonding area. Some results indicate that failure during the microbond experiments generally occurred at the ZnO NWs/fiber interface [28, 29]. However, there is no ZnO NWs found on the debonded surface of the pulled out CF, implying that all ZnO NWs were sheared off from the CF and embedded in the epoxy, so it can be concluded that failure occurred at the CF/ZnO interface, which limited further increase of the IFSS more or less.

4.3. Interlaminar fracture toughness of CFRP composite with hierarchical CF/ZnO fibers

Since ZnO NWs on CF are similar to toughening methods such as z-pinning [30] and CNTs grown on CFs [13], CF/ZnO hybrid composites can be used to manufacture laminates for the aerospace applications. Z-pinning and CNTs grown on CFs techniques have been applied in laminates for interlaminar toughening but some loss of in-plane strength may occurred in them, which is undesirable for laminate applications. By contrast, the hierarchical CF/ZnO NWs is prepared under low temperature without strong acid treatment, thus retaining the CF strength [31]. In addition, unlike CNTs which may collapse easily on the CFs during epoxy infusion, the rigid ZnO NWs can maintain their upright geometry during processing and provide strong mechanical interlocks with epoxy matrix [31] thus yielding more effective toughness improvement for composite laminates, hence, we [26] conducted the Double-cantilever-beams (DCB) and three-point end notched flexure (ENF) tests to evaluate mode I and mode II interlaminar fracture toughness of CF/ZnO NWs laminates. As **Figure 8a** shown, the fracture toughness of control laminate is 0.49 kJ/m^2 and this value is increased by 43 and 63% with introducing CF/ZnO NWs and CF/PDA/ZnO NWs, respectively. Mode II fracture toughness value for three types of laminates can be found in **Figure 8b**, which are 1.4, 1.61 and 1.71 kJ/m^2 for the Control, CF/ZnO NWs and CF/PDA/ZnO NWs modified composites laminate, respectively, indicating 15% and 22% increases respect to the Control. It can be concluded that both mode I and mode II interlaminar toughness of CF/ZnO NWs laminates were indeed found to be increased, and further increases in these toughness values were achieved for the CF/PDA/ZnO NWs hybrid laminates due to the enhanced interfacial interaction between ZnO NWs and PDA-modified CF.

Table 4 gives existing results on the mode I and mode II interlaminar fracture toughness for CFRP composites modified by various hierarchical reinforcement such as ZnO NWs [26], SCF

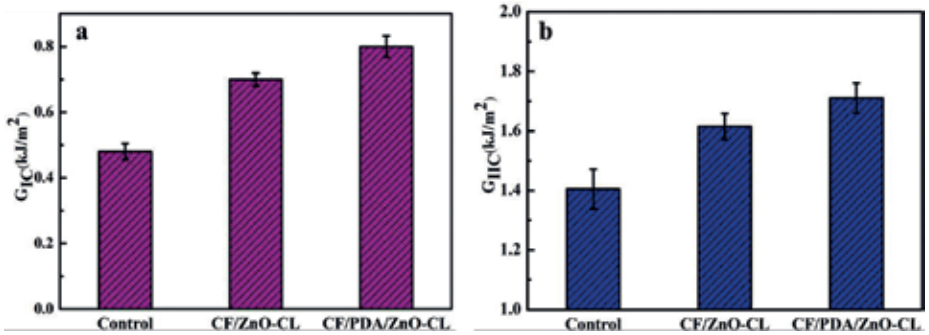

Figure 8. (a) G_{IC} and (b) G_{IIC} of three types of CFRP composite laminates [26].

Reinforcement material for laminate	Test method	Fracture toughness increment (%)	Ref
ZnO NWs	DCB	43–63	[28]
	ENF	15–22	
SCF tissue	DCB	73	[18]
CNT-SCF tissue	DCB	125	[18]
CNT forests by flame	DCB	67	[13]
	ENF	59	
CFF by our brushing method	DCB	62.4	[32]
	ENF	83.2	

Table 4. Improvement on the interlaminar fracture toughness of CFRPs with existing hierarchical reinforcements approaches.

tissue [18], CNT-SCF tissue [18], CNT forests by flame [13] and CFF by brushing method [32]. It is noticed that the interlaminar fracture toughness of composites laminate with ZnO NWs is lower than composites laminate with carbon reinforcement. It can be seen that the hierarchical short carbon reinforcement (see SCF tissue or CFFs in **Table 4**) or flame synthesis CNT forests could only give the limited toughness improvement for laminate while CNT-SCF tissue exhibits the highest toughness improvement due to its synergistic effect with incorporation of CNTs and SCF.

The toughening mechanisms in mode I and mode II was conducted [26] as well, it is found that the interlaminar failure largely occurs at the CF/ZnO NWs interface which consists with the single fiber microbond pull-out tests. It is claimed that the increased toughness mainly comes from the large matrix deformation induced by the ZnO NWs. From the CF/PDA/ZnO NWs, the cohesive rather than adhesive failure during crack propagation could be the main toughening mechanisms, ZnO NWs strongly bonded on CF can serve as pin-like materials. Their toughening effect works by a crack-wake bridging mechanism that includes their spanning across the matrix crack, thereby, increase the mode I and mode II interlaminar fracture toughness.

http://dx.doi.org/10.5772/intechopen.74706

5. Conclusion

In this chapter, three novel carbon fibers surface treatment methods, typically carbon nanotubes (CNTs) grafted on CFs using catalysts formed in an ethanol flame, carbon fiber forests on carbon fibers, ZnO nanowire grown onto CFs through a facile hydrothermal method respectively, were presented and detailed. The conclusions are as follows:

Firstly, the flame synthesis method is demonstrated to be an efficient technique for the in situ growth of CNTs onto the surface of carbon fabric to build up the hierarchical reinforcement in multi-scale laminate composites for improved interfacial and fracture properties. The CNTs growing temperature is as low as 450°C and the tensile performance of single carbon fiber did not degrade evidently after the CNTs deposition. The flame synthesized CNT interface developed here has been shown to offer a significant enhancement in the interfacial properties. ~70% increase of IFSS was achieved after the modification by flame growth CNTs for 3 min onto CFs. The G_{IC} and G_{IIC} of the composite reinforced by carbon fabric with CNTs growth for only 3 min could be enhanced about 60 and 67% over those without CNT grafting, respectively. Analysis of the surface following failure showed the lamina samples reinforced with bare carbon fabric were dominated by adhesive failure while the CNT-modified ones were predominantly cohesive matrix failure. The simple and open environmental deposit process together with the decreased growth time of the flame synthesis method make it a promising technology to fabricate hierarchical carbon reinforcement.

Secondly, the presented simple surface brushing and abrading method was demonstrated to significantly enhance the delamination resistance of the composite with moderate in-plane tensile strength loss. The fabric surface brushing and abrading method was simple, economic, environment friendly and chemical free. Moreover, there is no any additional reinforcement applied in the composites. Furthermore, the defective fabric surface texture structure with most fibers in the CFF interleaf rooting in the fabrics benefits the improvement of the delamination resistance of the laminates. It is believed that the method was compatible with large scale manufacturing processes for CFRP laminate composites, and could find its real applications with the balance and compromising of toughness and in-plane tensile properties of the composites.

At last, a dopamine functionalization method was proposed to give a PDA layer on the CF surface. ZnO nanowires were then grafted on the PDA-modified CF through a hydrothermal method to obtain a hierarchical ZnO nanowire/carbon fiber composites. In situ pull-off experiments of a single ZnO NW from the CF demonstrated that the PDA functionalization on the fiber surface was critical for the strong chemical adhesion of the ZnO nanowires with the CF substrate caused by the coordination reaction between the catechol groups and Zn^{2+} ion, which yielded a 200% increase in pull-off force and adhesion strength compared to bare CF/ZnO NWs. The interfacial shear strength was also increased by 64% after the growth of ZnO NWs on the PDA-modified CF. It was noteworthy that PDA modification and ZnO NWs growth did not degrade the CF strength. Furthermore, both mode I and mode II interlaminar toughness were increased for CF/ZnO NWs and CF/PDA/ZnO NWs. In particular, for the latter laminates, the improvements were 63% for mode I and 22% for mode II due to the strong chemical bonding between PDA-modified CF and ZnO NWs as well as the mechanical interlocking between ZnO NWs and epoxy.

Acknowledgements

Feng Xu is grateful for the research support of the National Natural Science Foundation of China (No. 11702224) and the Fundamental Research Funds for the Central Universities (No. 3102017zy034). Du Xusheng also wish to thank the support of the Guangdong Province Science and Technology Plan (No. 2017B090903005).

Author details

Feng Xu[1], Xusheng Du[2]* and Helezi Zhou[2]

*Address all correspondence to: xdusydjn@email.jnu.edu.cn

1 School of Astronautics, Northwestern Polytechnical University, Xi'an, Shaanxi Province, PR China

2 Institute of Advanced Wear and Corrosion Resistance and Functional Materials, Jinan University, Guangzhou, PR China

References

[1] Domun N, Hadavinia H, Zhang T, et al. Improving the fracture toughness and the strength of epoxy using nanomaterials–A review of the current status. Nanoscale. 2015;**7**(23): 10294-10329. DOI: 10.1039/C5NR01354B

[2] Xu F, Du XS, Liu HY, et al. Temperature effect on nano-rubber toughening in epoxy and epoxy/carbon fiber laminated composites. Composites Part B: Engineering. 2016;**95**: 423-432. DOI: 10.1016/j.compositesb.2016.04.019

[3] Qian H, Greenhalgh ES, Shaffer MSP, Bismarck A. Carbon nanotube-based hierarchical composites: A review. Journal of Materials Chemistry. 2010;**20**:4751-4762. DOI: 10.1039/C000041H

[4] Thostenson ET, Li WZ, Wang DZ, Ren ZF, Chou TW. Carbon nanotube/carbon fibre hybrid multiscale composites. Journal of Applied Physics. 2002;**91**:6034-6037. DOI: 10.1063/1.1466880

[5] Li Y, Hori N, Arai M, Hu N, Liu Y, Fukunaga H. Improvement of interlaminar mechanical properties of CFRP laminates using VGCF. Composites: Part A. 2009;**40**(12):2004. DOI: 10.1016/j. compositesa.2009.09.002

[6] Arai M, Yukihiro N, Sugimoto KI, Endo M. Mode I and mode II interlaminar fracture toughness of CFRP laminates toughened by carbon nanofiber interlayer. Composites Science and Technology. 2008;**68**:516-525. DOI: 10.1016/j.compscitech.2007.06.007

[7] Garcia EJ, Wardle BL, Hart AJ. Joining prepreg composite interfaces with aligned carbon nanotubes. Composites: Part A. 2008;**39**:1065-1070. DOI: 10.1016/j.compositesa.2008.03.011

[8] An Q, Rider AN, Thostenson ET. Electrophoretic deposition of carbon nanotubes onto carbon-fiber fabric for production of carbon/epoxy composites with improved mechanical properties. Carbon. 2012;**50**:4130-4133. DOI: 10.1016/j.carbon.2012.04.061

[9] Schaefer JD, Rodriguez AJ, Guzman ME, Lim CS, Minaie B. Effects of electrophoretically deposited carbon nanofibers on the interface of single carbon fibers embedded in epoxy matrix. Carbon. 2011;**49**:2750-2759. DOI: 10.1016/j.carbon.2011.02.070

[10] Kepple KL, Sanborn GP, Lacasse PA, Gruenberg KM, Ready WJ. Improved fracture toughness of carbon fiber composite functionalized with multi walled carbon nanotubes. Carbon. 2008;**46**:2026-2033. DOI: 10.1016/j.carbon.2008.08.010

[11] Sager RJ, Klein PJ, Lagoudas DC, Zhang Q, Liu J, Dai L, Baur JW. Effect of carbon nanotubes on the interfacial shear strength of T650 carbon fiber in an epoxy matrix. Composites Science and Technology. 2009;**69**:898-904. DOI: 10.1016/j.compscitech.2008.12.021

[12] Du XS, Liu HY, Zhou CF, Moody S, Mai YW. On the flame synthesis of carbon nanotubes grafted onto carbon fibers and the bonding force between them. Carbon. 2012;**50**(6):2347-2350. DOI: 10.1016/j.carbon.2012.01.003

[13] Du X, Liu HY, Xu F, Zeng Y, Mai YW. Flame synthesis of carbon nanotubes onto carbon fiber woven fabric and improvement of interlaminar toughness of composite laminates. Composites Science and Technology. 2014;**101**:159-166. DOI: 10.1016/j.compscitech.2014.07.011

[14] Qian H, Bismarck A, Greenhalgh ES, Shaffer MSP. Carbon nanotube grafted carbon fibres: A study of wetting and fibre fragmentation. Composites Part A: Applied Science and Manufacturing. 2010;**41**(9):1107-1114. DOI: 10.1016/j.compositesa.2010.04.004

[15] Lv P, Feng YY, Zhang P, Chen HM, Zhao NQ, Feng W. Increasing the interfacial strength in carbon fiber/epoxy composites by controlling the orientation and length ofcarbon nanotubes grown on the fibers. Carbon. 2011;**49**(14):4665-4673. DOI: 10.1016/j.carbon.2011.06.064

[16] Qian H, Bismarck A, Greenhalgh ES, Kalinka G, Shaffer MSP. Hierarchical composites reinforced with carbon nanotube grafted fibers: The potential assessed at the single fiber level. Chemistry of Materials. 2008;**20**(5):1862-1869. DOI: 10.1021/cm702782j

[17] Du X, Xu F, Liu HY, Miao YG, Guo WG, Mai YW. Electrical conductivity and Interface improvement of carbon fibers reinforced composites by the low temperature flame growth of CNTs onto them. RSC Advances. 2016;**6**(54):48896-48904. DOI: 10.1039/C6RA09839H

[18] Zhou H, Du X, Liu HY, Zhou H, Zhang Y, Mai YW. Delamination toughening of carbon fiber/epoxy laminates by hierarchical carbon nanotube-short carbon fiber interleaves. Composites Science and Technology. 2017;**140**:46-53. DOI: 10.1016/j.compscitech.2016.12.018

[19] Sohn MS, Hu XZ. Comparative study of dynamic and static delamination behaviour of carbon fibre/epoxy composite laminates. Composites. 1995;**26**:849-858. DOI: 10.1016/ 0010-4361(95) 90878-4

[20] Lee SH, Aono Y, Noguchi H, Cheong SK. Damage mechanism of hybrid composites with nonwoven carbon tissue subjected to quasi-static indentation loads. Journal of Composite Materials. 2003;**37**:333-339. DOI: 10.1177/0021998303037004334

[21] Wang Q, Li QH, Chen YJ, Wang TH, He XL, Li P, Lin CL. Fabrication and ethanol sensing characteristics of ZnO nanowire gas sensors. Applied Physics Letters. 2004;**84**(18): 3654-3656. DOI: 10.1063/1.1738932

[22] Law M, Greene LE, Johnson JC, Saykally R, Yang P. Nanowire dye-sensitized solar cells. Nature Materials. 2005;**4**(6):455-459. DOI: 10.1038/nmat1387

[23] Geng C, Jiang Y, Yao Y, Meng X, Zapien JA, Lee CS, et al. Well-aligned ZnO nanowire arrays fabricated on silicon substrates. Advanced Functional Materials. 2004;**14**(6):589-594. DOI: 10.1002/adfm.200305074

[24] Wang X, Song J, Liu J, Wang ZL. Direct-current nanogenerator driven by ultrasonic waves. Science. 2007;**316**:102-105. DOI: 10.1126/science.1139366

[25] Wang ZL, Song J. Piezoelectric nanogenerators based on zinc oxide nanowire arrays. Science. 2006;**312**:242-246. DOI: 10.1126/science.1124005

[26] Zheng N, Huang Y, Sun W, Du X, Liu HY, Moody S, Gao J, Mai YW. In-situ pull-off of ZnO nanowire from carbon fiber and improvement of interlaminar toughness of hierarchical ZnO nanowire/carbon fiber hydrid composite laminates. Carbon. 2016;**110**:69-78. DOI: 10.1016/j. carbon.2016.09.002

[27] Galan U, Sodano HA. Intermolecular interactions dictating adhesion between ZnO and graphite. Carbon. 2013;**63**:517-522. DOI: 10.1016/j.carbon.2013.07.027

[28] Galan U, Lin Y, Ehlert GJ, Sodano HA. Effect of ZnO nanowire morphology on the interfacial strength of nanowire coated carbon fibers. Composites Science and Technology. 2011;**71**:946-954. DOI: 10.1016/ j.compscitech.2011.02.010

[29] Ehlert GJ, Sodano HA. Zinc oxide nanowire interphase for enhanced interfacial strength in lightweight polymer fiber composites. ACS Applied Materials & Interfaces. 2009;**1**(8): 1827-1833. DOI: 10.1021 /am900376t

[30] Mouritz AP. Review of z-pinned composite laminates. Composites: Part A. 2007;**38**(12): 2383-2397. DOI: 10.1016/j.compositesa.2007.08.016

[31] Lin Y, Ehlert G, Sodano HA. Increased interface strength in carbon fiber composites through a ZnO nanowire interphase. Advanced Functional Materials. 2009;**19**(16): 2654-2660. DOI: 10.1002/adfm.200900011

[32] Xu F, Huang DD, Du XS. Improving the delamination resistance of carbon fiber/epoxy composites by brushing and abrading of the woven fabrics. Construction and Building Materials. 2018;**158**:257-263. DOI: 10.1016/j.conbuildmat.2017.10.015

Chapter 6

Carbon Fibers in Biomedical Applications

Naveen Kumar, Anil Kumar Gangwar and
Khangembam Sangeeta Devi

Additional information is available at the end of the chapter

http://dx.doi.org/10.5772/intechopen.75826

Abstract

Three-dimensional growth of fibroblasts on carbon fibre mesh and assessment of biocompatibilty by *in vitro* and *in vivo* examination was done. Suitable size carbon fiber mesh after sterilization, placed in six well cell culture plate. The mesh was co-cultured with p-MEF cells. At different time intervals the viability and proliferation of the p-MEF cells was evaluated. The primary objective of this study was biological evaluation of carbon fibre mesh which can be used for creation of three-dimensional scaffolds for tissue engineering. Among the possible forms of implants, fibrous matrices are highly promising for the tissue regeneration by acting as a cell-supporting scaffold. Results of in vitro observations of the morphology p-MEF cells seeded on the surface of carbon fibre mesh shows adhesions and attachment of fibroblasts cells to carbon fibres on day 3 post seeding. They attached firmly and were uniformly spread along the fibres on day 5 postseeding and mostly spindle-shaped and cover almost all their surface on day 7 postseeding and such a spreading of cells indicates good adhesions and biocompatibility of carbon fibres. In vivo examination of retrieved sample on day 30 post implantation shows that carbon fibre mesh was covered by dense thick fibrous connective tissue.

Keywords: carbon fibers, carbon fiber mesh, primary mouse embryo fibroblasts (p-MEF), in vitro examination, in vivo examination

1. Introduction

Carbon fiber (CF) consists of a multitude of unique physical, chemical and biological characteristics that can be utilized and exploited for a number of diverse applications. Being light weight, high strength, and chemically stable, so they are applied in various fields including aeronautical

science and space science. Investigation of applications of carbon fibers to biomaterials was started 30 or more years ago, and various products have been developed. It is used widely in imaging equipment structures to support limbs being X-rayed or treated with radiation.

Carbon fiber is frequently supplied in the form of a continuous tow wound onto a reel. The tow is a bundle of thousands of continuous individual carbon filaments held together and protected by an organic coating, or size, such as polyethylene oxide (PEO) or polyvinyl alcohol (PVA). Each carbon filament in the tow is a continuous cylinder with a diameter of 5–10 micrometers and consists almost exclusively of carbon. The earliest generation had diameters of 16–22 micrometers and later fibers have diameters that are approximately 5 micrometers. Precursors for carbon fibers are polyacrylonitrile (PAN), rayon and pitch.

The latest technological progress has realized nanolevel control of carbon fibers, applications to biomaterials have also progressed to the age of nanosize. Carbon fibers with diameters in the nanoscale (carbon nanofibers) dramatically improve the functions of conventional biomaterials and make the development of new composite materials possible. Carbon nanofibers also open possibilities for new applications in regenerative medicine and cancer treatment. The first three-dimensional constructions with carbon nanofibers have been realized, and it has been found that the materials could be used as excellent scaffolding for bone tissue regeneration. We have developed an innovative approach for the use of CF as a scaffold in the repair of tendon and ligaments and as a suture material for repair of hernial ring.

Carbon as an inert element has advantages over other materials because it is a basic constituent of tissues. The high proportion of tissues of living organisms is composed of carbon compounds so it should be tolerated by the tissues. Over the past 25 years various carbon materials have been investigated in many areas of medicine [1, 2].

The physical and chemical properties of CFs are also determined by their microstructure. This is particularly important in the case of CFs used in medicine. One of the earliest medical uses of CFs was replacement or repair of ligaments and tendons [3–5]. Most of the studies on carbon fibrous implants confirm that CFs do not inhibit tissue growth, and thus can act as a scaffold for tissue proliferation [3, 6]. Controversy surrounds the mechanism of the disintegration and removal of the implanted CFs. A histological study showed that the CFs gradually broke down and migrated into the nearest lymph nodes with no apparent detrimental effect [6]. In all instances the CFs acted as a scaffold that allowed the regeneration of tendon and ligament. In contrast to these investigations, Morris et al. [7] showed that fragmentation of fibers did not occur and implant debris was not found in the regional nodes. Moreover, CFs induced significantly more tissue ingrowth than polypropylene mesh at 6–12 months postoperatively. A probable elimination mechanism by erosion of carbon particles and their retention in the fibrous capsule surrounding the implant [8]. Although the results of most investigations of CFs in vivo were evaluated as good, several authors were skeptical as to the superiority of carbon fibrous implants over other prosthetic materials [9, 10]. Carbon fibers were considered to be a good candidate biomaterial for total hip replacement and internal fixation in the form of composites [11]. In spite of controversial results with CFs used for replacement and reconstruction of ligaments and tendons, several other clinical studies were undertaken. The different results obtained in evaluating CFs as a biomaterial can probably be explained by the

use of different types of carbon fibers of different physical, structural and chemical properties, resulting from many technological parameters. Most of the papers concerning examinations of CFs for medical purposes describe neither the type of carbon fibers used nor their fundamental properties determining their behavior in a biological environment. We will discuss the use of carbon fibers in biomedical applications under different headings:

- In vitro biocompatibility evaluation
- In vivo biocompatibility evaluation
  - Subcutaneous implantation of carbon fibers
  - Carbon fibers in repair of abdominal wall defects
  - Carbon fiber mesh in reconstruction of abdominal wall defects
  - Carbon fibers for gap repair of flexor tendons
- Clinical applications

2. In vitro biocompatibility evaluation

2.1. Introduction

Tissue engineering is the process of creating functional three dimensional (3-D) tissue by combining cells with scaffolds to facilitate cell growth, organization and differentiation. The most important aspect of tissue engineering is the adhesion and proliferation of cells on scaffold material. Biocompatibility of CFs has been the subject of numerous researches. Some of investigators concluded that CFs induces the growth of new tissue [12]. However, there were also announcements questioning biocompatibility of CFs [13–15]. The different opinions regarding biocompatibility of CFs may be explained by the use of different types of CFs of different physical, structural and chemical properties, resulting from many technological parameters [15, 16]. It has been demonstrated that the cellular response to the fibrous carbon material depends on the degree of crystallinity of the material; therefore only selected types of CFs are suitable for tissue treatment purposes [16–18].

The fibroblasts are common cells present in the connective tissue that synthesizes and continuously secretes precursors of extra cellular matrix. Fibroblasts play an important role in regeneration of new tissue due to their growth accelerating property of tissue cells by secreting several growth factors and extra cellular matrix (ECM). Primary mouse embryonic fibroblasts (p-MEFs) have a number of properties making them an attractive cell culture model. Compared to other primary explant cultures they are easy to establish and maintain, proliferate rapidly resulting in large numbers of cells produced from a single embryo within several days. Major histocompatibility complex (MHC) Class II antigens are present on the transplanting cells which is responsible for graft rejection. Fibroblasts lack these surface molecules and this makes them relatively immunologically inert.

In the present study, carbon fiber mesh was cut in desired size and after sterilization, placed in six well cell culture plates. The mesh was co-cultured with p-MEF cells. At different time intervals the viability and proliferation of the MEF cells was evaluated. The primary objective of this study was biological evaluation of carbon fiber mesh which can be used for creation of three-dimensional scaffolds for tissue engineering. Carbon fiber used as scaffold for tissue regeneration could simultaneously serve as a support for drug delivery or biologically active agents which would stimulate the tissue growth. Therefore, in this study, we investigated the behavior of carbon fiber mesh in biological environments and their interaction with cells and tissues under in vitro and in vivo conditions.

2.2. Materials and methods

In vitro tests in cell cultures were performed in Biomaterials and Bioengineering Laboratory, Division of Surgery, Indian Veterinary Research Institute, Izatnagar, Uttar Pradesh, India. Prior to cell culture, the carbon fiber mesh was autoclaved at the temperature of 120°C for 30 min. The primary mouse embryo fibroblasts culture (p-MEF) was done as per standard protocol. The cells obtained were washed twice with DMEM containing antibiotics and were centrifuged at 2500 rpm for 8–10 min. The cells were resuspended in cell growth media (DMEM-Low glucose) containing 10% FBS and antibiotics (Mixture of 100 units/ml penicillin and 100 μg/ml streptomycin). The cells were counted countess cell counting kit (Invitrogen) and plated at an average of 2.2×10^5 cells/cm^2 in T-25 flasks. They were maintained at 37°C in a humidified atmosphere of 5% CO_2 in CO_2 incubator. Day after the primary culture, the spindle shaped fibroblast cells were observed and the non-adherent/dead cells were removed by changing the medium. When the cells attained 80–90% confluency (as assessed by observing under inverted microscope, the cells were passaged into new culture flask. Culture medium was removed and cells were washed twice with HBSS (with antibiotic). The cells were detached from the culture flask by using 2 ml of 0.5% of trypsin. The trypsin activity was stopped by adding equal volume of culture medium containing FBS and flushed properly to get the attached cells in the suspension.

After the primary culture, when adherent cells reached to 90% confluency, they were detached with 0.25% trypsin-EDTA solution. Growth medium i.e. DMEM containing 10% fetal bovine serum was added and mixed properly to get single cell suspension. The carbon fiber mesh was cut into small pieces and washed 4–5 times with antibiotics containing Dulbecco's Modified Eagle Medium (DMEM) and was placed in wells of the culture plate. The cells were seeded at the rate of 2×10^4 cells/cm.^{2} It was maintained at 37°C in a humidified atmosphere of 5% CO_2 in a CO_2 incubator. The growth media was changed after 48 h. The seeded mesh was observed and processed for morphological assessment on day 3, 5 and 7 postseeding. Morphological examination was performed using Scanning Electron Microscopic Examination. The seeded mesh was fixed in 2% glutaraldehyde for SEM examination.

2.3. Results and discussion

A good amount of p-MEF cells were cultured from a single pregnant mouse. Cells were plated in a T-25 flask. A large number of spherical cells were observed under phase contrast microscope. Cells were maintained in CO_2 incubator and observed daily under inverted

phase contrast microscope to assess the viability and proliferation of cells. The cells showed characteristic growth and adherence pattern in vitro and proliferated rapidly to complete the monolayer in 4 days. The morphology of in vitro cultured cells clearly indicated the presence of primary mouse embryo fibroblasts. Effects of the tested materials on the adhesion, growth and morphology of cells on the fibers were evaluated by SEM examination.

Morphology of carbon fiber mesh showed that carbon fibers filaments were closely woven. In vitro observations of the morphology of cells seeded on the surface of carbon fiber mesh showed that they attached firmly and were uniformly spread along the fibers on day 5 post seeding and mostly spindle-shaped. They cover almost all their surface on day 7 post seeding and such a spreading of cells indicates good adhesions and biocompatibility of carbon fibers. The assumption that carbon as the fundamental element in biological tissues would not induce adverse reactions encouraged scientists to use carbon fibers in medicine as the implantable biomaterial [18]. In the field of regenerative medicine carbon materials are becoming increasingly attractive as they can be modified to be integrated into human bodies for promotion of tissue regeneration and treatment of various diseases.

3. In vivo biocompatibility evaluation

3.1. Subcutaneous implantation of carbon fibers

3.1.1. Materials and methods

Carbon fibers and mesh were implanted subcutaneously on either side of the spine in four Wistar rats. Animals were anesthetized using xylazine and ketamine anesthetic combination. The animals were restrained in sternal recumbency. Dorsal thoracic area was prepared for aseptic surgery. On either side of the spine 1 cm long skin incision was given lateral to the spine on both left and right side and subcutaneous pouches were created. The implants were pushed in the pockets and the skin incision was closed with simple interrupted sutures using polyamide suture no 1-0. The Carbon fibers and mesh were retrieved back on day 30 post-operatively. The retrieved implants were preserved in 10% formalin saline solution. The tissues were processed by routine paraffin embedding technique and the sections were cut at 5 micron thickness. The sections were stained with hematoxylin and eosin (H & E) stain.

3.1.2. Results and discussion

Retrieved sample on day 30 post implantation shows that carbon fibers and mesh were covered by dense thick fibrous connective tissue. Complications like infection or pus formation was not seen in the vicinity of any implanted biomaterials. The tissue response to implanted materials was more pronounced as observed in SEM examination. The implant was agglomerated and surrounded with granulation tissue. Individual carbon fiber was adhered with thick granulation tissue which included different types of cells and shows high biocompatibility of carbon fibers which was clearly observed in high magnification (**Figure 1**).

In histopathological examination foreign body-type multinucleated giant cells were observed to be accompanied with some eosinophils and mast cells. The structure of the muscle tissue surrounding the implant was regular. There was increased number of fibroblasts at day 30 post implantation. Histological observation revealed that carbon fibers stimulated extensive fibrocellular reaction with minimal infiltration of inflammatory cells at the site.

Based on microscopic observations we have confirmed that adhesion of cells to carbon fiber mesh. According to in vivo studies, carbon fiber mesh due to their porosity enables more efficient growing of cells and connective tissue within the structure of implant. Biocompatibility of carbon fibers has been the subject of numerous researches, however individual researchers implemented it in their own experiments without further physical and chemical characterization, and also without specifying the sterilization methods, so that cases of toxic effects of fiber degradation products on the human body were also reported [19–21].

Carbon fibers in many cases were well tolerated by the recipient and did not cause the around foreign body reactions [16]. Moreover the tendon or ligament newly developed on a carbon scaffold was morphologically very similar and functionally identical to the replaced natural structure [22]. It has been demonstrated by the later studies that the cellular response to the fibrous carbon material depends on the degree of crystallinity of the material; highly crystalline, high modulus fibers are not suitable for medical purposes, while amorphous fibers are excellent for implants [16]. Grabinski et al. [23] reported that toxicity of carbon materials depends also of dimensions and after 24 h the carbon nanotubes showed increased cellular toxicity when compared to the carbon fibers and carbon nanofibers. Our results clearly demonstrated the excellent biocompatibility of those carbon fibers; however, they also clearly

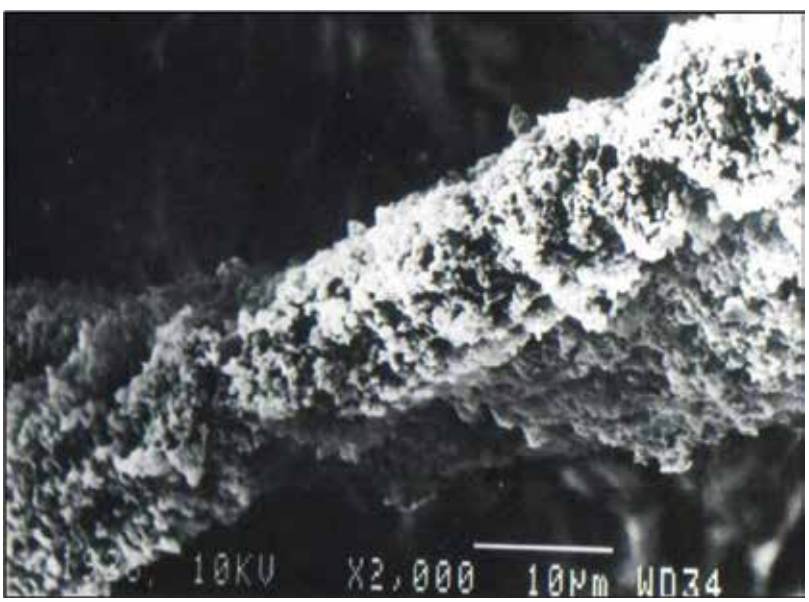

Figure 1. SEM examination showing individual carbon fiber adhered with thick granulation tissue having different types of cells.

confirmed that biological activity is even more desirable. Three thousand filaments of carbon fibers were used to reconstruct the experimentally created full thickness linear abdominal wall defects in rabbits [24].

3.2. Carbon fibers in repair of abdominal wall defects

3.2.1. Introduction

The successful reconstruction of abdominal wall defect is challenge to surgeon. Prosthetic materials like small intestine mucosa [25], human dura mater [26], polyester fabric [27], expanded polytetrafluoroethylene [28] have been used in reconstruction of large abdominal wall defects. Problems peculiar to each of these prosthetic materials have reduced prolonged and widespread clinical acceptance. Ideally, carbon fiber not only provides structural strength, but also acts as a scaffold on which the body may lay down collagen to complete the repair particularly in long term [29]. Braided carbon fibers have a place in the repair of tendon [30, 31]. So we have studied the carbon fibers in repair of abdominal wall defect in rabbits.

3.2.2. Materials and methods

Sixteen New Zealand white rabbits of either sex were randomly divided into two equal groups (group I and II) of 8 animals. Mid ventral abdominal region was chosen for the purpose of study. Food for 18 h and water for 6 h was withheld before operation. The ventral abdominal area was prepared for aseptic surgery and the operation was performed under general anesthesia. The animals were retained in dorsal recumbency. After skin incision a linear full thickness defect of 3 cm in the mid ventral aspect of abdominal wall was created and repaired with continuous suture pattern using 3000 filaments of carbon fiber and 1-0 black braided nylon, in-group I and II, respectively. Injection streptopenicillin @ 100 mg/kg body wt. and Injection diclofenac sodium @ 2 mg/kg body wt. were given intramuscularly for 3 days in all animals. The surgical wound was cleaned with povidone iodine and dressed daily with antiseptic ointment. Skin sutures were removed till the completion of skin healing.

3.2.3. Results and discussion

Surgical wounds appeared apparently healthy throughout the period of observation in both the groups. None of the wound showed any complication like gaping or infection. Gross observations at day 7 shows more vascularity around carbon fibers at the site and on day 30, the carbon fibers were covered by white fibrous tissue. On day 60 the carbon fibers including knots were completely buried under the newly formed tissue. Carbon fibers were well tolerated macroscopically with no evidence of infection or sinus formation. Increased vascularity observed in the present study at the site repaired with carbon fibers was also observed by Kumar et al. [31] following reconstruction of superficial digital flexor tendon with carbon fibers in crossbred calves. Increased vascularity at the reconstruction site is the normal response to injury which is essential for reabsorption of clot and dead cells and finally in the

laying down of fibrous tissue [32]. Uniform covering of prosthetic material with a layer of white connective tissue of variable thickness due to formation of fibrous connective tissue and subsequently laying of collagen fibers was observed [27].

On the contrary, in group I, the carbon fiber implant in the rabbit abdominal wall defect had induced extensive fibrous tissue (collagen fiber) reaction. The inflammatory cells were almost found negligible in the stroma, which indicates the host tissue tolerance to carbon fibers as described by Kumar [33]. The deposition of more collagen fibers in the healing tissue and chronic cell reaction adjacent to the carbon fibers/fibrils along with macrophages, few foreign body giant cells and microgranulomas have similarly been observed by earlier workers in relation to carbon fibers and Mersilene mesh [29, 34]. Subsequent to repair of abdominal wall defect with PTFE and Marlex mesh similar findings were also reported [35]. The chronic cellular reaction persisted throughout the observation period of 90 days in the form of microgranulomas and foreign body giant cells around carbon fibrils [31].

3.3. Carbon fiber mesh in reconstruction of abdominal wall defects

3.3.1. Introduction

A large abdominal wall defect presents a difficult problem for the surgeon. Conventional techniques involving no artificial reinforcement of the abdominal wall run a high risk of recurrence. In repairing the large abdominal wall defects, surgeons have used prosthetic materials of different composition and structures to replace lost tissue [36]. Carbon fibers have been used successfully for reconstruction of tendon [30, 31]. It elicits a strong stimulus to collagen formation and grows stronger with age [37]. Ideally, carbon fibers not only provide structural strength, but also act as a scaffold on which the body may lay down collagen to complete the repair process, particularly in long term [29]. Keeping in view the possible advantage of carbon fibers, the present study was conducted for reconstruction of abdominal wall defects with carbon mesh in rabbits.

3.3.2. Materials and m`ethods

Clinically healthy adult New Zealand white rabbits (12) of either sex were divided randomly into groups I and II having 8 animals in group I and 4 animals in group II (control). Mid-ventral abdominal region was chosen for the purpose of study. Food for 18 h and water for 6 h was withheld before operation. The ventral abdominal area was prepared for aseptic surgery and operation was performed under general anesthesia. Thiopental sodium (2.5%) was injected intravenously in the ear vein "to effect" for anesthesia. A full thickness 2 × 3 cm defect in mid-ventral abdominal wall was created and immediately repaired with carbon mesh in animals of group I. The carbon mesh was prepared from the carbon sheet. The carbon sheet was cut in desired shape and size. The carbon mesh was washed in acetone and autoclaved before use. In animals of group II the linear abdominal muscular wall incision was made and repaired with black braided nylon. Daily dressing of suture line with povidone iodine was done till recovery.

3.3.3. Results and discussion

Collagen and hydroxyproline content increased gradually up to 30 days in both the groups. However, significant ($P < 0.05$) increase was observed up to day 60 in group I and up to day 30 in group II animals. Elastin percentage increased in the healing tissue in both the groups up to 30th day. On the basis of the present study it can be concluded that the carbon mesh can be used for the reconstruction of large abdominal wall defects. Carbon fibers were used for the repair of experimental large abdominal incisional hernias in sheep [34]. The carbon fibers were well tolerated by animals and no herniation was reported in 20 sheep repaired with carbon fibers. Greenstein et al. [38] used polylactic acid carbon mesh for repair of experimentally created ventral hernias in rats. In another experimental study fascial defects in dogs were repaired with carbon fibers. Bilateral defects (1 cm square) were made in the fascia of the back and mechanical strength and stiffness at the sites were measured 3–12 months after operation. Defects repaired with carbon fibers were significantly stronger 12 months after operation compared with defects repaired with polypropylene mesh and unrepaired defects [39]. It is concluded that carbon fiber mesh act as biocompatible material and significantly increases mechanical strength at the repair site. It stimulated fibroplasias, resulted in strong fibrous reaction at the site. Experimental results in animals have been reported but on perusal in literature no report was found using carbon fiber mesh for the repair of external abdominal hernias in clinical cases.

3.4. Carbon fibers for gap repair of flexor tendons

3.4.1. Introduction

Formation of gap between cut ends and peritendinous adhesions after surgical repair are the major problems in tendon reconstruction. Carbon fibers have been used to fill the gap between the cut ends of the tendon in hoses, rabbits, dogs, sheep and donkey. Biocompatibility and non-carcinogenicity coupled with the ability to sustain tissue growth are the rationale for the utilization of filamentous carbon as a synthetic substitute. Carbon as an inert element has advantages over other materials because it is a basic constituent of tissues. The high proportion of the tissues of living organisms is composed of carbon compounds so it is well tolerated by the tissues. An ideal biomaterial is that "instead of fighting" biology it should "smoothly integrate into living tissue." The present study describes the use of carbon fibers for gap repair of tendon.

3.4.2. Materials and methods

Twenty-four tenorrhaphies were performed at the mid-metatarsal region in 12 crossbred calves under xylazine–ketamine spinal analgesia having 6–18 months of age and weighing 120–250 kg. A 2.5-cm long gap was created in the superficial digital flexor (SDF) tendon and immediately repaired with carbon fibers. About 3000 carbon fibrils (diameter of each filament was 7.5 micron) were taken and allowed to recoil upon themselves to form a two ply twist implant of 6000 carbon fibrils filament. They were threaded in straight cutting suturing needle with fine nylon suture material used to tow these carbon fibers. This implant was

washed with acetone for 2 min before autoclaving. Under epidural anesthesia a curvilinear incision was made at mid medial metatarsal region and superficial digital flexor tendon (SDF) was exposed. A 2.5 cm long defect was created in the SDF. The cut ends of SDF tendon were repaired with carbon fibers using modified locking loop suture pattern (**Figure 2**). The skin incision was closed with nylon sutures. Both the hind limbs were utilized for the study. The animals were evaluated on the basis of clinical, radiological, gross, histopathological and scanning electron microscopic observations.

3.4.3. Results and discussion

Clinical examination revealed a slight increase ($P > 0.05$) in rectal temperature, heart and respiratory rate for 2–4 days post-operation. Milder pain and exudation as well as earlier restoration of tendon gliding movements and weight bearing were seen. Air-tendogram in the carbon fiber group on day 30 revealed restoration of continuity across the defect of the tendon. Regression of peritendinous adhesions and swelling at the reconstructed site at later stages was observed indicative by the clear demarcation among these structures. On day 90 the tendon at the reconstructed site attained near normal thickness and density. Angiography

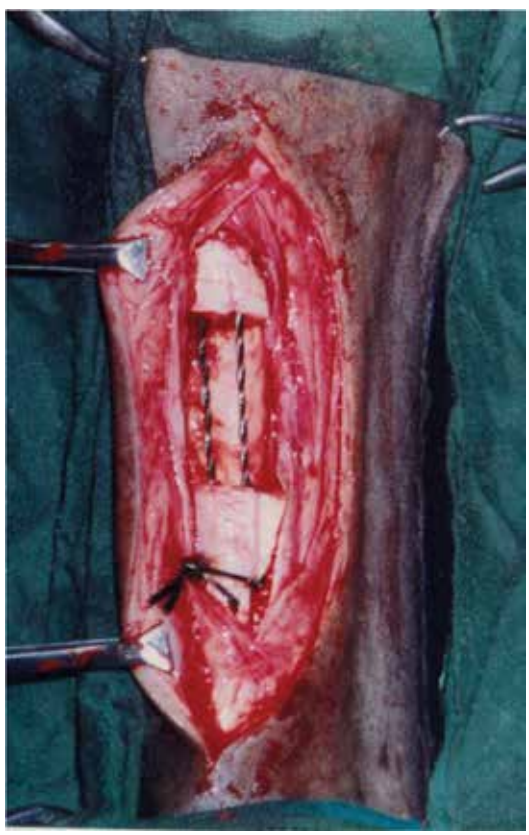

Figure 2. Repair of 2.5 cm long defect in SDF tendon using carbon fibers.

http://dx.doi.org/10.5772/intechopen.75826

showed hypervascularization at the reconstructed site on day 14 in the carbon fiber group. On days 30 and 90, blood vessels were normally organized.

Gross observations showed filling of the defect with granulation tissue with more vascularity on day 7, which was less prominent at day 14). On day 30, the neotendon formed was slightly thicker and comparable to normal tendon in appearance and texture (**Figure 3**). On day 90, it exhibited all the characteristics of a fully developed tendon. A longitudinal split section showed intact carbon fibers strand surrounded by neo tendon. Peritendinous adhesions were maximum on day 7, and later on reduced gradually (**Figure 4**). Microscopically, an acute inflammatory reaction in the periphery of carbon fibers was observed on day 7. Immature fibroblasts were arranged in a haphazard pattern at this stage. By day 14, numerous newly formed capillaries and comparatively more mature fibroblasts were present in between and

Figure 3. Gross observation on day 30, split section showing formation of neotendon.

Figure 4. Gross observation on day 90 and its split section exhibiting all characteristics of a fully developed tendon.

around the carbon fibers which were aligning parallel to the longitudinal axis of the tendon. By day 30 the healing tissue exhibited longitudinal orientation of collagen fibers and was at a more advance stage of maturation. By day 90, the neotendon formed simulated the picture of normal tendon. Scanning electron microscopic observation revealed formation of neotendon between carbon fiber strands, resulting in thickening of the implant. Longitudinal grooving on the carbon fiber filaments was also observed. In later stages parallel collagen fibers resembling normal tendon were observed.

4. Clinical applications

Successful repair of abdominal wall defect requires closure of defect without undue tension on suture line. To reduce the recurrence rates, surgeons had used prosthetic materials of different structures and composition to bridge the tissue defects of large hernias that cannot

be approximated primarily without placing excess tension on the suture line. Carbon mesh is available as a prosthetic sheet for bridging abdominal wall defects. This material is inert and has been proved to be biocompatible in experimental trials in rabbits [40]. In the present study carbon mesh was utilized in the treatment of cattle with abdominal wall hernias where repair by direct tissue approximation could not be accomplished without unacceptable tension across the suture line.

4.1. Materials and methods

Six crossbred heifers aged between 12 and 18 months with congenital umbilical hernias without complication were taken up in this study. After washing with acetone for 2 min, the mesh was autoclaved. The animals were kept on fasting for 24 h before surgery. Preoperatively all these animals received antibiotic therapy and surgery was carried out in dorsoventral recumbency. Analgesia at the site of operation was achieved by field block by using 2% Lignocaine hydrochloride. After preparing the site aseptically, a semicircular skin incision was made over the swelling. The subcutaneous tissue, abdominal muscles and hernial rings were separated. Carbon mesh was implanted subfascially. Interrupted sutures were then placed 1.5 cm from the edge of prosthesis and 1.5 cm apart, circumscribing the edges of the musculofascial defect by using Vetafil (1.1 mm). In all herniorrhaphies, the mesh was strengthened with Vetafil by using vest over pant technique. The skin incision was closed in routine manner. Injection Oxytetracycline for 5 days and Injection Diclofenac sodium for 3 days were administered intramuscularly. Antiseptic dressing was done with Betadine till suture removal. Sutures were removed on 12th postoperative day.

4.2. Results and discussion

All the animals were partially anorectic for 2 days thereafter feeding pattern was completely normal. Carbon mesh was well tolerated by all animals. Carbon mesh acted as a biocompatible scaffold and did not degrade or loose strength [38]. Slight inflammatory swelling was observed at the operated site, which may be due to tissue reaction to surgical trauma [41].

Seroma formation after hernioplasty with different biomaterials in human beings was also reported [42] and this complication was treated by aspiration and compression [36]. In present study, infection at the mesh-implanted site was not observed. It may be due to preoperative use of antibiotics in all the animals. Judicious use of local and systemic antibiotics was useful in decreasing the infection rate. Excessive tension on suture line forced the suture line to cut the tissue by progressive aseptic necrosis [43]. Hard swelling at the reconstruction site was recorded on day 12 in all animals, which gradually decreased and subsided completely between 34 and 40 days. This may be due to excessive production and deposition of fibrous tissue in the interstices of the mesh [29]. Later on decrease in hard swelling may be due to gradual disintegration of carbon fibers, phagocytosis and removal of debris. Carbon fiber implant induced extensive fibrous tissue reaction with neovascularization around it. The inflammatory cells were almost negligible in the stroma which indicated the host tissue reaction tolerance to carbon fibers [44]. The deposition of more collagen fibers in the healing tissue and chronic cell reaction adjacent to the carbon fibrils along with macrophages, few foreign body giant cells and microgranulomas has been reported [29].

Two cases of umbilical hernia in dogs have been successfully repaired using carbon fibers as suture materials [45]. The hernial ring was about 3 cm in diameter in both the cases. Carbon fibers filaments (6000 filaments of 7.5 micron diameter) were used to repair the hernial ring. There was an uneventful recovery without untowards reaction. Braided carbon fibers as a suture material for the repair of hernia in a buck and in buffalo calf with no untoward reaction have been used successfully [46]. Use of carbon fibers for the reconstruction of abdominal wall defects has been reported [47]. About 3000 carbon fibrils were taken and allowed to recoil upon themselves to form a two ply twist implant of 6000 carbon fibrils filament. This implant was washed with acetone for 2 min before autoclaving. They were used as sutures for the closing hernial ring. Carbon fibers have the advantage of being a non-irritable biomaterial of reasonable tensile strength. These fibers evoked less inflammatory response. Abundant fibrous tissue was produced around the carbon fibers.

During a 3-year period (2001–2004) 18 animals were surgically treated because of abdominal wall defects [48]. Out of 18 animals 8 were bovines, 5 caprines and 5 canines. In each case the defect was repaired with carbon fibers. Carbon fibers were placed either in simple interrupted pattern or as mattress overlapping pattern. All the cases were successfully treated and no complication was observed up to 6 months postoperatively. In the present study 6000 filaments of carbon fibers have been used for the repair of external abdominal wall defects/hernias in 18 clinical cases of different species of animals having the hernial ring size range from 1.5 to 8 cm in diameter with good results.

Carbon fibers for the *repair* of congenital *umbilical hernias* in five buffalo calves aged 5–13 months have been used. The size of the hernial rings in different animals ranged from 5 to 7 cm in diameter [49]. About 3000 carbon fibrils were taken and allowed to recoil upon themselves to form a two ply twist implant of 6000 carbon fibrils filament. This implant was washed with acetone for 2 min before autoclaving. Carbon fibers have the advantage of being a non-irritable biomaterial of reasonable tensile strength. These fibers evoked less inflammatory response and abundant fibrous tissue response around the carbon fibers. The amount of fibrosis increased with time with a gradual transition of stress from the carbon fibers to the induced fibrous tissue. The wound was healed by first intention in all the animals. Gangwar et al. [50] reported the *use* of carbon fibers for the *repair* of *umbilical hernias* in six cow calves. The size of the hernial rings in different animals ranged from 5 to 7 cm in diameter. About 3000 carbon fibrils were taken and allowed to recoil upon themselves to form a two ply twist implant of 6000 carbon fibrils filament. All the animals recovered completely. No complication was observed at the repair site.

Successful repair of large umbilical hernia in a crossbred heifer has been reported using carbon sheet. The hernial ring size was 12 × 10 cm in diameter. The carbon sheet was applied as inlay graft and sutured with hernial ring by silk sutures. The animal show uneventful recovery and no complication were observed up to 6 months postoperatively [51]. Similarly in another case carbon mesh was used to repair large umbilical hernia in a crossbred male calf as inlay graft where the hernial ring size was 8 × 10 cm in diameter. The animal show uneventful recovery and no complication were observed up to 3 months postoperatively [52] (**Figure 5a–c**).

http://dx.doi.org/10.5772/intechopen.75826

(a)

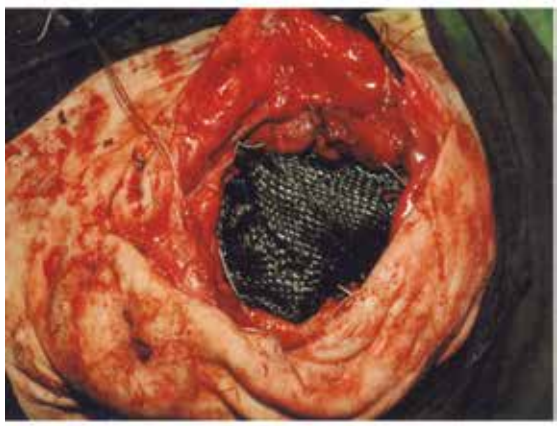

(b)

(c)

Figure 5. Large umbilical hernia in a crossbreed male calf repair with carbon mesh (a) crossbred male calf showing large umbilical hernia (b) opening of hernial sac and placing of carbon mesh for repair of hernial ring as inlay graft (c) complete closure of defect after skin suturing.

During a 4-year period (2001–2005) 9 animals (8 bovines and 1 caprine) were surgically treated for abdominal wall defects (hernia). In each case the defect was repaired with carbon mesh. All the cases were successfully treated and no complication was observed up to 6 months postoperatively. In the present study carbon fiber mesh have been used for the repair of external abdominal wall defects/hernias having the hernial ring size ranged from 6 to 15 cm in diameter with good results. This is probably the first report in which carbon fiber mesh has been successfully used for the repair of abdominal wall defects in clinical cases [53].

Use of carbon cloth/carbon fiber mesh for the repair of abdominal hernias in animals was reported with good results [54]. Similarly, Gangwar et al. [55] used carbon fiber mesh for the repair of external abdominal wall defect in a calf having the hernial ring size of 8 cm in diameter with satisfactory results. Kh Sangeeta Devi et al. [56] operated six crossbred heifers, 12–18 months old, with congenital umbilical hernia using carbon mesh. Results revealed that all animals were clinically healthy after the surgery. Inflammation gradually decreased between 34 and 40 days postoperatively. With significant increase in erythrocyte sedimentation rate up to 30 days. Total leukocyte count and neutrophils returned to normal after 30 days. Histopathological lesions showed that the carbon fiber implant induced extensive fibrous reaction with neovascularization. It is concluded that the carbon mesh can be used for successful reconstruction of umbilical hernia in cattle.

Author details

Naveen Kumar[1]*, Anil Kumar Gangwar[2] and Khangembam Sangeeta Devi[3]

*Address all correspondence to: naveen.ivri1961@gmail.com

1 Division of Surgery, ICAR-Indian Veterinary Research Institute, Bareilly, Uttar Pradesh, India

2 Department of Surgery and Radiology, College of Veterinary Sciences and Animal Husbandry, Narendra Deva University of Agriculture and Technology, Faizabad, Uttar Pradesh, India

3 Department of Surgery and Radiology, College of Veterinary Sciences and Animal Husbandry, Narendra Deva University of Agriculture and Technology, Faizabad, Uttar Pradesh, India

References

[1] Blazewicz M, Blazewicz S, Wajler C. Mechanical and implant behaviour of chemically modified carbon braids. Ceramics International. 1994;**20**:99-103

[2] Carranza-Bencano A, Armas-Padron JR, Gili-Miner M, Lozano MA. Carbon fiber implants in osteochondral defects of the rabbit patella. Biomaterials. 2000;**21**:2171-2176

[3] Forster IW, Ralis ZA, McKibbin B, Jenkins DHR. Biological reaction to carbon fiber implants. Clinical Orthopaedics and Related Research. 1978;**131**:299-307

[4] Miller JH. Comparison of the structure of neotendons induced by implantation of carbon or polyester fibres. Journal of Bone and Joint Surgery. 1984;**66**:131-139

[5] Jenkins DHR. Ligament induction by filamentous carbon fibre. Clinical Orthopaedics. 1985;**197**:86-90

[6] Becker HP, Rosenbaum D, Zeithammel G, Gnann R, Bauer G, Gerngross H, Claes L. Tenodesis versus carbon fiber repair of ankle ligaments: A clinical comparison. Clinical Orthopaedics. 1996;**325**:194-202

[7] Morris DM, Haskins R, Marino AA, Misra RP, Rogers S, Fronczak S, James AA. Use of carbon fibres for repair of abdominal wall defects in rats. Surgery. 1990;**107**:627-631

[8] More N, Baquey C, Barthe X, Rouais F, Rivel J, Trinqueste M, Marchand A. Biocompatibility of carbon-carbon materials: In vivo study using ^{14}C labelled samples. Biomaterials. 1988;**9**:198-202

[9] Strover AE, Firer P. The use of carbon fibre implants in anterior ligament surgery. Clinical Orthopaedics. 1985;**196**:88-98

[10] Alexander H, Weiss AB, Parsons JR. Ligament repair and reconstruction with absorbable polymer coated carbon fibre. Journal of Orthopaedic Surgery and Research. 1987;**3**:1-14

[11] Christel P, Claes L, Brown SA. Carbon-reinforced composites in orthopedic surgery. In: Szycher M, editor. High Performance Biomaterials. A Comprehensive Guide to Medical and Pharmaceutical Application. Lancaster, PA: Technomic Publishing Company; 1991. pp. 499-518

[12] Jenkins DHR, Forster IW, McKibbin B, Ralis ZA. Induction of tendon and ligament formation by carbon implantation. Journal of Bone and Joint Surgery. 1977;**59B**:53-57

[13] Jenkins DHR. The repair of cruciate ligaments with flexible carbon fibre. A longer term study of the induction of new ligaments and of the fate of the implanted carbon. Journal of Bone and Joint Surgery. 1978;**60B**:520-522

[14] Rohe K, Braun A, Cotta H. Ligament replacement with carbon fibre implants in rabbits: Light and transmission electron microscopic studies. Zeitschrift für Orthopädie und Ihre Grenzgebiete. 1986;**124**:569-577

[15] Pesakova V, Klezl Z, Balik K, Adam M. Biomechanical and biological properties of the implant material carbon-carbon composite covered with pyrolytic carbon. Journal of Materials Science. Materials in Medicine. 2000;**11**:793-798

[16] Blazewicz M. Carbon materials in the treatment of soft and hard tissue injuries. European Cells & Materials. 2001;**2**:21-29

[17] Czajkowska B, Blazewicz M. Phagocytosis of chemically modified carbon materials. Biomaterials. 1997;**18**:69-74

[18] Debnath UK, Fairclough JA, Williams RL. Long-term local effects of carbon fibre in the knee. The Knee. 2004;**11**:259-264

[19] Adams D, Williams DF. Carbon fiber-reinforced carbon as a potential implant material. Journal of Biomedical Research. 1978;**2**:35-42

[20] Bokros JC, Arkins RJ, Shim HS, Houbold AD, Agrawal NK. Carbon in prosthetic devices. In: Deviney ML, O'Grady TM, editors. Petroleum Derived Carbons. Washington, DC: American Chemical Society; 1976

[21] Mortier J, Engelhardt M. Foreign body reaction in carbon fiber prosthesis implantation in the knee joint-case report and review of the literature. Zeitschrift für Orthopädie und Ihre Grenzgebiete. 2000;**138**:390-394

[22] Demmer P, Ed FRCS, Glas FRCS, Fowler M, Marino AA. Use of carbon fibre in the reconstruction of knee ligaments. Clinical Orthopaedics and Related Research. 1991;**271**: 225-232

[23] Grabinski C, Hussain S, Lafdi K, Braydich-Stolle L, Schlager J. Effect of dimension on biocompatibility of carbon nanomaterials. Carbon. 2007;**45**:2828-2835

[24] Gangwar AK, Sharma AK, Kumar N, Maiti SK, Gupta OP, Goswami TK, Singh R. Carbon fibres for the repair of abdominal wall defects in rabbits. Carbon Science. 2005;**6**:15-24

[25] Dalla-Vecchia L, Engum S, Kogon B, Jensen E, Davis M, Grosfeld J. Evaluation of small intestine submucosa and acellular dermis as diaphragmatic prostheses. Journal of Pediatric Surgery. 1999;**34**:167-171

[26] Takahashi M, Ono K, Wakakuwa R, Sato O, Tsuchiya Y, Kamya G, Nitta K, Tajima K, Wada K. Use of human dura mater allograft for the repair of a contaminated abdominal wall defect. Surgery Today. 1994;**24**:468-472

[27] Shoukry M, El-Keiey M, Hamouda M, Gadallah S. Commercial polyester fabric repair of abdominal hernias and defects. The Veterinary Record. 1997;**140**:606-607

[28] Gillion JF, Begin GF, Marecos C, Fourtaniar G. Expanded polytetrafluoroethylene patches used in the intraperitoneal or extraperitoneal position for repair of incisional hernias of the anterolateral abdominal wall. American Journal of Surgery. 1999;**174**:16-19

[29] Cameron AEP, Taylor DEM. Carbon-fibre versus Marlex mesh in the repair of experimental abdominal wall defects in rats. The British Journal of Surgery. 1985;**72**:648-650

[30] Kumar N, Sharma AK, Sharma AK, Satish K. Carbon fibres and plasma preserved tendon allografts for gap repair of flexor tendon in bovines: Gross, microscopic and scanning electron microscopic observations. Journal of Veterinary Medicine Series A. 2002;**49**(5):269-276

[31] Kumar N, Sharma AK, Singh GR, Gupta OP. Carbon fibres and plasma preserved tendon allografts for gap repair of flexor tendon in bovines: Clinical, radiological and angiographical observations. Journal of Veterinary Medicine Series A. 2002;**49**(3):161-168

[32] Silver IA. Basic physiology of wound healing in the horse. Equine Veterinary Journal. 1982;**14**:7-15

[33] Kumar N. Carbon fibres and plasma preserved homologous grafts for gap repair of flexor tendon in bovines [PhD thesis]. Izatnagar, Uttar Pradesh: Deemed University, Indian Veterinary Research Institute; 1997

[34] Nurse CJ, Jenkins DHR. The use of flexible carbon fibre in the repair of experimental large abdominal incisional hernias. The British Journal of Surgery. 1980;**67**:135-137

[35] Bellon JM, Bujan J, Contreras LA, Mastin ACS, Junado F. Comparison of a new type of polytetrafluoroethylene patch (Mycro mesh) and polypropylene prosthesis (Marlex) for repair of abdominal wall defects. Journal of the American College of Surgeons. 1996;**183**:11-118

[36] Deysine M. Hernia repair with expanded polytetrafluoroethylene. American Journal of Surgery. 1992;**163**:422

[37] Layson RL, Channon GM, Jenkins DHR, Ralis ZA. Flexible carbon fibre in late ligamentous reconstruction for instability of the knee. Journal of Bone and Joint Surgery. 1984;**66B**:196-200

[38] Greenstein SM, Murphy TF, Rush BF Jr, Alexander H. Evaluation of polylactic acid-carbon mesh for repair of ventral herniorrhaphy. American Journal of Surgery. 1986;**151**:635-639

[39] Morris DM, Hindman J, Marino AA. Repair of fascial defects in dogs using carbon fibres. The Journal of Surgical Research. 1998;**80**:300-303

[40] Gangwar AK, Sharma AK, Kumar N, Sangeeta Devi K, Maiti SK, Gupta OP, Singh R. Reconstruction of large abdominal wall defects with carbon mesh in rabbits: Gross, histopathological and histochemical studies. The Indian Journal of Animal Sciences. 2010;**80**:117-120

[41] Bauer JJ, Salky BA, Gelernt IM, Kreel I. Repair of large abdominal wall defects with expanded polytetrafluoroethylene (PTFE). Annals of Surgery. 1987;**206**:765

[42] Koukourou A, Lyon W, Rice J, Wattchow DA. Prospective randomized trial of polypropylene mesh compared with nylon darn in inguinal hernia repair. The British Journal of Surgery. 2001;**88**:931

[43] Kennedy GM, Matyas JA. Use of expanded polytetrafluoroethylene in the repair of difficult hernias. American Journal of Surgery. 1999;**168**:304

[44] Ralis ZA, Forster IW. Choice of the implantation site and other factors influencing the carbon fiber tissue reaction. Journal of Bone and Joint Surgery. 1981;**63-B**:295-296

[45] Sharma AK, Kumar N, Gangwar AK, Maiti SK, Kumar N. Use of carbon fibres for the repair of umbilical hernia in dogs. Journal of Canine Development and Research. 2002;**2**:65-68

[46] Kumar N, Sharma AK, Gangwar AK, Maiti SK, Gupta OP. Use of braided carbon fibres for the repair of hernia in buck and buffalo calf. In: Xth IAAVR Conference; 14-15 April 2003; Palampur; 2003, Abstract 03:25

[47] Kumar N, Sharma AK, Kumar S. Use of carbon fibres for the reconstruction of abdominal wall defects. In: International Workshop on Carbon Materials for Energy Applications; 24-25 November 2004; New Delhi; Abstract in Fibres and Composites; 2004. p. 52

[48] Kumar N, Sharma AK, Gangwar AK, Maiti SK, Gupta OP, Kumar N, Mathur RB. Carbon fibres for the repair of external abdominal hernias in bovines, caprines and canines: A review of 18 clinical cases. Carbon Science. 2006;**7**:81-86

[49] Sangeeta Devi K, Gangwar AK, Singh HN. Carbon fiber as a prosthetic material for reconstruction of congenital umbilical hernias in buffalo calves. Indian Journal of Veterinary Surgery. 2008;**29**(1):42

[50] Gangwar AK, Sharma AK, Kumar N, Sangeeta Devi K. Use of braided carbon fibres in the repair of umbilical hernia in bovines. The Indian Veterinary Journal. 2008;**85**:430-431

[51] Kumar N, Sharma AK, Gangwar AK, Maiti SK, Kumar N. Successful use of carbon sheet in surgical management of large umbilical hernia in a crossbred heifer. In: 90th Indian Science Congress Association, Part-II, Advance Abstract, Section of Animal, Veterinary and Fishery Sciences; 2003. p. 97

[52] Kumar N, Sharma AK, Gangwar AK, Maiti SK, Kumar N. Use of carbon mesh in surgical management of large umbilical hernia. In: XXVI ISVS Annual Conference; 2003. pp. 31-32

[53] Kumar N, Sharma AK, Maiti SK, Gangwar AK, Kumar N. Carbon fibre mesh for the repair of abdominal hernias in bovines and caprines: A review of nine clinical cases. Carbon Letters. 2007;**8**:269-273

[54] Kumar N, Sharma AK, Maiti SK. Carbon cloth for repair of abdominal hernias in animals. In: 95th Indian Science Congress; Visakhapatnam, 3-7 January, 2008; Section II: Animal, Veterinary and Fishery Sciences, Abstract 118; 2008. p. 90

[55] Gangwar AK, Sharma AK, Kumar N, Sangeeta Devi K. Prosthetic hernioplasty with carbon mesh in a calf. The Indian Veterinary Journal. 2008;**85**:658-659

[56] Sangeeta Devi K, Gangwar AK, Singh HN, Kumar N. Studies on carbon mesh repair of congenital umbilical hernia in bovine. The Indian Veterinary Journal. 2010;**87**:139-141

Chapter 7

Characterization of Carbon Fibers Recovered by Pyrolysis of Cured Prepregs and Their Reuse in New Composites

Andrea Fernández, Cláudio S. Lopes,
Carlos González and Félix A. López

Additional information is available at the end of the chapter

http://dx.doi.org/10.5772/intechopen.74281

Abstract

The applications of composite materials are rapidly growing. In the aeronautical sector, composites account for up to 50% of the weight of a modern typical commercial aircraft. However, the amount of composites currently recycled is less than 5% of the total amount produced. With environmental concerns becoming an increasingly influential topic, recyclability of composite materials is a key issue. Furthermore, several related European laws have been passed to minimize the environmental impact of composite structures and to make rational use of landfills. In this chapter, the authors analyze recycling techniques for carbon fiber composites with thermoset polymer matrix. The objective is to reuse the fibers in new, lower cost composites with similar properties. Starting from a pyrolysis step, followed by oxidation, an evaluation of the different parameters of the recycling process has been performed. The characterization of the fibers includes tensile tests, scanning electron microscopy, and Raman spectroscopy. The recycled fibers presented a reduction of their initial tensile strength lower than 10%. Then, remanufacturing of laminates using the recycled fibers was achieved by resin film infusion, obtaining laminates with properties similar to the brand-new composites. These results have the potential to be exploited by the automotive, aeronautical, wind energy, construction, and other sectors.

Keywords: composites, recycling, pyrolysis, carbon fiber, fracture toughness, resin film infusion

1. Introduction

Composites are made from at least two constituents that together produce material properties that are different from the properties of those materials on their own. In practice, most composites consist of a bulk material (plastic matrix), and a reinforcement (typically fibers, i.e. carbon fibers), added primarily to increase the strength and stiffness of the material.

While they offer fantastic durability, high specific stiffness, and strength-to-weight ratio, their properties are essentially controlled by those of their constituents, including fiber/matrix interfaces, their volume fraction, and spatial distribution. The remarkable characteristics of fiber-reinforced plastics (FRPs) led to rapid increase of their use. In the aeronautical sector, the use of composites reaches up to 50% of the total weight of a modern commercial aircraft [1]. But, FRPs are not only used in the aeronautic/aerospace sector. Other industries where weight-efficient performance is a key factor, such as the automotive, naval, and wind energy sectors, are likewise increasing the use of composite materials (annual growth rate of 12–14% **Figure 1**).

Naturally, the increment in demand and use of composites results in more and more waste being generated throughout the life cycle of these materials; in fact, it is estimated that 30–40% of pristine carbon fibers are wasted during the manufacturing process, and significant amounts of off-cuts, rejects, and put-of-date prepregs are generated, causing a significant negative impact on the environment. The excess of carbon fibers that is generated per year equals about 20–25% of the total amount consumed during 2015 [2]. Evidently, the recycling of composite materials is a high priority.

The recycling of carbon fiber-reinforced plastics (CFRPs) not only makes sense from environmental and economic perspectives but also could be a key in increasing the penetration

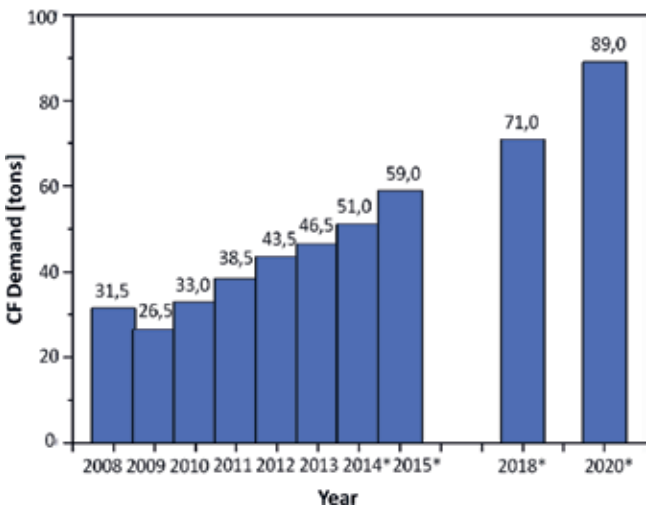

Figure 1. Global demand of carbon fibers over the years [3].

of these lightweight but expensive materials in high-volume markets such as automotive and aeronautical industry.

The principal waste management options that have been adopted for composites are burying, landfilling, or incinerating. Several European Directives and regulations were implemented in order to make better use of landfills (EU 1999/31/EC) [4]; to reduce waste management (EU 2000/53/EC on End-of-Life vehicles) [5]; to prevent or limit the emission levels produced by incineration plants (Directive 2000/76/EC) [6]; as well as to prevent and remedy the environmental damage (2004/35/EC on Environmental Liability) [7]. To reduce the consumption of natural resources and landfill allocations, recycling composite elements for reusing in different applications is postulated as a promising solution. Because of their high initial cost and energy consumption during manufacture, fibers are the most attractive constituent for recycling. In addition to these economic incentives and compared to the production of virgin materials, recycling will also reduce air, water, pollutant emissions (90–95% of CO_2 emissions), as well as energy demand. Therefore, recycling results in a substantial improvement on the environmental impact of composite materials.

The economic costs can be reduced by about 70% (from €30–58/kg to €15–23/kg for carbon fibers) and the energy requirement by nearly 98% (from 55 to 166 kWh/kg to 3–10 kWh/kg), since the majority of energy consumption occurs during production of virgin carbon fibers [8]. Substituting virgin carbon fibers with recycled ones would save enough electricity to power 175,000 homes in a year [9]. However, the amount of composites currently recycled is less than 5% due to their complex composition; the nature of the resin (i.e., thermoset resins have a cross-linked matrix that cannot be simply reprocessed by remelting or remolding); their combination with other materials; and the high variability among waste products [9]. Furthermore, the use of the recycled carbon fibers in industrial applications is currently very limited due to the low quality control of the fibers, i.e., the length, surface quality, and origin of the fibers are difficult to control. In addition, the hierarchical structure of composites is destroyed during recycling; and the resultant laminates composed of recycled fibers present disorientation. Then, these composites do not meet the standards of high-value structural applications.

There are three main general technical approaches to the recovery of the fibers in thermoset-matrix composites: mechanical, thermal, and chemical. The mechanical recycling consists of reducing the size of the scrap composite components by shredding, crushing or milling. Nevertheless, in industry, this technology has not been extensively exploited to treat carbon fiber-reinforced polymers (CFRCs) due to the poor bonding between the recycled fibers and the new resin.

Thermal recycling of composites involves the separation of the matrix from the fibers by applying heat. There are two main types of thermal recycling methods: pyrolysis and fluidized-bed recycling process. In both, the resin is volatilized into lower weight molecules to produce mainly oil and gases, while fibers are recovered, usually with char on their surfaces. These thermal processes have been widely implemented in industry. Among them, pyrolysis is the most widespread technology. Both glass and carbon fiber-reinforced composites can be recycled through pyrolysis. Because of the much higher market value of carbon fibers,

pyrolysis of carbon fiber-reinforced composites has higher economic attractiveness. The first continuous pyrolysis recycling line, commercially producing recycled carbon fibers, has been introduced by the company Recycled Carbon Fiber Ltd. (RCF) in 2008 [10]. One of the most famous cases of recycling composites is BMW: up to 95% of the BMW, i3 is recyclable [11]. In Spain, the company Thermal Recycling of Composites (TRC, SL) has technology for the thermochemical recycling of composite materials reinforced with both glass and carbon fibers, with a special recycling line for wind turbine blades [12]. ELG Carbon Fiber (ELG-CF), Coseley, UK, develops a pyrolysis process in which they treat around 24,000 tons per year of carbon fiber waste. The process yields a tough and abrasive cotton-wool-like fuzz of carbon fiber, which maintains 90–95% of its original mechanical properties [13].

The recycling of CFRP waste through pyrolysis poses the additional problem of managing the liquids that are produced in the process, as a consequence of the thermochemical degradation of the resins (usually epoxy) [14]. Therefore, other less expensive alternatives are being studied. In this regard, many researchers have investigated the decomposition of resin matrix and CFRP carbon fiber recovery using chemical treatment to break and degrade the resin. The solvent can be water (hydrolysis) or organic (solvolysis). Solvolysis offers a large number of possibilities, thanks to a wide range of solvents, temperatures, pressures, and catalysts. Depending on the amount of solvent and on the temperature, the fluid can be vapor, liquid, biphasic, or supercritical. The latest have gained much attention since 2000 because characteristics between liquid and gas phases can be achieved through combinations of temperature and pressure, allowing the enhancement of the diffusion effect [15]. The results of recent research on the use of supercritical or subcritical fluids including water and alcohol are very promising [16–18].

In this chapter, we propose a two-step carbon-fiber recycling process: pyrolysis followed by oxidation. An optimization of the method in terms of sustainability of the technique and the characteristics of the fibers will be carried by performing surface, microstructure, and mechanical testing of the recovered fibers. With respect to mechanical performance, fiber strength distribution and fracture toughness were the properties analyzed. In addition, the remanufacture of laminates by means resin film infusion using the recycled fibers is proposed. The mechanical performance of the resulting laminates will be evaluated and compared to that of pristine ones.

2. Recycling process

A common scrap material from the aeronautic sector was selected for recycling. The recycling steps and process optimization parameters are detailed below.

2.1. Scrap material

The composite material used as the basis for the optimization of the experimental parameters was a scrap (HexPly® F593, supplied by AIRBUS OPERATIONS S.L., Getafe, Spain) composed

of a plain woven prepreg made of epoxy resin reinforced with Toray T300/3 k carbon fibers [19] (55–60% carbon fibers [by mass] and 40–45% resin; fiber area weight = 193 g/m^2) [20]. The carbon fibers were made of PAN. This process is as follows. First, there is a pre-oxidation treatment under 200–300°C; second, a carbonization in high purity inert gas under 1000–1500°C takes place; third, there is a graphitization under 2500–3000°C; and finally, a sizing.

2.2. Recycling approach

The process used to recover the fibers was pyrolysis. It is a thermochemical decomposition of the organic part of the composite materials at temperatures between 450°C and 700°C in the nearly absence of oxygen. It is widely performed in the industry due to its easy and cheap implementation.

The recycling process was done in a thermolysis installation (**Figure 2**). It consists of a heating system and a gas condensation device [21]. The muffle furnace (1) contains a 9.6 L steel reactor, sealed by a screw-on lid. The flue gases circulate across four condensers (3–6) connected to each other by six cooling pipes. Each condenser allows the collection of distilled oils as cool gases and has four collection holes for the withdrawal of the distilled liquids and a thermometer to measure their temperature. The noncondensable gases are led to a water-cooling tower (7), where the last fraction of the distilled liquids is collected. These gases pass through a set of three filters (8 and 9) to eliminate pollutant gases and solid particles. The gases can then be mixed with air and burned off or collected for analysis. When the thermolysis is complete (the rotameter (10) inside the tubing no longer detects any distillation gas), the reactors are cooled and the thermolytic solid residues removed, which are mainly composed of pieces of dimensions equal to those of the input material but completely black.

The complete process consists of two steps: a thermolysis or pyrolysis (heat rate of 20°C/min) and a gasification or oxidation (air flow of 5 L/min). In the first one, the separation fiber/resin takes place; on the second stage, there is the removal of the char deposited on the

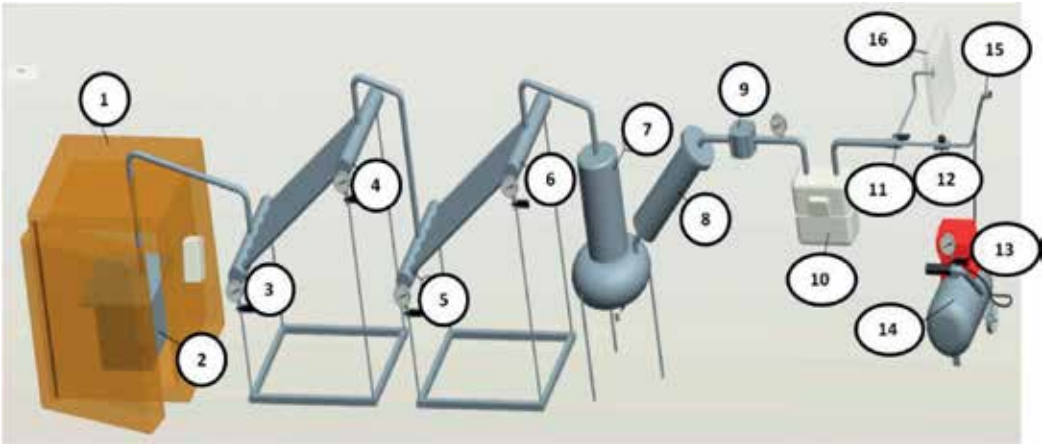

Figure 2. Installation used for the pyrolysis of the carbon fibers [15].

surface of the fibers. However, this second step, if not properly designed, is likely to reduce the mechanical properties of the fibers.

2.3. Process optimization

With the purpose of designing the experimental procedure toward achieving the best recyclability and keeping the original fiber properties as intact as possible, the pyrolysis and oxidation steps were studied and optimized.

The design of the pyrolysis temperature for the degradation of the resin was performed by conducting tests runs at 500, 600, and 700°C for 6 h. Values below 500°C did not effectively remove all the resin; and values higher than 700°C caused a high degradation of the recovered fibers. The temperature of the pyrolysis (P) stage was then set to 500°C, because for 550°C and above, the preliminary thermogravimetric analysis and surface element concentration tests showed the fibers to be damaged.

The optimum oxidation (O) step was determined by varying the oxidation times between 30 and 90 min. This was done with the following objectives: efficiently removing the char on the fiber surface, while maintaining fiber microstructure intact and retaining fiber mechanical properties as much as possible. Section 3 details the results of this optimization study.

3. Recycled fibers

To determine the optimum oxidation time, analyses of fiber surface quality, fiber composition and mechanical properties of the recovered fibers were performed, as described in this section.

3.1. Surface quality

Scanning electron microscope (SEM) was used to evaluate the presence of char on the surface of the recycled fibers and compare with pristine ones. The images of the morphology change of the virgin and the recycled carbon reveal that pristine fibers exhibit a rough and irregular surface, while the recycled fibers are free of resin char, with a much more regular and smooth surface (**Figure 3(a)–(d)**). Only a few traces of micron-sized resin residues can be seen in few regions on the fiber surface. It can be concluded that, independently the oxidation time, the surface of recycled fibers presented a low amount of residual char and was otherwise clean and showed no evidence of fiber damage. This means that the removal of char from the fiber surface was efficient, and that this process requires only short oxidation times, e.g., 30 min.

3.2. Composition

3.2.1. Surface chemistry

The surface chemistry of virgin and recycled carbon fibers was examined by X-ray photoelectron spectroscopy by López et al. [20]. As shown in **Table 1**, the surface of all the examined fibers was composed of carbon (C), oxygen (O), and nitrogen (N). While the C content

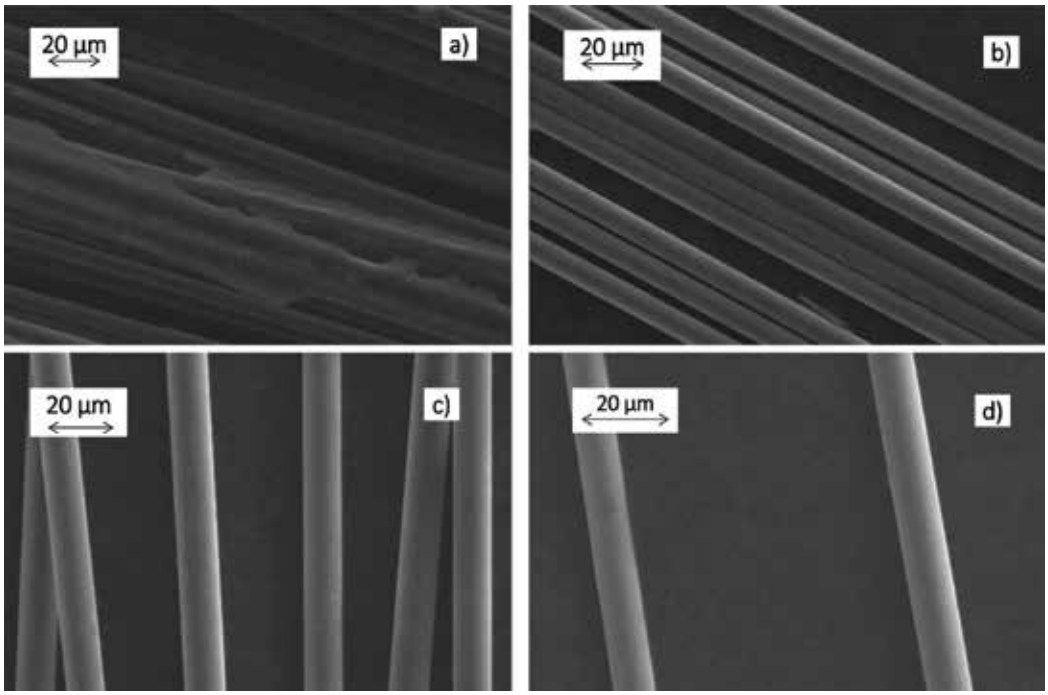

Figure 3. SEM images of the virgin (a) recovered carbon fibers after thermolysis at 500°C and gasification times of 30 min (b), 60 min (c), and 90 min (d).

Fiber sample	C (at.%)	N (at.%)	O (at.%)	Si (at.%)	O/C (at.%)
Virgin	90.1	1.0	8.9	—	0.082
Recycled: P-500°C	89.3	4.5	6.0	0.1	0.067
Recycled: P-500°C/O-30 min	81.2	7.1	10.0	1.7	0.123
Recycled: P-500°C/O-60 min	83.3	4.6	11.7	0.4	0.140

Virgin: virgin TORAY T300/3 k fibers; values provided by manufacturer TORAY JAPAN [22].

Table 1. Surface atomic concentration (at.%) of the recovered fibers obtained at the different gasification times, plus concentrations for pristine fibers.

remains practically constant, the O content increases with gasification time and the N content decreases. The increase in the O/C ratio with gasification time is indicative of the degree of fiber oxidation, which can lead to undesirable alterations. The smaller ratio obtained, i.e., the less oxidized recovered fiber (compared to 0.082% of the virgin ones) indicates that the optimum gasification time is 30 min.

Moreover, according to the thermolytically derived solid residue, 500°C is the condition in which the best atomic surface composition was obtained, due to the smallest quantity of C═O and COOH groups, which suggests the formation of oxygenated compounds on the surface of the solid residue, potentially caused by secondary repolymerization reactions in the gaseous phase.

3.2.2. Crystallite structure

Raman spectra of the surface and transversal section of the carbon fibers (**Figure 4**) were obtained at room temperature to detect the changes in crystallite structure of the recycled carbon fibers at a penetration depth of the order of 60 nm. Independently of the zone evaluated, all first-order Raman spectra for the recycled carbon fibers exhibited two broad peaks at about 1350 and 1580 cm^{-1} corresponding to the D and G bands, respectively.

The G band is associated with a single crystal of graphite, whereas the D peak is from the structural imperfections created by the attachment of hydroxyl and epoxide groups on the carbon basal plane. The ratio of the intensity of the D and G bands (I_D/I_G) indicates the measurement of the graphitic plane size, so the lateral crystallite size (L_a) of the recycled fibers had become smaller [23]. The recycling process generated surface defects caused by the reduced L_a values through the oxidation effect, as is indicated in **Table 2**. The general expression that gives the crystallite size form the integrated intensity ratio is given by Ref [24].

$$L_a\,(nm) \;=\; (2.4 \cdot 10^{-10}) \cdot (\lambda_1)^4 \cdot \left(\frac{I_D}{I_G}\right)^{-1} \tag{1}$$

where λ_1 is the laser line wavelength in nanometer units.

The variation of L_a is generally indicative of a change in material strength. It can be inferred that the larger the reduction in L_a, the lower the tensile strength of the recycled fibers. Therefore, these results indicate that the lowest reduction in fiber tensile strength is likely to be achieved for an oxidation step of 30 min.

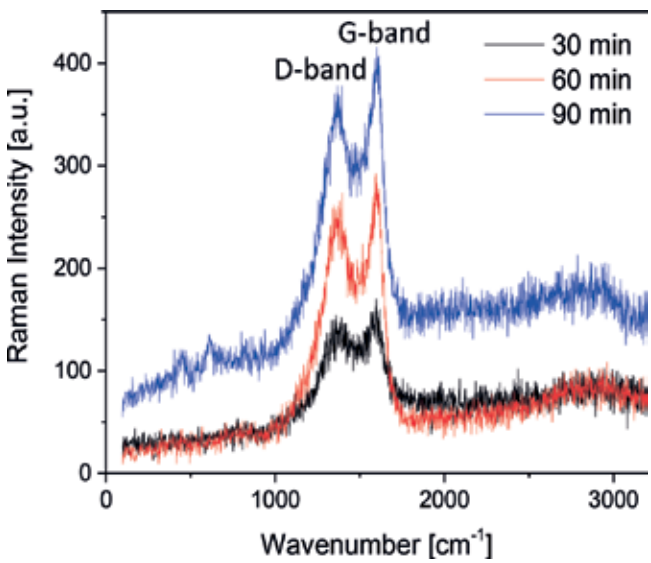

Figure 4. Raman spectra for the recycled carbon fibers.

Fiber sample	D band position (cm^{-1})	G band position (cm^{-1})	I_D/I_G	L_a (nm)
P-500°C/O-30 min	1357	1588	0.93	21
P-500°C/O-60 min	1364	1582	0.98	20
P-500°C/O-90 min	1364	1580	0.98	20

Table 2. Microstructure parameters of the recycled T300 carbon fibers at different gasification times using Raman spectrometer.

3.3. Mechanical properties

To achieve an objective determination of the optimum oxidation time based on mechanical properties, evaluations of the tensile strength and of the fracture toughness of the recovered fibers were performed.

3.3.1. Fiber tensile strength

The tensile properties of the carbon fibers were determined through tensile tests at a gage length of 20 mm in the fiber tensile tester at room temperature. Each single fiber was directly connected to the mechanical grips and then submitted to uniaxial straining up to failure under stroke control at 1 mm min^{-1}. Then, the natural frequencies were extracted to determine the linear density (using the frequency method according to the ASTM D1577 standard [25]), and subsequently, the cross-section area was calculated with the known fiber density, in order to finally determine the average fiber diameter at 20 mm gage length [26].

During the test, the force-strain curve was recorded. These curves indicate linear and elastic behavior up to failure (**Figure 5**). The maximum load attained was used to calculate the strength of each individual fiber, and the elastic modulus in the fiber direction was determined from the slope of the stress-strain curve.

The large reductions in tensile strength with increases of the gasification time are attributed to the large number of micropits on the fiber surfaces generated due to the severity of the oxidation. The higher void content also contributes to strength degradation. Overall, the oxidative effect results in a higher amount of surface defects, which leads to a reduction in the tensile strength and lateral crystallite size, as demonstrated above.

The average fiber diameter (D), elastic moduli (E), and tensile strength (σ_u) of fibers recycled with different gasification times are given in **Table 3**. It is shown that the decrease in strength is more significant compared to that of the modulus. This is caused by the presence of large number of defects on the thermally oxidized surface of fibers. At 30 min of oxidation time, the modulus seems to be slightly higher than the one of the virgin fibers (+2%). This can be due the presence of a layer of residual matrix or char on the surface of some recycled fibers. The modulus for the recovered fibers drops by about 10% with respect to virgin fibers after 90 min of gasification. With longer oxidation times, the modulus further reduces, which can be attributed to the removal of the amorphous carbon layer resulting from the oxidizing thermal treatment (corroborated with the decrease of the fiber diameter). This is consistent with

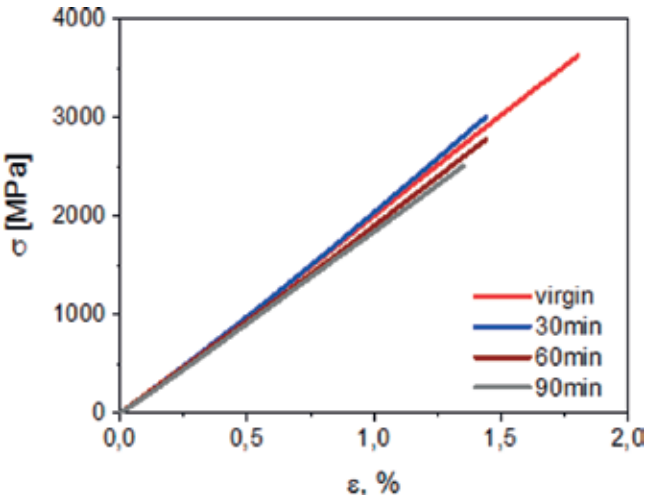

Figure 5. Strain vs. strain relationship for a pristine and recovered carbon fiber at different oxidation times.

Fiber sample	Diameter *D* (μm)	Elastic modulus *E* (GPa)	Tensile strength σ_u (GPa)
Virgin	7.5 ± 0.2	197 ± 18	3.4 ± 0.4
Recycled: P-500°C/O-30 min	7.2 ± 0.1 (−4%)	200 ± 4 (+2%)	3.0 ± 0.3 (−10%)
Recycled: P-500°C/O-60 min	7.1 ± 0.2 (−5%)	189 ± 9 (−4%)	2.7 ± 0.3 (−20%)
Recycled: P-500°C/O-90 min	6.6 ± 0.6 (−12%)	178 ± 5 (−10%)	2.4 ± 0.4 (−30%)

Table 3. Average diameter and mechanical properties of the fibers analyzed as function of the oxidation time.

the finding that heat treatment affects the diameter of the fibers. Consequently, gasification times of 60 min already lead to severe reductions in elastic modulus and tensile strength.

3.3.2. Fiber fracture toughness

In spite of the remarkable specific properties mentioned above, fracture of fiber-reinforced composite materials tends to occur in a brittle way due to their low capacity for plastic deformation and relatively low fracture toughness. In combination with the fiber/matrix interface, fiber fracture plays a role on the ultimate failure stress and energy dissipation mechanisms in brittle unidirectional composites. However, this property is less widely reported owing to the experimental difficulties associated with evaluation fracture in small-diameter fibers.

The methodology used consists on the introduction of artificial notches in the fibers by removing material using a focused ion beam (FIB) (**Figure 6**) [26–28]. A fine tungsten pin covered with liquid gallium (Ga) is used as an ion source from which Ga atoms are extracted and ionized via high voltage. This methodology allows precise monitoring of the notch geometry in terms of length, depth, and tip radius.

http://dx.doi.org/10.5772/intechopen.74281

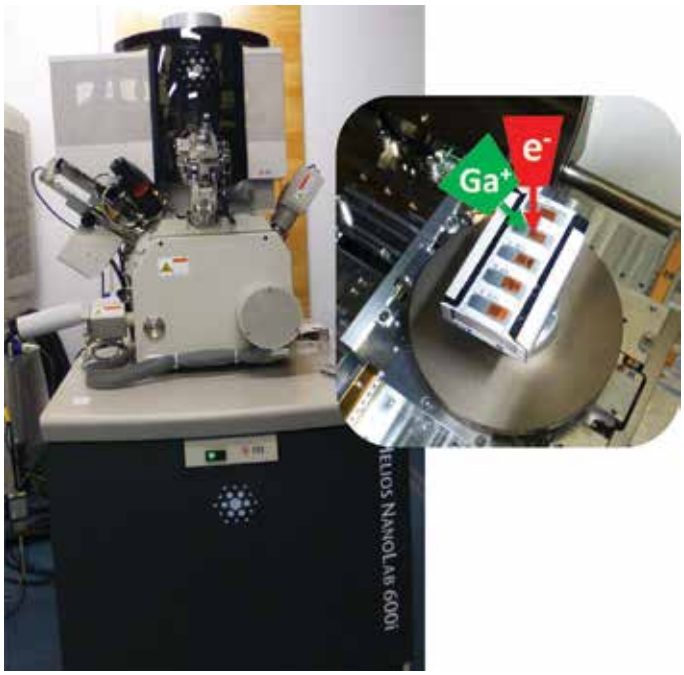

Figure 6. Fiber-milling system by focused ion beam (FIB).

Straight and sharp notches perpendicular to the fiber axis were introduced, as shown in **Figure 7**. The fiber diameter and the notch length of each test specimen were measured with a SEM associated to the FIB apparatus. Once the notch was milled into the fiber, the fibers were submitted to uniaxial loading up to failure in similar form as for the plain tensile strength tests described previously.

The fracture process started from the crack tip induced by FIB milling, and the response was also linear and elastic up to failure. The residual strength of the notched fiber was determined from the failure load and the corresponding area of the cross section of the fiber. The mode-I apparent fracture toughness, K_{IC}, was evaluated from the residual strength based on Linear Elastic Fracture Mechanics (LEFM) postulates. It is assumed that neither the small crack tip radius (≈50 nm) nor the possible material modification induced during the milling will excessively affect the fracture behavior of the fiber, and thus, the result can be considered a good approximation of the real material property. Hence, the failure of the fiber is dictated by

$$K_{IC} = \left(\frac{a}{D}, a, \sigma\right) = Y\left(\frac{a}{D}\right) \cdot \sigma_c \cdot \sqrt{\pi\, a} \tag{2}$$

where K_I depends on the specimen geometry, the crack depth, and the far-field stress applied. The parameter Y is a dimensionless stress intensity factor calculated according to the literature that assumes the geometric effects and the elastic anisotropy of the material [29].

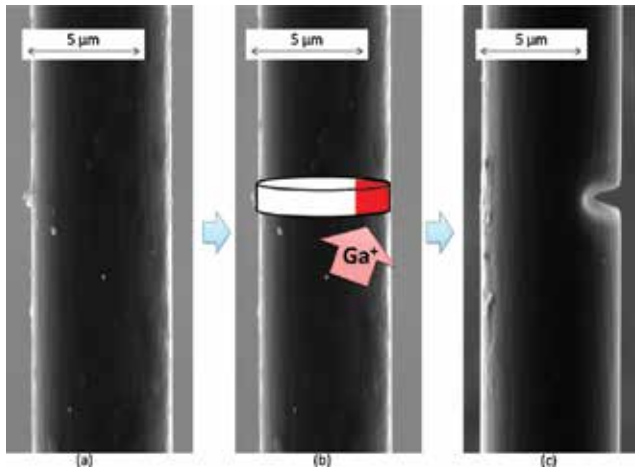

Figure 7. SEM micrographs the milling procedure; (a) original fiber; (b) gallium ions focusing and (c) notched fiber.

The critical energy release rate, or fracture energy, G_{Ic}, is computed through Irwin's equation, assuming the validity of LEFM, as

$$G_{Ic} = \frac{K_{IC}^{\ 2}}{E^*} \tag{3}$$

where E^* is the effective modulus which is taken as $E^* = E$, assuming plane strain conditions. The calculation of the plastic region length ahead of the crack tip, l_p, is based on

$$l_p = \frac{1}{2\pi} \cdot \left(\frac{K_{IC}}{\sigma_0}\right)^2 \tag{4}$$

where σ_0 is the average tensile strength of the Weibull statistics given by

$$F = 1 - exp\left(-\frac{L}{L_0}\left(\frac{\sigma}{\sigma_0}\right)^m\right) \tag{5}$$

The function F above is the cumulative fracture probability function, wherein L is the fiber length, L_0 is an arbitrary reference length, and σ_0 and m are the characteristic strength and the Weibull modulus of the fiber [26].

The average fracture toughness and fracture energies obtained for virgin and recycled fibers, at different oxidation times, are given in **Table 4**. The small value of the plastic radius compared to the fiber diameter demonstrates the validity and applicability of LEFM postulates. Very large reductions in fracture toughness and fracture energy (in the order of 50% for K_{Ic} and 70% for G_{Ic}) result of the recycling process, independently of the oxidation time, and they are presumably affected mostly during the thermolysis step. The operated material modifications that lead to these property reductions are also unclear. Hence, these aspects are under

Fiber sample	a_0/D	Apparent fracture toughness K_{Ic} (MPa $m^{1/2}$)	Apparent fracture energy G_{Ic} (J m^{-2})	Irwin plastic radius l_p (μm)
Virgin	0.15 ± 0.01	2.4 ± 0.5	24 ± 8	0.19 ± 0.01
Recycled: P-500°C/O-30 min	0.10 ± 0.03	1.2 ± 0.2	8 ± 3	0.15 ± 0.06
Recycled: P-500°C/O-60 min	0.15 ± 0.02	1.2 ± 0.3	7 ± 4	0.20 ± 0.03
Recycled: P-500°C/O-90 min	0.12 ± 0.02	0.9 ± 0.1	4 ± 1	0.15 ± 0.03

Table 4. Geometry and mechanical properties of the pristine and the recovered fibers for different gasification times.

investigation. However, it should be noted that the reduction in fiber fracture toughness is bound to have a limited influence on the fracture of the fiber-reinforced composite ply, as this property ($G_{Ic}^{ply} \approx 100$ kJ/m^2) is mostly determined by the fiber/matrix interface behavior.

Given the results achieved in terms of tensile strength and fracture toughness, it can be concluded that the optimal recycling process conditions consist on a thermolysis step at 500°C, for 6 h followed by gasification step for another 30 min. These conditions result in retentions of 100% of fiber elastic modulus and 90% of fiber tensile strength, although the brittleness of the fibers is seriously increased.

4. Remanufacturing of composites

Remanufacturing of unidirectional composites was pursued with the optimal fibers resulting from the optimization of the recycling process (thermolysis at 500°C for 6 h and oxidation at 500°C for 30 min). This section describes the adopted fabrication route and the preliminary evaluation of the mechanical performance of the resulting laminates.

4.1. Resin film infusion of recycled fibers

A tow-spreading technique was used to compact the nearly unidirectional fiber tows in order to obtain a high fiber volume fraction in plies of thin thickness. The fibers passed through a spreading machine, which is equipped with an air duct and rolls (**Figure 8**). The air pressure can be regulated and flows between two guide rolls, making the tows sag downward toward the air direction. This creates a momentary free tension stage that allows the tow to be spread.

Afterward, the resin film infusion technique (RFI) was used for manufacturing new laminates. In this way, the recycled fiber tows were laid down next to each other to complete a thin fiber bed layer. The fiber layers were interleaved with layers of semi-solid epoxy resin film Letoxit® LFX 060 [30] for subsequent consolidation. The fibers/resin consolidation is characterized by

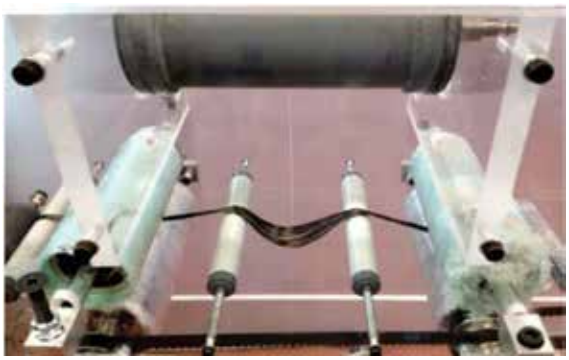

Figure 8. Tow-spreading equipment.

three major steps: intimate contact, adhesion, and fiber impregnation. The configurations carried out were [2x rCF layer/2x LFX 060 film/ …], with three LFX 060 film epoxy sheets placed on the top and bottom layer (the number of repetitions depends on the desired thickness). The final kit was introduced in a close-mold and cured in a hot-plate press, applying pressure (0.7 MPa) and heat (125°C for 25 min) simultaneously. The steps followed to make a laminate are depicted in **Figure 9**. It was then confirmed that the degree of resin curing was optimal by means of Differential Scanning Calorimeter (DSC) tests.

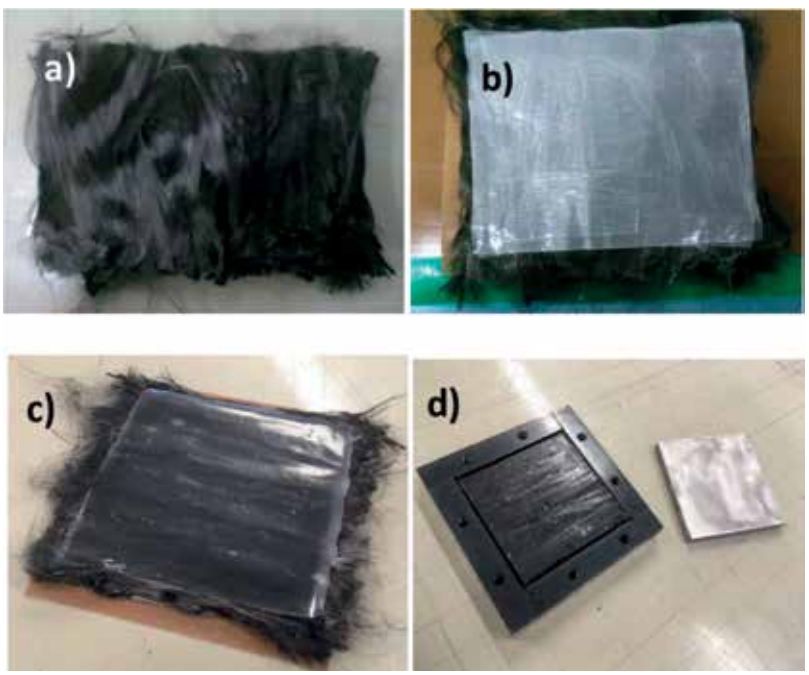

Figure 9. Staking sequence: (a) recycled carbon fiber layer; (b) LFX 060 film; (c) laminate after 2 h in the thermal plate; and (d) laminate in the close-molding.

4.2. Quality and properties of remanufactured composites

The quality of the composites recycled according to the methodology described above was evaluated by means of ultrasonic C-scan laminates. It was confirmed that the laminates were free of major porous, voids, or delaminations.

Thermogravimetric analyses (TGA) were carried to evaluate the composition of the laminates. It was determined that the nominal fiber volume fraction, V_f, was approximately 50%, a value not far from the typical $V_f \approx 60–65\%$ of high-performance unidirectional composites.

As means of rapidly assessing the mechanical performance of the remanufactured laminates, their interlaminar shear strength (ILSS) was evaluated by means of Short Beam Shear tests. This consists on flexural testing method using a very short beam relative to its thickness in order to promote interlaminar shear failure [31]. According to the test standard ASTM D2344 [32], all specimens ($27 \times 9 \times 4.5\ mm^3$) were loaded in a three-point bending configuration. The interlaminar shear strength was calculated using the equation:

$$F^{sbs} = \frac{3}{4} \cdot \frac{P}{b \cdot h} \tag{6}$$

where P is the maximum applied load, b is the measured specimen width, and h is the measured specimen thickness. The measured average ILSS of the remanufactured laminate was 64.3 ± 1.8 MPa, a value close to the lower bound of typical carbon fiber composite laminates (60–120 MPa). This might be a result of the lower V_f and flexural stiffness but also of the degradation of fiber/matrix interface properties. In fact, this aspect was previously reported in other researcher works [33] and will be investigated by the authors in the future. The interlaminar shear mode of failure confirms that this test is valid in terms of fracture mechanism.

5. Conclusion

This chapter dealt with the study of recycling technologies, of properties of the recovered fibers, and of the composites formed from these fibers. Regarding the recycling methodology, a thermolysis process at 500°C, for 6 h, followed by an oxidation/gasification step in air atmosphere at the same temperature, for 30 min, has been found to constitute the optimum recycling process. The combination of pyrolysis and gasification provides high process reliability, repeatability, product quality, and cost reduction. Moreover, remanufacture of composites was successfully achieved. As a whole, this constitutes a complete process of recycling carbon fibers that significantly reduces the environmental footprint and improves the life cycle of lightweight CFRP structures.

Regarding the properties of the recovered fibers, an oxidation time of 30 min leads to a full retention of elastic modulus and a 90% retention of tensile strength, relatively to pristine fibers. Longer gasification times lead to more significant decreases in these properties and undesirable alterations in the atomic composition of the surface of the fiber (increase of the O/C ratio). Moreover, the fracture toughness of the recycled fibers was found to decrease

significantly, independently of the oxidation time. These results still have to be investigated but are judged not to impact the properties of the remanufacture composites.

With respect to the composites remanufacturing process, tow-spreading of the unidirectionally aligned recycled fibers followed by means of resin film infusion is postulated to be an appropriate method in terms of resulting ply thickness, disposition of the fiber, fiber/resin ratio, and porosity control. It provides a potential solution to prepreg production scraps with enhanced quality assurance, resulting in the reduction of toxic emissions. The resulted laminates presented similar fiber content and interlaminar shear properties as compared to the brand new composites.

Acknowledgements

The authors are grateful to the Spanish Ministry of Economy and Competitiveness for support via the projects HYDTCOMP (MAT2015-69491) and R3FIBER (CTM2013-48887). A.F. gratefully acknowledges the Spanish Ministry of Education, Culture and Sports for financial funding through the FPU Fellowship. C.S.L. acknowledges the support of the Spanish Ministry of Economy, Industry and Competitiveness through the Ramón y Cajal fellowship (grant RYC-2013-14271). The help of Miguel Herráez and Dr. Miguel Castillo in the experimental work is also acknowledged.

Author details

Andrea Fernández[1], Cláudio S. Lopes[1], Carlos González[1,2] and Félix A. López[3]*

*Address all correspondence to: f.lopez@csic.es

1 Institute IMDEA Materials, Madrid, Spain

2 Department of Materials Science, E.T.S. de Ingenieros de Caminos, Madrid, Spain

3 Centro Nacional de Investigaciones Metalúrgicas (CENIM-CSIC), Madrid, Spain

References

[1] Marsh G. Airbus A350 XWB update. Materials Today. 2010. Available from: https://www.materialstoday.com/composite-applications/features/airbus-a350-xwb-update/

[2] ELG Carbon Fibre [Internet]. [cited 2016 Oct 24]. Available from: http://www.elgcf.com/

[3] Boeing [Internet]. 2017 [cited 2017 Jun 12]. Available from: Boeing.com/commercial/aeromagazine%0A

[4] Council Directive. Council directive 1999/31/EC on the landfill. Official Journal of the European Communities. 1999;**10**:L182/1-L18219

[5] European Parliament, Council of the European Union. Directive 2000/53/EC of the European Parliament and of the Council of 18 September 2000 on end-of life vehicles—Commission Statements. Official Journal of the European Union. 2000;**269**(September 2000):34

[6] Council Directive. Council directive 2000/76/EC on the Incineration of Waste. Official Journal of the European Communities. 2000;L **332**(February 1997):91-111

[7] European TEP& TC of. Directive 2004/35/CE of the European Parliament and of the Council of 21 April 2004 on environmental liability with regard to the prevention and remedying of environmental damage. Regulation. 2004;**2003**(807):56-75

[8] Oliveux G, Dandy LO, Leeke GA. Current status of recycling of fibre reinforced polymers: Review of technologies, reuse and resulting properties. Progress in Materials Science [Internet]. 2015;**72**:61-99. Available from: http://linkinghub.elsevier.com/retrieve/pii/S0079642515000316

[9] Roberts T. Rapid growth forecast for carbon fibre market. Reinforced Plastics. 2007; **51**(2):10-13

[10] ELG CArbon Fibre Ltd. [Internet]. 2017 [cited 2018 Jan 3]. Available from: http://www.elgcf.com/home

[11] BMW i3 [Internet]. [cited 2018 Jan 3]. Available from: https://secure.bmw.com/com/en/newvehicles/i/i3/2016/showroom/sustainability.html

[12] Thermal Recycling of Composites. Available from: http://www.trcsl.com

[13] Recycling carbon fibres. Engineering Materials. Available from: http://www.materials-forengineering.co.uk/engineering-materials-features/recycling-carbon-fibre/160324/

[14] Yang YX, Boom R, van Heerden I, Kuiper PH, de Wit PH. Recycling of composite materials. Chemical Engineering and Processing. 2012;**51**:53-68

[15] Hyde JR, Lester E, Kingman S, Pickering S, Wong KH. Supercritical propanol, a possible route to composite carbon fibre recovery: A viability study. Composites. Part A, Applied Science and Manufacturing. 2006;**37**(11):2171-2175

[16] Okajima I, Sako T. Recycling of carbon fiber-reinforced plastic using supercritical and subcritical fluids. Journal of Material Cycles and Waste Management. 2017;**19**:15-20

[17] Oliveux G, Bailleul JL, Le Gal La Salle E. Chemical recycling of glass fibre reinforced composites using subcritical water. Composites: Part A. 2012;**43**:1809-1818

[18] Morin C, Loppinet-Serani A, Cansell F, Aymonier C. Near- and supercritical solvolysis of carbon fibre reinforced polymers (CFRPs) for recycling carbon fibers as a valuable resource: State of the art. Journal of Supercritical Fluids. 2012;**66**:232-240

[19] Torayca. T300 Data Sheet. No CFA-001 [Internet]. 2002;6-7. Available from: www.toray-cfa.com/pdfs/T300DataSheet.pdf

[20] López FA, Rodríguez O, Alguacil FJ, García-Díaz I, Centeno TA, García-Fierro JL, et al. Recovery of carbon fibres by the thermolysis and gasification of waste prepreg. Journal of Analytical and Applied Pyrolysis. 2013;**104**:675-683

[21] López FA, Martín MI, Alguacil FJ, Rincón JM, Centeno TA, Romero M. Thermolysis of fibreglass polyester composite and reutilisation of the glass fibre residue to obtain a glass-ceramic material. Journal of Analytical and Applied Pyrolysis [Internet]. 2012;**93**:104-112 Available from: http://dx.doi.org/10.1016/j.jaap.2011.10.003

[22] TORAY—Innovation by Chemistry [Internet]. [cited 2018 Jan 12]. Available from: http://www.toray.com/

[23] Tanaka F, Okabe T, Okuda H, Ise M, Kinloch IA, Mori T, et al. The effect of nanostructure upon the deformation micromechanics of carbon fibres. Carbon [Internet]. 2013;**52**:372-378. Available from: http://dx.doi.org/10.1016/j.carbon.2012.09.047

[24] Caṇado LG, Takai K, Enoki T, Endo M, Kim YA, Mizusaki H, et al. General equation for the determination of the crystallite size la of nanographite by Raman spectroscopy. Applied Physics Letters. 2006;**88**(16):2-5

[25] Test Method for Linear Density of Textile Fibers, ASTM Standard D 1577-79

[26] Herráez M, Fernández A, Lopes CS, González C, Materials I, Kandel CE. Strength and toughness of structural fibres for composite material reinforcement. Philosophical Transactions. Series A, Mathematical, Physical, and Engineering Sciences. 2016;**374**: 20150274. Available from: http://dx.doi.org/10.1098/rsta.2015.0274

[27] Kant M, Penumadu D. Fracture behavior of individual carbon fibers in tension using nano-fabricated notches. Composites Science and Technology [Internet]. 2013;**89**:83-88. Available from: http://dx.doi.org/10.1016/j.compscitech.2013.09.020

[28] Tanaka F, Okabe T, Okuda H, Kinloch IA, Young RJ. Factors controlling the strength of carbon fibres in tension. Composites Part A: Applied Science and Manufacturing [Internet]. 2014;**57**:88-94. Available from: http://dx.doi.org/10.1016/j.compositesa.2013.11.007

[29] Ogihara S, Imafuku Y, Yamamoto R, Kogo Y. Application of FIB technique to introduction of a notch into a carbon fiber for direct measurement of fracture toughness. Journal of Physics Conference Series. 2009;**191**:12009

[30] Technical data sheet Letoxit LFX 060. 2011;1-5. Available from: www.5M.cz

[31] Shah DU, Schubel PJ. On recycled carbon fibre composites manufactured through a liquid composite moulding process. Journal of Reinforced Plastics and Composites. 2015;**35**(7):533-540

[32] Standard Test Method for Short-Beam Strength of Polymer Matrix Composite Materials and Their Laminates-ASTM D2344

[33] Pimenta S, Pinho ST. Recycling carbon fibre reinforced polymers for structural applications: Technology review and market outlook. Waste Management [Internet]. 2011; **31**(2):378-392. Available from: http://dx.doi.org/10.1016/j.wasman.2010.09.019

Chapter 8

Recent Development of Reused Carbon Fiber Reinforced Composite Oriented Strand Boards

Bo Cheng Jin

Additional information is available at the end of the chapter

http://dx.doi.org/10.5772/intechopen.77085

Abstract

There is a growing interest for the reused composite oriented strand board (COSB) for stiffness-critical and contoured applications. COSBs are made of rectangular shape prepreg strands that are randomly oriented within the structure. Development of this product form could markedly reduce the scrap generated during aerospace manufacturing processes. COSBs retain high modulus and drapability during processing and manufacturing. However, before any material can be deployed in industrial applications, its various properties must be well understood so that proper design analysis can be performed. Nondestructive testing (NDT) is widely used in research and industry to evaluate the quality of a variety of materials including composite materials and structures. NDT, as the name indicates, has the benefit that it does not alter or destroy the sample like other techniques, such as cross-sectional imaging. In this chapter, two nondestructive techniques, ultrasound and micro-computed tomography (micro-CT), were used to characterize carbon fiber epoxy composites, particularly comparing conventional laminates and reused COSB. The void content and morphology of samples cured using a range of materials and process parameters were determined using NDT and conventional microscopic analysis of cross sections. The mass distribution of fiber and resin within each sample was also determined. The manufacturing and NDT of COSB were introduced, and provided most detailed information on composite microstructure, including void size, void morphology, void distribution, and overall void content. Conventional micro-CT was determined to be ill-suited to scan large samples because of long scan times and large file sizes. To enhance the capabilities of micro-CT for evaluation of composite materials and structures, a micro-CT postprocessing method using stitching computer programming algorithms was developed. The method presented markedly increases the resolution that micro-CT can achieve, as well as the maximum feasible sample size, thus overcoming some of the primary drawbacks to conventional micro-CT. The primary objective of this work was to evaluate the feasibility of NDT methods in the assessment of both conventional composite laminates and the reused COSB fabricated from prepreg scrap. To this end, the advantages and limitations of ultrasound and micro-CT were discussed. The results showed that with stitching up postprocessing, micro-CT can be used

to detect global void morphology structure wide, making the technique competitive with ultrasound, yet with greater resolution and equivalent scan size.

Keywords: composite oriented strand board (COSB), reuse, recycle, NDE, micro-CT, ultrasound computer numeric control (CNC)

1. Introduction

Production waste and end-of-life (EOL) materials from one industrial process can serve as the raw materials for another, thereby reducing the environmental impact of an industry or process [1]. This concept is drawing attention in the aerospace industry as commercial aircraft designs transition from primarily metallic structure to carbon and glass fiber composite materials reduce weight and increase durability. Over the next 20 years, approximately 12,000 aircraft currently utilized for different purposes will be at the end of service life. In 2015, Boeing projects a demand of 38,050 new airplanes at a total value of $5.6 trillion [2] over the next 20 years, an increase of 3.5% from the previous year's forecast. With current trends in aircraft design, these airplanes are likely to contain increasing quantities of composite materials. The Boeing 787 Dreamliner, for example, is about 50% composite by weight, equating to roughly 32,000 kg of carbon fiber reinforced polymer (CFRP). The increased use of composites in aerospace has benefits in terms of fuel efficiently and durability. An immediate concern, however, is the large amount of thermosetting composite scrap generated during the manufacturing process.

In current aerospace and automotive production lines, 10–20% or more of virgin carbon fiber reinforced prepreg sheets end up as production wastes (**Figure 1**), as large prepreg rolls are cut into desired shapes to manufacture parts. This production scrap accounts for a significant source of composite waste. A second waste stream is end-of-life (EOL) thermoset composites. The total combined volume of end of life and production waste generated by the thermoset composites market in Europe is expected to reach 304,000 tons by 2015 [5]. Composite waste reduction and disposal are pressing concerns worldwide. Traditional disposal routes include landfilling and incineration. The financial and environmental costs of these methods, however, are steadily increasing. The composite industries, from suppliers and part manufacturers to customers, are seeking more sustainable solutions for reusing and recycling composite materials.

Jin et al. have been actively seeking viable methods and processes to turn in-process waste into useful products and components [6–9]. Research efforts thus far have focused on the repurposing of prepreg scrap into reused composite products including consumer products like skateboards and structural materials like reused composite oriented strand board (COSB), hat stiffened panels, etc. These components are fabricated by cutting prepreg trim waste into rectangular strands and curing them using out-of-autoclave (OoA) techniques like vacuum bag only (VBO), oven cure, and hot pressing. The work presented here originated from an NSF G8 Research Council funded project on "Sustainable Manufacturing through Out-of-Autoclave Processing". The first phase of the project focused on evaluating the manufacturing feasibility and mechanical properties of components made from scrap prepreg. As part of this work, finite element analysis (FEA) was utilized to predict the mechanical properties of scrap-based composites. Jin et al. and Jain et al. [7, 8] used FEA and mean field homogenization hybrid

http://dx.doi.org/10.5772/intechopen.77085

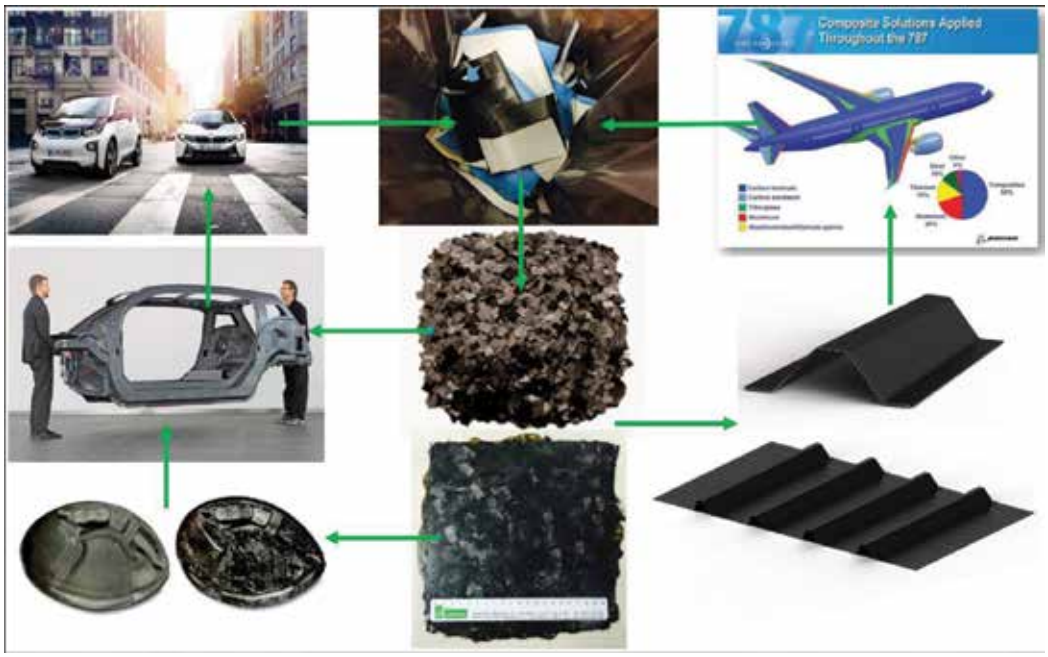

Figure 1. Motivation and potential applications of the composite oriented strand board (COSB), top middle shows the scrap generated during manufacturing, the scrap is trimmed to rectangular strands (center) and subsequently used for a variety of applications [3, 4].

methods to predict equivalent modulus of the COSB. Jin et al. [10] built a 3-D parametric FE model for random fiber composites with high volume fraction and fiber aspect ratio based on innovative 3-D spatial mathematic algorithm. In related work, Faessel et al. [11] created a finite element model on low-density wood-based fiberboards to study their local thermal conductivity, using a model based on X-ray tomography. While preliminary experimental and model results have shed light on the processing and mechanics of composites fabricated from prepreg scrap, a more detailed understanding of the microstructure of the materials is required, including voids. Details of void morphology and microstructure, as obtained through nondestructive techniques, can be utilized to build detailed and FEA models. This work describes results of NDT analysis of COSB fabricated from rectangular prepreg strands of uniform size.

2. Experiments

A reused carbon fiber epoxy COSB demonstrator panel was produced using OoA techniques [9]. The part was then analyzed for mass and void distribution using ultrasonic C-scan. After scanning, the COSB was cut down using a CNC milling machine. Void content and void morphology were investigated using both microscopic examination of polished cross sections and state-of-the-art stitched high-resolution micro-CT techniques. The results, pros and cons of the three techniques are compared and discussed later in this chapter.

Figure 2. Composite oriented strand board (COSB, left), similar to wood OSB (right).

A demonstrator COSB panel (**Figure 2**, Left) was first manufactured. Fresh prepreg (UD Tape T40/800B with Cytec CYCOM 5320-1 epoxy resin) was manually cut into rectangular strands (10 × 20 mm) and distributed evenly on an aluminum plate. The prepreg was subsequently cured using a compression molding hot press (Wabash) into a flat COSB panel measuring 215.9 × 215.9 mm. The manufactured panel is analogous to a composite version of the ubiquitous wood-based strand board (**Figure 2**). A CNC milling machine with a diamond cutting wheel was used to section the COSB into seven individual plain tensile specimens (25 × 200 mm) in accordance with ASTM D3039 [12] standard for quasi-static tensile testing. Six coupons were tested in a loading frame (INSTRON), and elastic modulus was determined from the resulting load-displacement curve, the details of which are presented elsewhere [7].

The remaining coupons (prepared from the center of the COSB) were cut into smaller pieces (25 × 50 mm) for nondestructive evaluation (NDE) using ultrasound A and C scans, high-resolution micro-CT, as well as cross-sectional imaging analysis, that are discussed in Section 3 of this chapter.

3. Results and discussion

A commonly used nondestructive testing method used for composite materials is ultrasonic test [13]. Ultrasonic testing is a noncontact method, which typically requires a coupling agent (often water) and therefore an extensive setup. Ultrasound scans, when performed properly, enable defects such as delamination and debonding to be detected easily and accurately [14, 15].

3.1. Ultrasound scans

Ultrasonic A-scans were performed on both the demonstrator COSB sample and a reference panel. The reference laminate was an autoclave-cured Cytec 5320-1 composite panel with known low void content (<1%, by microscopic image study). To carry out the scans, the ultrasound transducer was fixed in position at the center of the specimen. A pulse-echo mode was utilized to

interrogate defects within each panel. The strength of the reflected ultrasonic echoes as function of time is presented in **Figure 3**. The A-scan of the reference laminate (**Figure 3**, Upper) reveals clear top surface and back surface reflections. The region between these top and bottom surfaces (Gate 2, the interior of the panel) shows <3% signal attenuation, indicating a low void content. The A-scan of the COSB (**Figure 3**, Lower), in contrast, shows roughly 20% signal attenuation between the top and back surface reflections, indicating greater void content within the composite.

While the A-scan mode reveals critical information about the ultrasound signal attenuation, visual maps of panel quality can be produced using a C-scan mode, which is one of the most suitable method for production inspection of composites using a conventional pulse-echo or pulsed through-transmission system. In this study, a 10-MHz transducer was focused on the top surface of the specimen and gated on the echo from a glass reflector plate (**Figure 4**). The pulse passed through the specimen twice. A quantized display was used, so the various attenuation levels are presented as finite changes to tone density on a plain view of the specimen. The white regions are of lowest attenuation. There is no attenuation in the absence of a specimen, which accounts for the white border outlining each sample.

Ultrasonic C-scans were performed on the following specimens: a quasi-isotropic reference panel that was manufactured using heated platen compression molding (**Figure 5**, Left), and the demonstrator COSB (**Figure 5**, Right). These two panels are both made of same prepreg material (Cytec 5320-1). The transducer moved in two dimensions within a range in the x-y plane covering the whole flat panel area. The total time for the transducer to cover the entire laminate (215.9 × 215.9 mm) was about 6 hours. The images in **Figure 5** display the peak signal response within a time or depth interval of interest as a function of transducer position. There are two observations from the examination of the C-scan images. First, the COSB displays high signal attenuations (max ~90%) when compared to continuous fiber laminates (max ~10–20%) This confirms that, not surprisingly, COSB has a much higher overall void volume fraction compared to that of the reference panel (void volume fraction <1%). Secondly, insights into the distribution of resin and fiber in each sample are revealed in the C-scan images. We observe that the distribution of matter in COSB is significantly more uneven than in the conventional continuous prepreg laminate. The uneven distribution of the matter in COSB is probably due to less free-flowing resin as compared to the continuous prepreg plies. Also, the discontinuity and random orientation and location of the strands play an important role.

3.2. Microscopy study of void contents

To gain more insight into void morphology and assess the validity of NDT analysis, the void contents of test laminates were also evaluated using optical microscopy. To investigate a method for reducing void content in COSB, two samples with smaller sizes (50 × 50 mm) were fabricated from prepreg aged for 14 and 28 days at room temperature, in addition to the demonstrator COSB made of fresh prepreg strands. The samples for cross-section imaging were prepared from the center of each panel, and measured 50 mm in length and 3 mm in thickness. Cross sections were prepared via mechanical polishing with silicon carbide abrasive papers on a grinder-polisher (Struers), at successive grits of 150, 240, 400, 600, 1200, and 2400. Cross-sectional images were acquired using a digital microscope (Keyence) at a magnification of 100×. Approximately, 20 images were obtained from each sample to assemble a full-scale

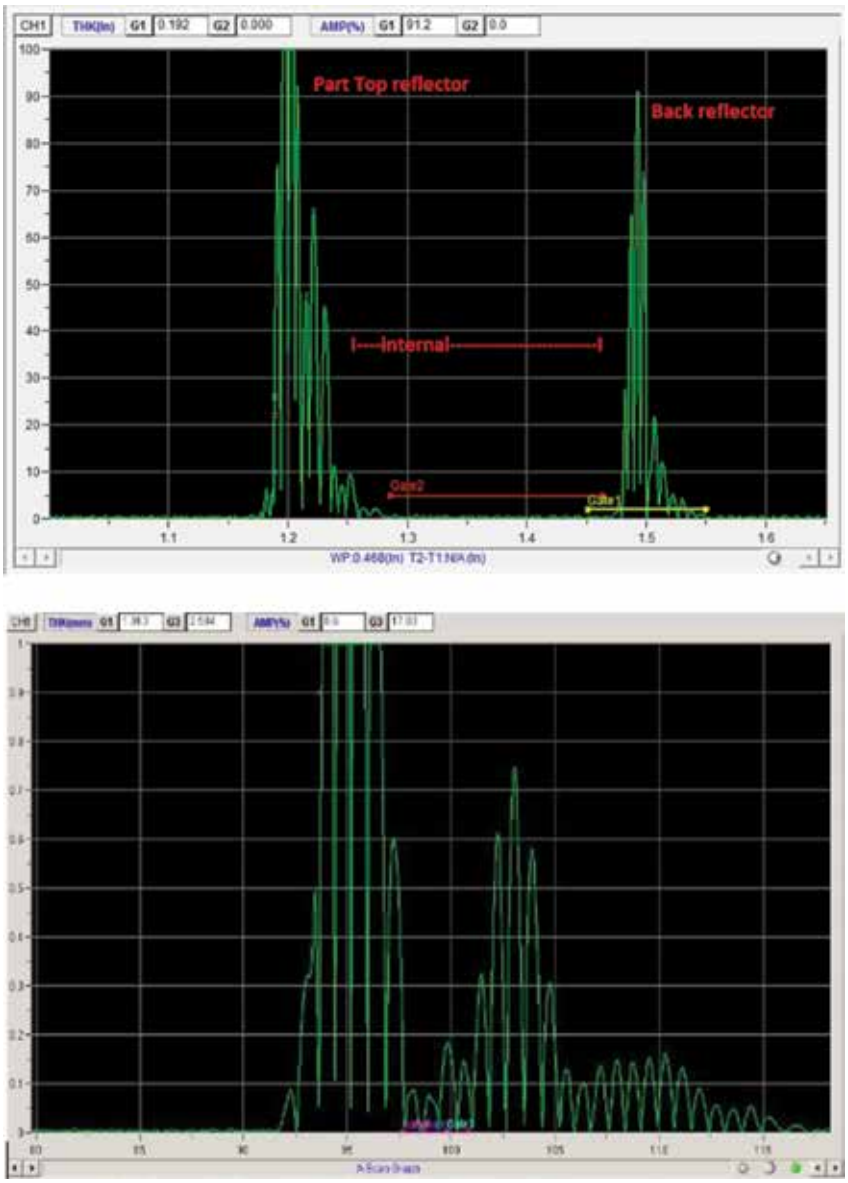

Figure 3. Upper: ultrasonic A-scan plot of the referenced autoclave cured composite laminates: void content <1%. Lower: the A-scan result of a COSB, indicating greater signal attenuation compared to the referenced laminate: void content ~6%.

image of the cross section. Images were processed and merged using image-processing software for void content analysis. The images were first converted to gray scale. Voids were manually selected and filled to distinguish from solid phases. An image analysis program (ImageJ [16]) was used to convert each image into a binary map of voids (black pixels) and solid (white pixels). The areal void contents was then calculated and used as a representation of void volume fraction (**Figure 6**).

http://dx.doi.org/10.5772/intechopen.77085

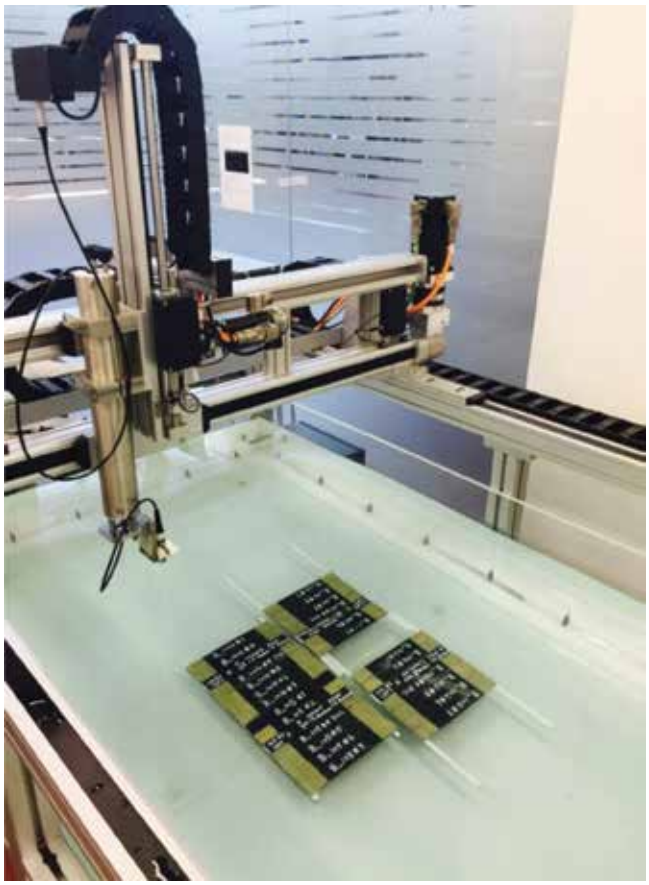

Figure 4. Ultrasonic scan setup. At the top is the arm with a 10-MHz transducer installed. The samples are placed in the water pool underneath.

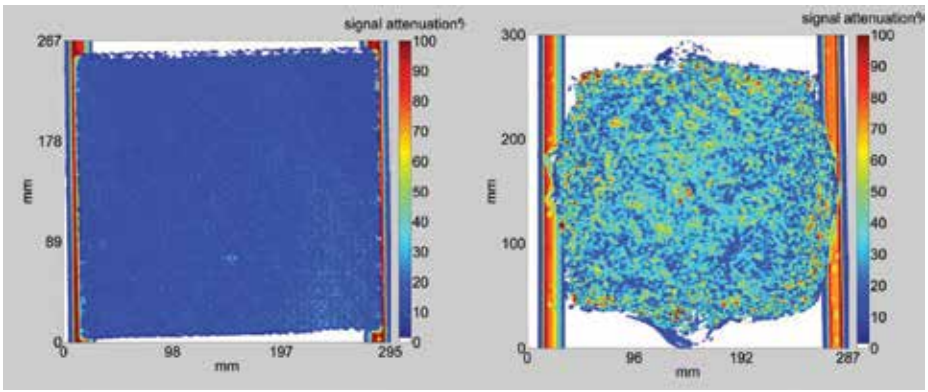

Figure 5. Ultrasonic C-scan results. Left: reference panel, quasi-isotropic layup, heated platen compression molding cured. Right: the demonstrator COSB.

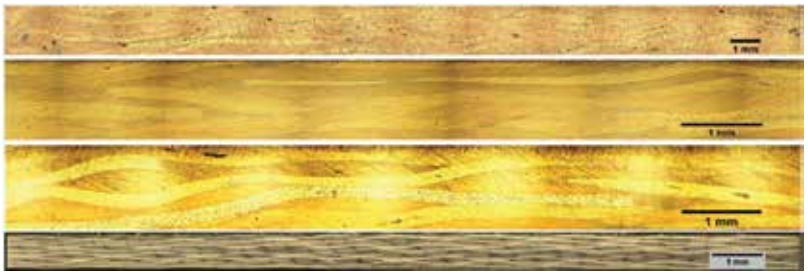

Figure 6. Microscopic scan results of (from top to bottom): (a) the demonstrator COSB (made of fresh prepreg strands). Void content = 2.07%, (b) COSB sample made from prepreg strands aged in room temperature for 14 days. Void content = 0.81%, (c) COSB sample made from prepreg strands aged in room temperature for 28 days. Void content = 2.41%, (d) an autoclave-cured reference sample with continuous prepreg fibers.

COSB made from fresh prepreg strands, 14-day room-temperature-aged-, and 28-day room-temperature-aged prepreg strands yielded void contents of 2.07, 0.81, and 2.41%, respectively. The COSB sample made from prepreg with 14 days of out time had the lowest void content. This is because prepreg is partially cured during room temperature aging time, resulting in decreased tack and easier manipulation during layup and more efficient air removal during cure. This aging process can have beneficial results in the short term, but when prepreg is aged over its shelf life (28 days), viscosity increases such that resin flow is hindered and flow-induced voids are formed.

3.3. Micro-CT analysis

X-ray CT is an effective nondestructive technique for studying the details of internal defects. This technique was first applied in designing medical CT device. Because nonmetal composite materials have a similar composition to human bodies, the medical CT devices were well suited to imaging of carbon fiber epoxy composite materials. The device can be used for 3-D image reconstruction to detect defects (microcracks, inclusions, voids, delamination and debonding), determine distribution of mass, and accurately measure and display internal structural configurations. Previous studies [14] have indicated that the resolution of micro-CT is well suited to the detection of internal and surface defects in carbon fiber epoxy composites. In this work, a Phoenix Nanotom Tomographic machine (General Electric) with a Hamamatsu C-7942 detector and an Mo anode was utilized to perform micro-CT scans on the demonstrator COSB. A micro-CT sample (25 × 50 × 3 mm, **Figure 7**, Left) was prepared from the center of COSB. Electric tensions between 30 and 55 kV and current intensities between 190 and 220 μA were used. Spatial resolutions between 2.5 and 14.5 μm/px were attained from the above setup.

Initial scans showed that clear boundaries between strands cannot be resolved using X-ray absorption tomography, even at the highest resolution. However, when viewing continuous frames of scanned images, an animation reveals strand boundaries. This observation was helpful in identifying the shape of deformed strands and stitching multiple volumes for further postprocessing and analysis. The technique proved to be valuable for estimating void content. Thus, all samples were scanned in sets of 3–4 simultaneous samples to optimize available tomography time. Updated settings used were 80 kV and 150 μA, with a 500 ms exposure time. The attained resolution was 13.04 μm/px.

http://dx.doi.org/10.5772/intechopen.77085

Figure 7. Left: a micro-CT sample prepared from the center coupon of COSB. Right: a 2-D micro-CT image of cured COSB sample (resolution: 2.5 μm/px). Deformed prepreg strands and their curvature were observed. Morphology of the voids was also presented.

Multiple scans were performed on different regions from a single sample in order to cover the entire sample volume. The obtained volumes were reconstructed using a user-defined computer program. By stitching and cropping, an individual volume containing the complete sample volume was obtained. Results are displayed in **Figure 8**. Detailed void content and void morphology information was extracted from the stitched volume, as presented in **Figure 9**. In the demonstrator COSB made of fresh prepreg strands, voids mostly appear as

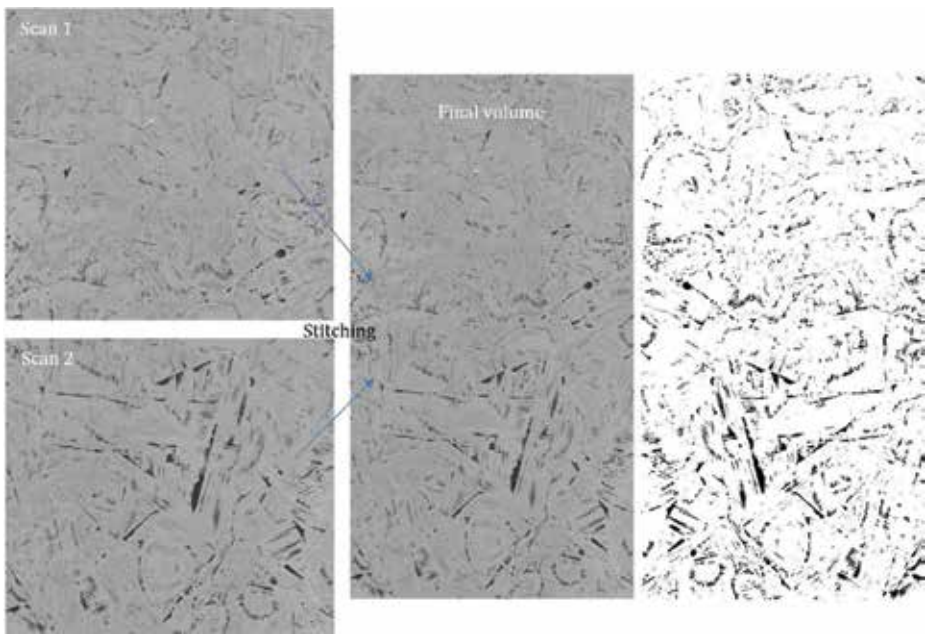

Figure 8. Stitching of multiple scanned volumes to obtain completed final micro-CT scanned volume.

needle shapes, and void content was determined to be 8.55%. This is considerably higher than the 2.07% void content determined via microscopic analysis. This is not surprising, as the void content from micro-CT is obtained from a 3-D volume, while the void content concluded from microscopic imaging is obtained from 2-D images. There is a difference of one spatial degree between two sources of data. Because micro-CT can reveal void information in 3-D, it has advantages compared to 2-D techniques such as microscopic images of polished sections.

The curvature of the deformed strands is a critical parameter when trying to predict and optimize the modulus and strength [7, 8] of COSBs using FEA techniques. Micro-CT allows for examination of this critical parameter. Several shapes of deformed strands (10 × 20 mm), extracted from the micro-CT data, are displayed in **Figure 10**. Strands have various deformed shapes after being cured within the COSB, due to the randomness and complex geometry of the material (**Table 1**).

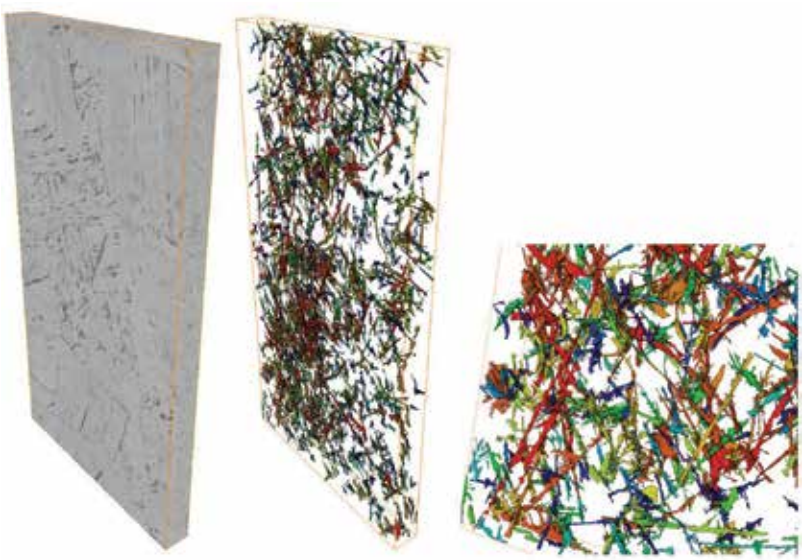

Figure 9. Extracted void content (8.55% voids) and void morphology of COSB (left and middle). Close-up view of void morphology (right).

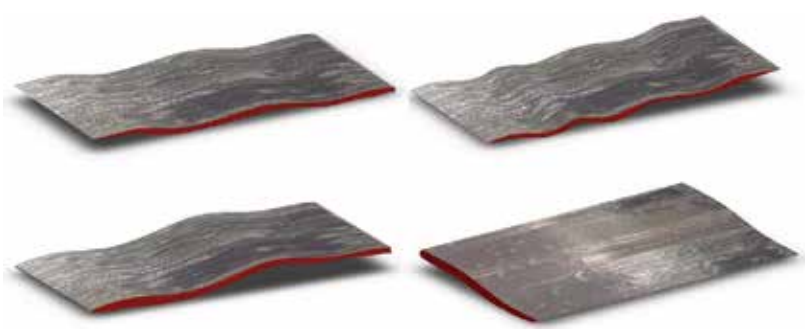

Figure 10. Extracted shape of deformed strands in COSB.

Technique	Approximate processing time	Maximum sample size
Ultrasonic scan (3-D)	4–6 hours	1 × 1 m by sample thickness
Microscopic image (2-D)	1–2 hours	5 × 5 cm
Micro-CT (3-D)	6–12 hours	3 × 5 cm × 5 mm by sample thickness

Table 1. Comparison of different techniques: approximate processing time and sample size.

3.4. Comparison of NDE techniques

In this chapter, the void content, void distribution, void morphology and deformed strand shapes of carbon fiber epoxy composite panels were examined. Microscopic cross-sectional analysis and NDE techniques (ultrasound and micro-CT) were employed. Traditional laminates and reused COSB were examined using these techniques. Conclusions on the pros and cons of each technique are discussed below:

3.4.1. NDT ultrasonic scans

a. Ultrasonic scans evaluate the overall void distribution in a panel-level scale. Macrolevel information such as void cluster regions, and distribution of matter, can be revealed by this technique. Ultrasound scans can also evaluate relatively large sample sizes.

b. Signal attenuation level does not directly link to void content. Ultrasonic scans cannot offer a void content number quantitatively and accurately without the use of reference panels. Overall relative panel level void content can be estimated when compared to ultrasonic image of a reference panel with low void content.

3.4.2. Microscopic image study

a. Microscopic imaging of cross sections is one of the most convenient methods in evaluating composite void content. The process of sample preparation including cutting, polishing and image postprocessing are relatively straightforward and less time consuming compared to other methods.

b. However, it is not nondestructive. Samples need to be cut and polished. Extra-damages are possible to be introduced during sample preparation procedure. Also, void content is only investigated in the area of the cross-sectional cut, which is a 2-D area but not a 3-D volumetric study. The results vary based on location within the sample.

3.4.3. Micro-CT

a. Micro-CT is a nondestructive method. It yields accurate void content values, and reveals void morphology. However, it is time consuming and requires a large amount of image-processing work. One high-resolution micro-CT scan can take up to dozens of hours and engage dozens of GBs of data space in computer system.

b. Limitation of the sample size cannot be ignored. Due to the limitation of scanning time and storage, the sample size of micro-CT is relatively small, normally within a few millimeters in length and width. As a result, some materials could potentially loose representativeness when examined via a micro-CT scan.

c. Due to this limitation of the sample size, overall void distribution in panel size level cannot be obtained. So, this technique does not work well for large panels with none-even mass distribution.

4. Conclusions

The void contents of COSB made of reused production scraps as well as conventional composite laminates were studied using different NDE methods, including ultrasonic C-scan, micro-CT scan, and microscopic image analysis of polished cross sections. Results were reported and the general pros and cons of the different techniques as well as specific observations relative to the COSB material have been identified. The void content, void distribution, void morphology and curvature and geometries of the deformed strands obtained by the NDE techniques in this study are valuable information for future COSB design and optimization. With these information, methods such as FEA [7] and hybrid methods using analytical solutions and homogenization schemes [8] can be used to predict various mechanical responses of such material. Future work will be focused in these directions.

Acknowledgements

The authors are grateful to NSF G8 program and to Airbus for supporting this research through Airbus Institute for Engineering Research (AIER) Program. M.C. Gill Composites Center in Los Angeles, U.S. and IMDEA Materials Institute in Madrid, Spain are thanked for supporting this work. Vanesa Martinez, Jose Luis Jimenez, Miguel De La Cruz Pacha, Dr. Federico Sket, Dr. Claudio Lopes, and Dr. Ignacio Romero are thanked for their useful suggestions and warm discussions in the summer of 2015.

Author details

Bo Cheng Jin[1,2,3]*

*Address all correspondence to: bochengj@usc.edu

1 M.C. Gill Composites Center, Department of Chemical Engineering and Materials Science, University of Southern California, Los Angeles, CA, United States

2 Department of Aerospace and Mechanical Engineering, University of Southern California, Los Angeles, CA, United States

3 NASTRAN (NASA Structural Analysis) Development, MSC Software, CA, United States

References

[1] Frosch RA Gallopoulos NE. Strategies for Manufacturing. Scientific American. 1989. Available from: http://www.umich.edu/~nppcpub/resources/compendia/IEORpdfs/IEOR_Reading.pdf

[2] Current Market Outlook 2015-2034. Report. Boeing Commercial Airplanes; 2015

[3] Boeing Commercial Aircraft. Available from: www.boeing.com/commercial

[4] SGL Carbon. Available from: www.sglgroup.com

[5] Harbers F. Annual Report of the European Composite Recycling Services Company. 2015

[6] Jin B, Li X, Jain A, Gonzalez Carlos, LLorca J, Nutt S. Optimization of microstructure and mechanical properties of composite oriented strand board from reused prepreg. Journal of Composite Structures. 2017;**174**:389-398

[7] Jin B, Li X, Jain A, Wu M, Mier R, Herraez M, Gonzalez C, LLorca J, Nutt S. Mechanical properties and finite element analysis of reused UD carbon fiber/epoxy OoA VBO composite oriented strand board. In: Proceedings of SAMPE 2016; Long Beach; 2016

[8] Jain A, Jin B, Li X, Nutt S. Stiffness predictions of random chip composites by combining finite element calculations with inclusion based models. In: Proceedings of SAMPE 2016; Long Beach; 2016

[9] Nutt S, Centea T. Sustainable manufacturing using OoA prepregs. In: Proceedings of CAMX 2014; Orlando, FL, United States; October 13-16, 2014

[10] Jin B, Pelegri A. Three-dimensional numerical simulation of random fiber composites with high aspect ratio and high volume fraction. Journal of Engineering Materials and Technology. 2011;**133**:41014

[11] Faessel M, Delisee C, Bos F, Castera P. 3D modelling of random cellulosic fibrous networks based on X-ray tomography and image analysis. Journal of Computer Science and Technology. 2005;**65**:1931-1940

[12] ASTM D 3039/D 3039 M. Standard Test Method for Tensile Properties of Polymer Matrix Composite Materials. ASTM International

[13] Garnier C, Pastor M, Eyma F, Lorrain B. The detection of aeronautical defects in situ on composite structures using non destructive testing. Review. Journal of Composite Structures. 2011;**93**:1328-1336

[14] Djordjevic BB. Advanced Ultrasonic Probes for Scanning of Large Structures. Ultrasonic International; 1993

[15] Djordjevic BB, Reis H. Sensors for Materials Characterization, Processing, and Manufacturing. NDE; 1998. p. 1

[16] https://imagej.nih.gov/ij/

Edited by Rita Khanna and Romina Cayumil

Carbon fibres are lightweight, chemically stable materials with high mechanical strength, and have state-of-the-art applications in aerospace, marine, construction and automotive sectors. The demand for carbon fibre–based components is expected to grow dramatically with expanding opportunities for lightweight metals and composites. Although this field has achieved a high level of maturity, nanoscale developments in carbon fibres have seen dramatic improvements in the functions of conventional biomaterials and composites. This book reveals several new developments in the field to enhance characteristics of carbon fibres and their composites, novel applications for tissue engineering, biological scaffoldings and implants, recycling and reuse of end-of-life CFRP and manufacturing waste and other issues of concern in the field of carbon fibres.

Published in London, UK

IntechOpen

ISBN 978-1-83881-562-2